Phase Transitions in Evolutionary Potential Games

Ph.D. Thesis

Balázs Király

Supervisor: György Szabó D.Sc.

Consultant: Csaba Tőke D.Sc.

BME, MTA EK MFA

2019

Nyilatkozatok

Alulírott Király Balázs kijelentem, hogy ezt a doktori értekezést magam készítettem és abban csak a megadott forrásokat használtam fel. Minden olyan részt, amelyet szó szerint vagy azonos tartalommal, de átfogalmazva átvettem, egyértelműen, a forrás megadásával megjelöltem.

Budapest, 2019. november 20.

Király Balázs

Alulírott Király Balázs hozzájárulok a doktori értekezésem korlátozás nélküli, interneten történő nyilvánosságra hozatalához.

Budapest, 2019. november 20.

Király Balázs

Alulírott Király Balázs nyilatkozom, hogy az értekezés és a tézisfüzetek leadott nyomtatott és elektronikus példányai mindenben azonosak.

Budapest, 2019. november 20.

Király Balázs

Abstract

Phase Transitions in Evolutionary Potential Games

by Balázs Király

In game theory, player–player interactions are usually defined by so-called payoff matrices, which can be considered as superpositions of elementary games. When an iterated multiplayer version of such a game lacks certain elementary components and the strategy updates of the players follow the logit rule, the game in question is equivalent to a classical spin model. This thesis exploits this correspondence: It deals with the analysis of the general features, phase transitions, and critical properties of a handful of these games systems using the concepts and methods of statistical physics. The models treated in this thesis are simple combinations of elementary games that represent archetypical interaction situations, and thus initiate the systematic analysis of the interplay between interaction components.

Összefoglaló

Fázisátalakulások evolúciós potenciáljátékokban

Király Balázs

Az értekezés első része a szimmetrikus mátrixjátékok egy olyan, a szuperpozíció elvét követő felbontását mutatja be, melyben az elemi játékok négy alapvető kölcsönhatási viszony valamelyikét képviselik: a kölcsönhatási osztályokat az ön- és társfüggő, a koordinációs, valamint a ciklikus dominanciát leíró játékok alkotják. Ezen felbontás alapján könnyen azonosíthatók az úgynevezett potenciáljátékok, ugyanis ezek nem rendelkeznek ciklikus dominanciát leíró komponenssel. A potenciáljátékok segítségével teremthető közvetlen kapcsolat az evolúciós játékelmélet és a statisztikus fizika között: ha a játékosok az úgynevezett logitszabály szerint választják meg stratégiáikat, akkor a sok játékos által játszott ismételt potenciáljátékok klasszikus spinmodelleknek feleltethetők meg. Az ekvivalencia részleteinek rövid áttekintését követően az értekezés néhány ilyen, négyzetrácsra helyezett játékmodell általános tulajdonságait és kritikus viselkedését tárgyalja a statisztikus fizika olyan jól ismert fogalmainak és módszereinek felhasználásával, mint például az átlagtér- és párközelítés, valamint a Monte-Carlo-szimuláció. Megmutatjuk, hogy a legegyszerűbb nem triviális potenciáljáték, az elemi koordinációs játék – ami az Ising-modell kiterjesztése közömbös stratégiákkal – egy, az Ising-modell univerzalitási osztályába tartozó folytonos rend–rendezetlenségi fázisátalakuláson megy keresztül, ha a közömbös stratégiák száma nem túl magas; ellenkező esetben az átalakulás elsőrendű. Míg egy szimmetriasértő önfüggő komponens jelenlétében a folytonos átalakulások mindenképpen kisimulnak, addig egy olyan önfüggő komponens, amelyik azonosan hat a két koordinált stratégiára, megváltoztathatja az átalakulás kritikus pontját és annak rendjét is, vagy akár el is tüntetheti azt. Ezen eredmények helyességét igazolja, hogy az utóbbi rendszer leképezhető a Blume–Capel-modellre. Az Ising-osztályú kritikus viselkedés robusztusságát vizsgálandó, néhány több elemi koordináció kombinációjaként előálló játékot is megvizsgálunk. A maximálisan nem átfedő koordinációs játékokat a lehetséges legnagyobb számú, közös koordinált stratégiákkal nem rendelkező elemi koordináció alkotja. Az ezek között fennálló permutációs szimmetria két koordinált pár esetén erősíti, három esetén viszont elnyomja az Ising-típusú viselkedést, noha a rendezett fázis mindkét esetben csak egyetlen pár szimmetriáját sérti. Végezetül egy Ising- és Potts-típusú részjátékok közötti versengést leíró modellt tárgyalunk, melynek kritikus viselkedése általában a két részjáték valamelyikének kritikus viselkedését követi. Ugyan a rendszer alapállapota mindig annak a részjátéknak a szimmetriáját sérti, amelyik magasabb nyereményeket biztosít, entrópiahatások következtében az Ising-osztályú viselkedés mégis stabilizálódhat a folytonos rend–rendezetlenségi átalakulás környezetében olyan esetekben is, amelyekben a Potts-komponens csupán kellően kis mértékben erősebb. Ekkor a két versengő rendezett fázis között egy újabb, elsőrendű fázisátalakulás is megfigyelhető.

Summary

Phase Transitions in Evolutionary Potential Games

by Balázs Király

This thesis begins with a review of the decomposition of symmetric matrix games as superpositions of elementary games representing four fundamental interaction types: players unilaterally setting either their opponent's or their own payoff, pure coordination, and games of cyclic dominance. This decomoposition scheme readily identifies so-called potential games as lacking cyclic dominance components. These potential games play a key role in bridging the gap between evolutionary game theory and statistical physics: Iterated multiplayer potential games that are governed by the logit strategy update rule are equivalent to classical spin models. After a brief overview of the details of this correspondence, the thesis proceeds to examine the general features and critical properties of a handful of these game models when the players are located at the sites of a square lattice using some well-established concepts and methods of statistical physics, including mean-field and pair approximations and Monte Carlo simulations. It is shown that the simplest nontrivial potential game, the elementary coordination game—an extension of the Ising model with neutral strategies—exhibits an order-disorder phase transition that is continuous and belongs to the Ising universality class as long as the number of neutral strategies is low enough but is of the first order otherwise. Whereas the presence of a symmetry-breaking self-dependent component invariably smooths out continuous phase transitions, a self-dependent component that equally affects both coordinated strategies can tune the critical point, change the order of the phase transition, or even abolish it altogether. These results are verified by mapping the system to the Blume–Capel model. Some simple combinations of multiple elementary coordinations are also discussed in order to further probe the robustness of Ising-type critical behavior. Maximally nonoverlapping coordination games are permutation symmetric combinations of a maximal number of elementary coordinations that do not share coordinated strategies. This symmetry enhances Ising-type behavior in the two-pair model, but suppresses it in the three-pair case, although both phase transitions break the symmetry of just one constituent coordination. Finally, a model of competing Ising- and Potts-type subgame components is examined, whose critical properties generally correspond to those of one of the subgames. Even tough the ground state always breaks the symmetry of the subgame that provides higher payoffs, Ising-type behavior is still stabilized by entropy effects near the order-disorder transition when the Potts component is only slightly stronger, introducing a second, first-order transition separating the competing ordered phases.

Acknowledgements

This work was supported by the Hungarian Scientific Research Fund (OTKA) under Grants No. TK-101490 and No. K-120785.

Contents

Chapter 1

Introduction

Recent years have seen increased interest in interdisciplinary applications of concepts and tools widely used in statistical physics in various, sometimes rather new research disciplines [1] such as theoretical ecology [2, 3], econophysics [4–6] and sociophysics [7–10], and network science [11, 12]. What is common in many of these applications is that they aim to model universal emergent collective behavior in complex systems of numerous interacting individual components by analogy to many-particle physical systems [13]. This often involves agent-based modeling [14]: identifying the autonomous microscopic elements of the system in question, determining the salient features of how these influence each other, and inferring macroscopic properties from these features.

In a system of inanimate particles, the interactions are generally fairly well-known, measureable, calculable, and derive from the universal laws of physics. In contrast, agents in a human system are conscious actors whose behavior does not necessarily follow easily discernible rules and may be quite sensitive to conditions, which makes comprehensive modeling extremely hard [8]. Consequently, sensible interaction models should be rooted in behavioral sciences and game theory, the mathematical study of strategic decision-making [15]. Similar things can be said about ecological systems, whose population dynamics is driven by Darwinian fitness [16].

The closest correspondence between game theoretic and statistical physical models lies in the formal equivalence of logit-rule-driven potential matrix games and classical spin models. Even within this narrowed field, it is hard to predict what most aspects of the resulting multiagent system's macroscopic phenomenology would be like at a glance of the microscopic interaction rule. The recently proposed concept of decomposing such interactions as superpositions of four fundamental interaction types (self- and cross-dependent, coordination-type, and cyclic-dominance components) could potentially help bridge that gap by providing an excellent framework for the investigation of the interplay

effects between these elementary game components, as well as the systematic exploration and classification of matrix games.

The overarching aim of the ongoing research work reported in this thesis is to lay a foundation for this analysis of the matrix game decomposition concept. After brief reviews concerning the anatomy of two-player matrix games in Chapter 2 and their relevance to statistical physics in Chapter 3, the thesis discusses the properties of a handful of multiagent logit-rule-driven potential matrix games that are composed of just a few elementary games in simple combinations. Chapters 4 and 5 deal with the elementary coordination game, the simplest nontrivial potential game, and its extensions with two types of self-dependent components, one that preserves and one that explicitly breaks the symmetry of the coordination; while Chapters 6 and 7 are about games composed of multiple elementary coordinations, a highly symmetric combination in the former and in a configuration geared towards competition between different components in the latter.

How coordination—and cooperation in particular—emerges and how it is sustained are among the central questions of game theory [17–20]. The game models treated in this thesis also contribute to these questions, as they all possess phase transitions between disordered states stable at high logit noise levels and coordinated ordered states stable at lower noise levels. On closer inspection, it turns out that the continuous Ising-type transition characteristic of the few-strategy elementary coordination game is robust and can be observed in the other, composite models as well, under appropriate circumstances. Deviations from this behavior seem to be closely related to both elementary game composition and entropy effects. The more available strategies (or spin states in the physical analogy) there are in a system, the higher the entropy of the disordered phase becomes, which expands the stability region of the disordered phase, and drives systems towards first-order transitions (Chapters 4 and 5). The universality class of the transition can also be changed by the presence of a strong higher-symmetry combination of elementary coordinations (Chapter 6), though the Ising-type phase associated with an otherwise weaker competing elementary coordination may still gain stability at the order-disorder transition due to its higher entropy content (Chapter 7) leading to a social trap situation and also introducing a first-order transition between the competing ordered phases.

Chapter 2

The anatomy of matrix games

2.1 Matrix Games

The following sections introduce some of the basic concepts of game theory. For in depth and more general discussions of the subject, we refer the reader to textbooks and reviews by von Neumann and Morgenstern [21], Karlin [22], Vorob'ev [23], Szép and Forgó [24], Fudenberg and Tirole [25], Gibbons [26], Osborne and Rubinstein [27], Weibull [28], Hofbauer and Sigmund [29], Samuelson [30], Cressman [31], Szabó and Fáth [32], Gintis [33], Sandholm [34], Sigmund [35], and Szabó and Borsos [36].

The normal or strategic form of a noncooperative game represents only its most important aspects by interpreting it as a single decision situation. Each player $x \in \{1, \ldots, N\}$ chooses independently and simultaneously one of her available pure strategies $s_x \in S_x$ that defines her complete sequence of actions throughout the game. The set of chosen actions, also called the strategy profile, $\mathbf{s} = \{s_1, \ldots, s_N\}$ determines the outcome of the game from which player x derives utility according to the payoff function $u_x(\mathbf{s})$. Usually players are assumed to be rational, and they intend to maximize their own payoff.

If there are only $N = 2$ players, and they both have a finite number of discrete strategies $S_1 = \{\sigma_1, \ldots, \sigma_n\}$ and $S_2 = \{\tau_1, \ldots, \tau_m\}$, then the possible payoff pairs can be conveniently arranged into a so-called bimatrix:

$$\mathbf{G} = (\mathbf{A}, \mathbf{B}^T) = \begin{pmatrix} (A_{11}, B_{11}^T) & \cdots & (A_{1m}, B_{1m}^T) \\ \vdots & \ddots & \vdots \\ (A_{n1}, B_{n1}^T) & \cdots & (A_{nm}, B_{nm}^T) \end{pmatrix}, \tag{2.1}$$

where $\mathbf{A}$ and $\mathbf{B}$ are the payoff matrices of the first player (the row player) and the second player (the column player), respectively, and their elements are defined through

$A_{ij} = u_i(\{\sigma_i, \tau_j\})$ and $B_{ji} = B^T_{ij} = u_j(\{\sigma_i, \tau_j\})$. (Here, $\mathbf{B}^T$ is the transpose of $\mathbf{B}$.) This notation is further simplified if the strategies are represented by Cartesian unit vectors:

$$\sigma_1 \equiv \mathbf{s}_1 = \begin{pmatrix} 1 \\ 0 \\ 0 \\ \vdots \\ 0 \\ 0 \end{pmatrix}, \qquad \sigma_2 \equiv \mathbf{s}_2 = \begin{pmatrix} 0 \\ 1 \\ 0 \\ \vdots \\ 0 \\ 0 \end{pmatrix}, \quad \ldots, \qquad \sigma_n \equiv \mathbf{s}_n = \begin{pmatrix} 0 \\ 0 \\ 0 \\ \vdots \\ 0 \\ 1 \end{pmatrix} \in \mathbb{R}^n, \tag{2.2}$$

$$\tau_1 \equiv \mathbf{t}_1 = \begin{pmatrix} 1 \\ 0 \\ 0 \\ \vdots \\ 0 \\ 0 \end{pmatrix}, \qquad \tau_2 \equiv \mathbf{t}_2 = \begin{pmatrix} 0 \\ 1 \\ 0 \\ \vdots \\ 0 \\ 0 \end{pmatrix}, \quad \ldots, \qquad \tau_m \equiv \mathbf{t}_m = \begin{pmatrix} 0 \\ 0 \\ 0 \\ \vdots \\ 0 \\ 1 \end{pmatrix} \in \mathbb{R}^m. \tag{2.3}$$

In this case the utilities of the players can simply be written in the following way as the result of consecutive matrix-vector and scalar products:

$$u_1(\{\mathbf{s}_i, \mathbf{t}_j\}) = \mathbf{s}_i \cdot \mathbf{A}\mathbf{t}_j, \tag{2.4}$$

$$u_2(\{\mathbf{s}_i, \mathbf{t}_j\}) = \mathbf{t}_j \cdot \mathbf{B}\mathbf{s}_i. \tag{2.5}$$

If the two players are identical, that is, they share the same strategy set ($S_1 = S_2$) and have identical payoff matrices ($\mathbf{A} = \mathbf{B}$), then the game is called symmetric. In the following, we will refer to such games, which are obviously completely defined by a single payoff matrix, simply as matrix games.

As mentioned earlier, all players aim to optimize their utility, but this task can easily become very complicated because of their conflicting interests that may prevent players from simultaneously realizing their maximal possible payoffs. Nash's equilibrium concept [37, 38] offers a minimal solution to this problem: In a Nash equilibrium no player can increase her utility as a result of a unilateral strategy change. This means that the strategy profile $s^* = (s_1^*, \ldots, s_n^*)$ is a Nash equilibrium[1] if it satisfies

$$u_x(s_x^*, s_{-x}^*) \geq u_x(s_x, s_{-x}^*) \qquad \forall x \in \{1, \ldots, N\},\ \forall s_x \neq s_x^*, \tag{2.6}$$

[1] More precisely, this is the definition of a pure (or pure strategy) Nash equilibrium, as opposed to a mixed strategy Nash equilibrium. A mixed strategy is a probability distribution over the strategies available to the players according to which a player randomly picks her strategy. In a mixed strategy Nash equilibrium no player can increase her expected utility by unilaterally switching to another mixed strategy. In this thesis, we are only interested in pure strategies and pure Nash equilibria.

where $s_{-x} = (s_1, \ldots, s_{x-1}, s_{x+1}, \ldots, s_N)$ denotes the strategy profile of player x's co-players.

2.1.1 Prisoner's dilemma

The most popular example of a matrix game is probably the prisoner's dilemma, devised by Merrill Flood and Melvin Dresher, but cast in its dilemma tale form by Albert W. Tucker [17, 39, 40]. Two prisoners are charged with committing the same crime, and held separately. The prosecutors are confident that the criminals would be sentenced to a year in prison for a lesser charge but lack sufficient evidence to convict them on the principal charge. They offer each prisoner the same bargain: If he testifies against his partner, he will be released while his partner will serve three years in prison for the main charge. However, should they both decide to turn state's evidence, both of them will be sentenced to two years in jail. The prisoners know that they were both offered the same deal and are not allowed to communicate before making their decision. The corresponding payoff matrix reads:

$$\mathbf{A}^{(\mathrm{PD})} = \begin{pmatrix} -1 & -3 \\ 0 & -2 \end{pmatrix}, \tag{2.7}$$

where the first strategy is refusing to testify, and the second is betrayal. Clearly, choosing to testify results in a shorter sentence, regardless of the other prisoner's choice. Therefore, if both prisoners are rational, they will mutually defect and testify against their partner in crime (this is a Nash equilibrium), and as a result both will be sentenced to two years in jail. The prisoners' dilemma lies in the fact that both prisoners would receive a shorter sentence if they cooperated and refused to testify.

2.1.2 Potential games

In general normal-form games each player has her own utility function she aims to maximize through her choice of strategy. In the special subset of so-called potential games [36, 41], however, there exists a single function, the game's potential, which contains all payoff changes any player may achieve by unilaterally switching her strategy. In particular, a game is a potential game, if it admits a potential $V(\mathbf{s})$ such that

$$V(s'_x; s_{-x}) - V(s_x; s_{-x}) = u_x(s'_x; s_{-x}) - u_x(s_x; s_{-x}) \tag{2.8}$$

for every $x \in \{1, \ldots, N\}$, every $s_x, s'_x \in S_x$, and every $s_{-x} \in \prod_{y \neq x} S_y$. A game's potential, if it exists, is unique up to an additive constant. An important property of

the potential is that it attains its maximal value where the original game has a preferred pure Nash equilibrium. For matrix games the potential can also admit a similar bilinear matrix form, and can be evaluated quite easily, as we will see later on.

The utility changes that figure into the definition of the potential can be tracked using a so-called dynamical graph whose nodes and edges represent strategy profiles and unilateral strategy changes, respectively. Monderer and Shapley have shown [41] that a normal-form game admits a potential if and only if the sum of the utility changes of deviators equals zero along any four-edge (and consequently any longer) loops (closed paths) of its dynamical graph. If the edges of the graph are directed in such a way as to point toward nodes with higher potentials, then finding pure Nash equilibria reduces to finding nodes that only have incoming edges. If the directed dynamical graph (flow graph) has any directed loops, then along this loop the sum of the payoff changes realized by each unique deviator is strictly positive, which means that the game does not admit a potential.

For example, the previously mentioned prisoner's dilemma game is a potential game. Its potential matrix (up to an additive constant matrix) is

$$\mathbf{V}^{(\mathrm{PD})} = \begin{pmatrix} -2 & -1 \\ -1 & 0 \end{pmatrix}, \tag{2.9}$$

whose maximal element 0 is attained when both players defect, and this is indeed the game's only Nash equilibrium, as we have seen earlier.

2.2 Decomposition of matrix games

A general two-player, n-strategy matrix game is defined by n^2 independent parameters, the elements of its payoff matrix. Yet, it can be easily shown that not all different parametrizations result in different games. For example, the prisoner's dilemma introduced in Subsection 2.1.1 is clearly not changed by switching the order of the strategies, and considering defection as the first and cooperation as the second strategy, and yet its payoff matrix becomes different from the one in Eq. (2.7), namely,

$$\mathbf{A}_{*}^{(\mathrm{PD})} = \begin{pmatrix} -2 & 0 \\ -3 & -1 \end{pmatrix}. \tag{2.10}$$

Shifting all payoffs by the same constant amount may change the framing of the game, but keeps many of the game's most important properties intact. For instance, consider

the payoff matrix

$$\mathbf{A}^{(\mathrm{DG})} = \begin{pmatrix} 1 & -1 \\ 2 & 0 \end{pmatrix}, \tag{2.11}$$

where all payoffs are 2 higher than the corresponding payoffs in Eq. (2.7). This payoff matrix defines a so-called donation game [35]. There are two players who may choose to either cooperate and provide a benefit worth 2 units of payoff at a personal cost of 1 unit of payoff, or defect and offer nothing. (Again, cooperation is the first, and defection is the second strategy.) Because of the uniform shifting of the payoffs, payoff differences remain the same as in the prisoner's dilemma, so the Nash equilibrium and the potential derived from these differences are also carried over.

Similarly, multiplying the payoffs by the same positive number can be thought of as changing the unit payoffs are measured in, which affects payoff differences and the potential in the same way. The Nash equilibria, however, are unchanged, because the multiplication of payoffs does not change their order.

These simple examples point toward the possibility of arranging matrix games into classes based on the similarity of their behavior and characteristics. The concept of linear payoff matrix decomposition provides such a classification scheme and gives rise to an anatomy of games that views complex general games as combinations of simple building blocks and their emergent properties as the manifestation of the interplay between these building blocks.

At the center of this idea lies the fact that the space of $n \times n$ real matrices is a vector space of n^2 dimensions and, as such, its elements can be expanded as linear combinations of basis matrices. It is the choice of this basis set that gives meaning to the decomposition. The simplest basis choice in essence follows the defining construction of the payoff matrix and singles out individual strategy pairings as elementary game components. This decomposition scheme resolves a general two-strategy game in the following way:

$$\mathbf{A} = \begin{pmatrix} A_{11} & A_{12} \\ A_{21} & A_{22} \end{pmatrix} = A_{11} \begin{pmatrix} 1 & 0 \\ 0 & 0 \end{pmatrix} + A_{12} \begin{pmatrix} 0 & 1 \\ 0 & 0 \end{pmatrix} + A_{21} \begin{pmatrix} 0 & 0 \\ 1 & 0 \end{pmatrix} + A_{22} \begin{pmatrix} 0 & 0 \\ 0 & 1 \end{pmatrix} \tag{2.12}$$

and can be straightforwardly generalized to higher strategy numbers. Although it is very easy to carry out this decomposition, and thus provides a clear illustration of the formal mathematical side of linear decomposition, it is hardly useful, as it offers no new insights into the properties of the game in question. The reason behind this is that individual strategy pairings in themselves are not intrinsically linked to any of the game properties of interest such as Nash equilibria and the existence of a potential.

In the following we introduce a basis set of $n \times n$ elementary matrices that lends itself to separating elementary games representing nonstrategic and proper player–player interactions, components that promote coordination or cause social dilemmas, or games that do and do not admit a potential. This decomposition scheme was developed by Szabó et al. in Refs. [36, 42–45]. Candogan et al. [46] and Hwang and Rey-Bellet [47, 48] take a different approach and arrive at a somewhat different decomposition without introducing a definite set of basis games.

2.2.1 The irrelevant elementary game

As we have said earlier, a uniform shifting of all payoffs does not change payoff differences and as a result does not significantly change the game's relevant properties. Our choice of the first elementary game reflects this by separating the game's average payoff from the remaining relevant part of the payoff matrix. The elements of this average payoff component are all equal to the arithmetic mean of the game's possible payoffs, that is,

$$A_{ij}^{(\mathrm{av})} = \mu = \frac{1}{n^2} \sum_{i,j} A_{ij}, \tag{2.13}$$

where the sum runs over all possible values of i and j, and A_{ij} is the payoff a player receives when playing strategy i against an opponent playing strategy j. μ can also be thought of as the strength of the irrelevant elementary game whose payoff matrix is the all-ones $n \times n$ matrix,

$$\mathbf{m}(n) = \begin{pmatrix} 1 & \cdots & 1 \\ \vdots & \ddots & \vdots \\ 1 & \cdots & 1 \end{pmatrix}. \tag{2.14}$$

The irrelevant elementary game is obviously a potential game with a constant potential.

2.2.2 Cross-dependent elementary games

Similar to the average payoff component, the so-called cross-dependent component of a game detaches the part of the payoff matrix that does not influence the incentives for an active player changing his or her strategy. In this sense, games that only differ in this part of their payoff are strategically equivalent. Such payoff changes are of the form $u(i', j) - u(i, j) = A_{i'j} - A_{ij}$, so for the elements of the cross-dependent component $A_{i'j}^{(\mathrm{cd})} = A_{ij}^{(\mathrm{cd})}$ holds for all $i, i', j \in \{1, \ldots, n\}$, which means that $\mathbf{A}^{(\mathrm{cd})}$ has the same entries in each of its columns. With the average payoff component in mind, let us define

the cross-dependent game component the following way:

$$A_{ij}^{(\mathrm{cd})} = \gamma_j = \frac{1}{n}\sum_i A_{ij} - \mu. \tag{2.15}$$

Here γ_j is the average deviation of a player's payoff from μ when playing against a j-strategist. To each coefficient γ_k belongs an elementary cross-dependent game with payoff matrix $\mathbf{g}(k;n)$. The k-th column of $\mathbf{g}(k;n)$ is filled with ones, while its remaining elements all equal zero:

$$\mathbf{g}(1;n) = \begin{pmatrix} 1 & 0 & \cdots & 0 \\ 1 & 0 & \cdots & 0 \\ \vdots & \vdots & \ddots & \vdots \\ 1 & 0 & \cdots & 0 \end{pmatrix}, \ldots, \ \mathbf{g}(n;n) = \begin{pmatrix} 0 & \cdots & 0 & 1 \\ 0 & \cdots & 0 & 1 \\ \vdots & \ddots & \vdots & \vdots \\ 0 & \cdots & 0 & 1 \end{pmatrix}. \tag{2.16}$$

Notice that the irrelevant elementary game is in fact a cross-dependent game, because

$$\mathbf{m}(n) = \sum_{k=1}^{n} \mathbf{g}(k;n), \tag{2.17}$$

which means that the irrelevant and the n cross-dependent elementary games are not linearly independent; however, any n of them are. This is also reflected by the γ_k expansion coefficients, which are also linearly dependent:

$$\sum_{k=1}^{n} \gamma_k = 0. \tag{2.18}$$

Thus the n cross-dependent elementary games and the irrelevant elementary game together only generate the space of cross-dependent payoff matrices, but do not form a basis set in this space, because they are not a minimal generator. As a result, expansions in terms of this set are not unique. One way to enforce uniqueness is to leave out one of the elementary games and use the remaining n that do form a basis set. As a downside, the aforementioned interpretation of the expansion coefficients as averages is lost. Conversely, the averages in Eq. (2.13) and Eq. (2.15) are by definition unique expansion coefficients in an $(n+1)$-element generator of the n-dimensional space of cross-dependent (including irrelevant) games. We can easily switch from this expansion to the other one by simply decomposing one of the elementary games in terms of the other n.

The cross-dependent game component also has a constant potential, because a player cannot change his or her cross-dependent payoff by simply switching to another strategy.

2.2.3 Self-dependent elementary games

Similar to the player's opponent being able to set part of the player's payoff through the cross-dependent component of the payoff matrix, the active player can also determine part of her payoff regardless of the opponent's choice of strategy. For such a game component we expect $u(i,j') - u(i,j) = 0$ to hold, which is satisfied for $A^{(\mathrm{sd})}_{ij'} = A^{(\mathrm{sd})}_{ij}$, that is, if the matrix has the same entries in each of its rows. Again with the average game component in mind, we can define a game's self-dependent component as

$$A^{(\mathrm{sd})}_{ij} = \varepsilon_i = \frac{1}{n}\sum_j A_{ij} - \mu, \tag{2.19}$$

where ε_i is the average deviation of a player's payoff from μ when playing strategy i. By definition these deviations satisfy

$$\sum_{k=1}^{n} \varepsilon_k = 0. \tag{2.20}$$

To each payoff ε_k we assign an elementary self-dependent game with payoff matrix $\mathbf{e}(k;n)$ whose entries equal one inside and zero outside its k-th row:

$$\mathbf{e}(1;n) = \begin{pmatrix} 1 & 1 & \cdots & 1 \\ 0 & 0 & \cdots & 0 \\ \vdots & \vdots & \ddots & \vdots \\ 0 & 0 & \cdots & 0 \end{pmatrix}, \ldots, \ \mathbf{e}(n;n) = \begin{pmatrix} 0 & 0 & \cdots & 0 \\ \vdots & \vdots & \ddots & \vdots \\ 0 & 0 & \cdots & 0 \\ 1 & 1 & \cdots & 1 \end{pmatrix}. \tag{2.21}$$

Notice that $\mathbf{e}^T(k;n) = \mathbf{g}(k;n)$.

Just like cross-dependent elementary games, self-dependent elementary games are also not linearly independent from the irrelevant elementary game, because

$$\mathbf{m}(n) = \sum_{k=1}^{n} \mathbf{e}(k;n). \tag{2.22}$$

This again raises the question of expansion uniqueness, which can again be solved by either dropping one of the $n+1$ self-dependent elementary games to get a basis, or imposing consistent rules like Eq. (2.13) and Eq. (2.19) on the expansion coefficients.

Elementary self-dependent games are potential games. The potential matrix of the k-th n-strategy elementary self-dependent game (up to an additive constant) can be written as

$$\mathbf{V}^{(\mathrm{sd})}(k;n) = \mathbf{e}(k;n) + \mathbf{e}^T(k;n) = \mathbf{e}(k;n) + \mathbf{g}(k;n), \tag{2.23}$$

or in matrix form as

$$\mathbf{V}^{(\mathrm{sd})}(1;n)=\begin{pmatrix}2&1&\cdots&1\\1&0&\cdots&0\\\vdots&\vdots&\ddots&\vdots\\1&0&\cdots&0\end{pmatrix},\ldots,\ \mathbf{V}^{(\mathrm{sd})}(n;n)=\begin{pmatrix}0&\cdots&0&1\\\vdots&\ddots&\vdots&\vdots\\0&\cdots&0&1\\1&\cdots&1&2\end{pmatrix}. \tag{2.24}$$

In a purely self-dependent game, both players choosing the strategy with the highest ε_k coefficient is a symmetric Nash equilibrium.

2.2.4 Elementary coordination games

After removing the irrelevant, cross-, and self-dependent components, the remaining game describes a proper player–player interaction where players cannot unilaterally set a nonzero average payoff for either of the players. Accordingly, the entries of the corresponding payoff matrix add up to zero in each of its rows and columns. It is worth further dividing this payoff matrix into its symmetric and antisymmetric parts. The symmetric part is the original game's coordination-type component,

$$\mathbf{A}^{(\mathrm{co})}=\frac{1}{2}\left[\left(\mathbf{A}-\mathbf{A}^{(\mathrm{av})}-\mathbf{A}^{(\mathrm{cd})}-\mathbf{A}^{(\mathrm{sd})}\right)+\left(\mathbf{A}-\mathbf{A}^{(\mathrm{av})}-\mathbf{A}^{(\mathrm{cd})}-\mathbf{A}^{(\mathrm{sd})}\right)^{T}\right]. \tag{2.25}$$

Due to its symmetry, the two players receive equal payoff from this component regardless of their choice of strategy. In general, the coordination-type component's payoff matrix is of the form

$$\mathbf{A}^{(\mathrm{co})}=\begin{pmatrix}\upsilon_1&-\nu_{12}&\cdots&-\nu_{1n}\\-\nu_{12}&\upsilon_2&\cdots&-\nu_{2n}\\\vdots&\vdots&\ddots&\vdots\\-\nu_{1n}&-\nu_{2n}&\cdots&\upsilon_n\end{pmatrix}, \tag{2.26}$$

where the rows and columns sum to zero, that is,

$$\upsilon_i=\sum_{j\neq i}\nu_{ij} \tag{2.27}$$

for all $i\in\{1,\ldots,n\}$ with $\nu_{ij}=\nu_{ji}$ if $i>j$.

To each of the $\binom{n}{2} = \frac{n(n-1)}{2}$ independent ν_{kl} $(k < l)$ parameters belongs an elementary coordination game $\mathbf{d}(k, l; n)$ whose entries are

$$d_{ij}(k,l;n) = \begin{cases} 1 & \text{for } i = j = k \\ 1 & \text{for } i = j = l \\ -1 & \text{for } i = k \text{ and } j = l \\ -1 & \text{for } i = l \text{ and } j = k \\ 0 & \text{otherwise.} \end{cases} \tag{2.28}$$

When players are restricted to pick either strategy k or strategy l, the game becomes the original coordination game that rewards players choosing the same strategy by giving one unit of payoff to both players and punishes anticoordinated behavior by deducting the same amount. The remaining $n-2$ strategies are neutral, in the sense that playing them provides zero payoff regardless of the opponent's strategy. These games are obviously linearly independent from each other and the elementary games mentioned earlier, and form a basis in the subspace of coordination-type games.

It is quite easy to check that elementary coordination games are potential games, and consequently their linear combinations, coordination-type games, are also potential games with $\mathbf{V}^{(\mathrm{co})} = \mathbf{A}^{(\mathrm{co})}$. As a result, a strategy profile that belongs to a maximal entry in the payoff matrix is a Nash equilibrium. (This is also true for local maxima with respect to unilateral strategy changes, but global maxima usually correspond to preferred Nash equilibria.) The maximal $A_{ij}^{(\mathrm{co})}$ value may be one of the diagonal elements v_k, in which case both players follow the corresponding strategy in the preferred Nash equilibrium. On the other hand, if the maximal payoff $\max(A_{ij}) = -\nu_{kl}$ is in an off-diagonal position, then in the corresponding Nash equilibrium strategy choices are anticoordinated, one of the players plays strategy k while the other follows strategy l, or vice versa.

2.2.5 Elementary cyclic dominance games

The antisymmetric part of the player–player interaction part of a payoff matrix is

$$\mathbf{A}^{(\mathrm{cy})} = \frac{1}{2}\left[\left(\mathbf{A} - \mathbf{A}^{(\mathrm{av})} - \mathbf{A}^{(\mathrm{cd})} - \mathbf{A}^{(\mathrm{sd})}\right) - \left(\mathbf{A} - \mathbf{A}^{(\mathrm{av})} - \mathbf{A}^{(\mathrm{cd})} - \mathbf{A}^{(\mathrm{sd})}\right)^{T}\right]. \tag{2.29}$$

in terms of the original payoff matrix and its mean-value (irrelevant, cross-, and self-dependent) components, and by this definition its row and column sums all equal zero.

This means that this so-called cyclic dominance component is of the general form

$$\mathbf{A}^{(\mathrm{cy})} = \begin{pmatrix} 0 & \xi_2 & \xi_3 & \cdots & \xi_n \\ -\xi_2 & 0 & \zeta_{23} & \cdots & \zeta_{2n} \\ -\xi_3 & -\zeta_{23} & 0 & \cdots & \zeta_{3n} \\ \vdots & \vdots & \vdots & \ddots & \vdots \\ -\xi_n & -\zeta_{2n} & -\zeta_{3n} & \cdots & 0 \end{pmatrix}, \tag{2.30}$$

and the parameters satisfy

$$\xi_i = -\sum_{j<i} \zeta_{ji} + \sum_{j'>i} \zeta_{ij'} \tag{2.31}$$

for all $i \in \{2, \ldots, n\}$, where $\zeta_{ij} = 0$ for $j \leq i$ or $j > n$ by definition. $\sum_i \xi_i = 0$ follows as a consequence. Notice that this game component can only be present if there are at least three available strategies.

The different ζ_{ij} parameters are linearly independent and completely determine the cyclic dominance component, so it is only sensible to think of these as expansion coefficients and choose the elementary games accordingly. Setting one of the ζ_{kl} to one and the rest to zero defines the following elementary payoff matrix:

$$C_{ij}(1,k,l;n) = \begin{cases} 1 & \text{for } i = 1 \text{ and } j = k \\ 1 & \text{for } i = k \text{ and } j = l \\ 1 & \text{for } i = l \text{ and } j = 1 \\ -1 & \text{for } j = 1 \text{ and } i = k \\ -1 & \text{for } j = k \text{ and } i = l \\ -1 & \text{for } j = l \text{ and } i = 1 \\ 0 & \text{otherwise.} \end{cases} \tag{2.32}$$

The corresponding game reduces to the rock-paper-scissors game, a zero-sum cyclic dominance game, if players are restricted to use only strategies 1,k, and l: strategy 1 dominates strategy k, strategy k dominates strategy l, and strategy l dominates strategy 1. The remaining strategies are neutral. These $\binom{n-1}{2} = \frac{(n-1)(n-2)}{2}$ elementary cyclic dominance games are linearly independent and span the space of cyclic dominance games.

It may seem somewhat surprising that this set is generated by the rock-paper-scissors games involving strategy 1, and suggests that strategy 1 somehow plays a special role. This just reflects the bias towards strategy 1 inherent in the parametrization used in Eq. (2.30). Of course, any other strategy could play the same role, and its elementary cyclic games could define a basis of the cyclic dominance subspace as well. A general

elementary cyclic dominance payoff matrix can be expanded as

$$\mathbf{C}(k,l,m;n) = \mathbf{C}(1,k,l;n) + \mathbf{C}(1,l,m;n) - \mathbf{C}(1,k,m;n), \tag{2.33}$$

where $1 < k < l < m \leq n$, and similar equations can be derived for bases defined by other strategies. Using this expression one of the elementary games of the basis set introduced in Eq. (2.32) can be replaced with $\mathbf{C}(k,l,m)$ and by repeating this step further bases can be generated. The main advantage of using a strategy-centered basis like the one in Eq. (2.32) is that it allows us to determine the expansion coefficients at a glance, without any further calculations. Nevertheless, choosing different bases may lead to simpler expansions into fewer terms in certain situations.

Cyclic dominance games do not admit a potential. Consider the general cyclic dominance game $\mathbf{A}^{(\mathrm{cy})}$ of Eq. (2.30) and strategy profile sequences of the form $(k,l) \to (k,m) \to (l,m) \to (l,l) \to (k,m)$ for all $k < l < m$ strategy labels. If this game is a potential game, then the payoff changes of deviating players add up to zero along each loop:

$$\begin{aligned}\left(-A^{(\mathrm{cy})}_{km} + A^{(\mathrm{cy})}_{kl}\right) + \left(A^{(\mathrm{cy})}_{lm} - A^{(\mathrm{cy})}_{km}\right) + \left(-A^{(\mathrm{cy})}_{ll} + A^{(\mathrm{cy})}_{lm}\right) + \left(A^{(\mathrm{cy})}_{kl} + A^{(\mathrm{cy})}_{ll}\right) = \\ = 2\left(A^{(\mathrm{cy})}_{kl} - A^{(\mathrm{cy})}_{km} + A^{(\mathrm{cy})}_{lm}\right) = 0.\end{aligned} \tag{2.34}$$

This gives two kinds of constraints on the parameters:

$$\zeta_{kl} - \zeta_{km} + \zeta_{lm} = 0 \text{ for } 1 = k < l < m \tag{2.35}$$

$$\xi_l - \xi_m + \zeta_{lm} = 0 \text{ for } 1 < k < l < m. \tag{2.36}$$

Plugging Eq. (2.31) into Eq. (2.36), rearranging the terms, and applying Eq. (2.35) yield

$$\begin{aligned}\xi_l - \xi_m + \zeta_{lm} &= \zeta_{lm} - \sum_{i<l}\zeta_{il} + \sum_{i'>l}\zeta_{li'} + \sum_{j<m}\zeta_{jm} - \sum_{j'>m}\zeta_{mj'} = \\ &= \zeta_{lm} + \sum_{i<l}(\zeta_{im} - \zeta_{il}) + \sum_{l\leq j<m}\zeta_{jm} + \sum_{l<i'\leq m}\zeta_{li'} + \sum_{j'>m}\left(\zeta_{lj'} - \zeta_{mj'}\right) = \\ &= \zeta_{lm} + \sum_{i<l}\zeta_{lm} + \zeta_{lm} + \sum_{l<j<m}(\zeta_{jm} + \zeta_{lj}) + \zeta_{lm} + \sum_{j'>m}\zeta_{lm} = \\ &= \zeta_{lm} + \sum_{i<l}\zeta_{lm} + \zeta_{lm} + \sum_{l<j<m}(\zeta_{lm}) + \zeta_{lm} + \sum_{j'>m}\zeta_{lm} = n\zeta_{lm} = 0.\end{aligned} \tag{2.37}$$

Thus, a general cyclic dominance game can only be a potential game if $\zeta_{lm} = 0$ for all $1 < l < m \leq n$, but that is a contradiction, because for a proper cyclic dominance game at least one of the ζ_{lm} has to be nonzero. As a consequence, the presence of the cyclic dominance component in a matrix game's decomposition precludes the game form having a potential.

2.2.6 Elementary external benefit and hierarchical games

Setting apart the symmetric and antisymmetric parts of the mean-value component of a game can also offer new insights into its properties. The symmetric part reads

$$\mathbf{A}^{(\mathrm{mvs})} = \frac{1}{2}\left[\left(\mathbf{A}^{(\mathrm{av})} + \mathbf{A}^{(\mathrm{cd})} + \mathbf{A}^{(\mathrm{sd})}\right) + \left(\mathbf{A}^{(\mathrm{av})} + \mathbf{A}^{(\mathrm{cd})} + \mathbf{A}^{(\mathrm{sd})}\right)^{T}\right], \tag{2.38}$$

which in terms of the previously introduced elementary payoff matrices becomes

$$\mathbf{A}^{(\mathrm{mvs})} = \mu\mathbf{m}(n) + \sum_{k=1}^{n} \frac{\varepsilon_k + \gamma_k}{2}\left[\mathbf{e}(k;n) + \mathbf{g}(k;n)\right], \tag{2.39}$$

because $\mathbf{e}^T(k;n) = \mathbf{g}(k;n)$. In the following, we will call the sum appearing beside the average game component $\mu\mathbf{m}(n)$ the external benefit component of the game and denote it by $\mathbf{A}^{(\mathrm{ex})}$. We can also introduce a matching set of elementary games and expansion coefficients for each term of the sum, namely,

$$\mathbf{f}(k;n) = \mathbf{e}(k;n) + \mathbf{g}(k;n) \qquad \text{and} \qquad \varphi_k = \frac{\varepsilon_k + \gamma_k}{2}. \tag{2.40}$$

Notice that the k-th elementary external benefit game's payoff matrix is identical to the potential matrix $\mathbf{V}^{(\mathrm{sd})}(k;n)$ of Eq. (2.24). In a possible interpretation of the k-th elementary external benefit game an outside actor offers to evenly distribute among the two players payoff equal to twice the number of players following strategy k. Equivalently, we can think of φ_k as a measure of the average benefit the presence of a k-strategist provides to the community.

The antisymmetric part of the mean-value game is

$$\mathbf{A}^{(\mathrm{hi})} = \frac{1}{2}\left[\left(\mathbf{A}^{(\mathrm{av})} + \mathbf{A}^{(\mathrm{cd})} + \mathbf{A}^{(\mathrm{sd})}\right) - \left(\mathbf{A}^{(\mathrm{av})} + \mathbf{A}^{(\mathrm{cd})} + \mathbf{A}^{(\mathrm{sd})}\right)^{T}\right]. \tag{2.41}$$

Expanding the above in terms of self- and cross-dependent elementary games yields

$$\mathbf{A}^{(\mathrm{hi})} = \sum_{k=1}^{n} \frac{\varepsilon_k - \gamma_k}{2}\left[\mathbf{e}(k;n) - \mathbf{g}(k;n)\right] = \sum_{k=1}^{n} \chi_k \mathbf{h}(k;n), \tag{2.42}$$

where $\mathbf{h}(k;n) = \mathbf{e}(k;n) - \mathbf{g}(k;n)$ is the k-th elementary hierarchical game and χ_k is the corresponding expansion coefficient; in matrix form

$$\mathbf{h}(1;n) = \begin{pmatrix} 0 & 1 & \cdots & 1 \\ -1 & 0 & \cdots & 0 \\ \vdots & \vdots & \ddots & \vdots \\ -1 & 0 & \cdots & 0 \end{pmatrix}, \ldots, \ \mathbf{h}(n;n) = \begin{pmatrix} 0 & \cdots & 0 & -1 \\ \vdots & \ddots & \vdots & \vdots \\ 0 & \cdots & 0 & -1 \\ 1 & \cdots & 1 & 0 \end{pmatrix}. \tag{2.43}$$

The k-th elementary hierarchical game is a zero-sum game that describe situations where k-strategists can take one unit of payoff from players following other strategies. We can also think of it as a stick to the elementary external benefit game's carrot: Whereas the external benefit game attracts players toward choosing strategy k by promising an increased payoff for each member of the whole community, the hierarchical game does not directly reward k-strategists, but instead allows them to exploit players following other strategies.

In this sense the external benefit game represents an extreme version of Adam Smith's invisible hand concept, insofar as the self-interested player's interests coincide with the interests of the community. On the other hand, the hierarchical game acts more like the invisible hand of Atë, the goddess of mischief, delusion, ruin, and folly in Greek mythology; it promises a higher payoff at the expense of other players, but actually withholds this incentive once all players have been swayed. This effect can also lead to social dilemma situations when such a component is strong enough to guide players away from what would otherwise be a mutually beneficial strategy arrangement.

From the linearity of the potential under matrix composition, it follows that the k-th elementary external benefit and hierarchical games both share their potential with the k-th elementary self-dependent game, that is, $\mathbf{V}^{(\mathrm{ex})}(k;n) = \mathbf{V}^{(\mathrm{hi})}(k;n) = \mathbf{V}^{(\mathrm{sd})}(k;n)$ as defined in Eq. (2.24). As a result, both players choosing the strategy with the highest $\varphi_k + \chi_k$ is a symmetric Nash equilibrium in games made up of only external benefit and hierarchical components. Since both the φ_k and the χ_k coefficients add up to zero, the highest φ_k, χ_k, and $\varphi_k + \chi_k$ are all non-negative, but they do not necessarily belong to the same strategy.

2.2.7 Dimensions of interaction subspaces

Finally, let us briefly check that the construction described above does indeed define a game through n^2 independent parameters. The average payoff component is defined by a single number μ, so it contributes $\mathcal{N}^{(\mathrm{av})} = 1$ parameter. There are n elementary cross-dependent games, but only $\mathcal{N}^{(\mathrm{cd})} = n - 1$ of them are independent from the elementary irrelevant game. This also reflected by the fact that their expansion coefficients are linearly dependent, in particular,

$$\sum_{k=1}^{n} \gamma_k = 0. \tag{2.44}$$

Similarly, only $\mathcal{N}^{(\mathrm{sd})} = n - 1$ of the n elementary self-dependent elementary games are linearly independent, and the same is also true for their expansion coefficients, because

$$\sum_{k=1}^{n} \varepsilon_k = 0. \tag{2.45}$$

All elementary coordination-type games can be chosen independently when constructing a general game. The number of these components is the number of combinations of two strategies selected from all n strategies, which is $\mathcal{N}^{(\mathrm{co})} = \binom{n}{2} = \frac{n(n-1)}{2}$. When $n \geq 3$ strategies are available, there are a total of $\binom{n}{3}$ elementary cyclic dominance games, the number of ways three strategies can be selected without regard for their arrangement. However, only

$$\mathcal{N}^{(\mathrm{cy})} = \binom{n}{3} - \binom{n-1}{3} = \binom{n-1}{2} = \frac{(n-1)(n-2)}{2} \tag{2.46}$$

of these can be chosen linearly independently, because by Eq. (2.33) $\binom{n-1}{3}$ of these games can be expressed as the linear combination of three cyclic dominance games that belong to the same fixed strategy. Notice that accordingly $\mathcal{N}^{(\mathrm{cy})}$ is the number of two-strategy combinations of the $n - 1$ remaining strategies. In the $n = 2$ case there are no cyclic game components. In conclusion, the total number of independent game components and their corresponding expansion coefficients is

$$\begin{aligned} \mathcal{N} &= \mathcal{N}^{(\mathrm{av})} + \mathcal{N}^{(\mathrm{cd})} + \mathcal{N}^{(\mathrm{sd})} + \mathcal{N}^{(\mathrm{co})} + \mathcal{N}^{(\mathrm{cy})} = \\ &= 1 + (n-1) + (n-1) + \frac{n(n-1)}{2} + \frac{(n-1)(n-2)}{2} = n^2, \end{aligned} \tag{2.47}$$

which is exactly the number of the traditional payoff parameters.

2.3 Summary

This section gives a brief summary of the anatomy of matrix games based on the linear decomposition of payoff matrices presented in this chapter.

Two-player symmetric normal-form games are defined by their payoff matrices. If players can choose among n strategies, then the payoff matrix is an $n \times n$ matrix that tabulates the outcome of the game for each n^2 possible strategy pairings. The central idea behind the linear payoff matrix decomposition concept is that different parametrizations may be better suited to adequately characterize games. The decomposition scheme presented in this chapter considers games as superpositions of simple games that describe archetypical interaction situations. Alternative approaches can be geared more toward employing

basis sets with advantageous algebraic properties like orthogonality and normality, such as the Fourier decomposition approach [42] or the construction of basis sets as dyadic products [43], or identifying games with certain characteristic features.

In our decomposition scheme, games are made up of elementary games describing five distinct interaction types. Accordingly, we write a game's payoff matrix as a sum of five components in the following way

$$\mathbf{A} = \mathbf{A}^{(\mathrm{av})} + \mathbf{A}^{(\mathrm{cd})} + \mathbf{A}^{(\mathrm{sd})} + \mathbf{A}^{(\mathrm{co})} + \mathbf{A}^{(\mathrm{cy})}. \tag{2.48}$$

The first three terms together comprise the mean-value part of the game $\mathbf{A}^{(\mathrm{mv})}$, and each represent decision situations where at least one of the players has no control over the outcome of the game.

$$\mathbf{A}^{(\mathrm{mv})} = \mathbf{A}^{(\mathrm{av})} + \mathbf{A}^{(\mathrm{cd})} + \mathbf{A}^{(\mathrm{sd})} \tag{2.49}$$

The average payoff component $\mathbf{A}^{(\mathrm{av})}$ considers the mean value of possible payoffs μ as a baseline for the outcome of the game, the initial capital players start the game with. Its payoff matrix is proportional to the irrelevant elementary game $\mathbf{m}(n)$, which gives one unit of payoff to both players regardless of their choice of strategy.

$$\mathbf{A}^{(\mathrm{av})} = \mu \mathbf{m}(n) \qquad \text{with} \qquad \mu = \frac{1}{n^2} \sum_{ij} A_{ij} \tag{2.50}$$

The cross-dependent payoff component $\mathbf{A}^{(\mathrm{cd})}$ establishes similar baselines for playing against each strategy by columnwise detaching the mean signed deviation of payoffs γ_k from the average payoff μ. This part of a player's payoff is solely defined by her opponent's chosen strategy. The cross-dependent component is the linear combination of elementary cross-dependent games $\mathbf{g}(k;n)$.

$$\mathbf{A}^{(\mathrm{cd})} = \sum_{k=1}^{n} \gamma_k \mathbf{g}(k;n) \qquad \text{with} \qquad \gamma_k = \frac{1}{n} \sum_{i} A_{ik} - \mu \tag{2.51}$$

The final mean-value-type component, $\mathbf{A}^{(\mathrm{sd})}$, is called the self-dependent component of the game. It accounts for partial payoffs that can be earned regardless of the opponent's strategy. The corresponding payoff matrix is the linear combination of the elementary self-dependent payoff matrices $\mathbf{e}(k;n)$ with coefficients ε_k, which are the row-wise mean

signed payoff deviations from the average payoff μ.

$$\mathbf{A}^{(\mathrm{sd})} = \sum_{k=1}^{n} \varepsilon_k \mathbf{e}(k;n) \qquad \text{with} \qquad \varepsilon_k = \frac{1}{n}\sum_j A_{kj} - \mu \tag{2.52}$$

Alternatively, the mean-value component can also be divided into its symmetric and antisymmetric parts to separate social and private interests.

$$\mathbf{A}^{(\mathrm{mv})} = \mathbf{A}^{(\mathrm{mvs})} + \mathbf{A}^{(\mathrm{hi})} \tag{2.53}$$

The symmetric part can be further split up into the average payoff component $\mathbf{A}^{(\mathrm{av})}$ and the external benefit component $\mathbf{A}^{(\mathrm{ex})}$.

$$\mathbf{A}^{(\mathrm{mvs})} = \mathbf{A}^{(\mathrm{av})} + \mathbf{A}^{(\mathrm{ex})} \tag{2.54}$$

The external benefit component combines elementary games $\mathbf{f}(k;n)$ in which both players receive φ_k payoff for each player following strategy k. Thus these games incentivize choosing their corresponding strategy only at the community level and equate community- and self-interest.

$$\mathbf{A}^{(\mathrm{ex})} = \sum_{k=1}^{n} \varphi_k \mathbf{f}(k;n) \qquad \text{with} \qquad \varphi_k = \frac{\varepsilon_k + \gamma_k}{2} \tag{2.55}$$

The antisymmetric part of the mean-value component $\mathbf{A}^{(\mathrm{hi})}$ is composed of elementary hierarchical games $\mathbf{h}(k;n)$ that also promote playing strategy k but instead of rewarding both players it allows k-strategists to exploit other players and directly take χ_k payoff away from them. These games, as opposed to external benefit games, incentivize following one of the strategies at the individual level without any benefit to the community as a whole.

$$\mathbf{A}^{(\mathrm{hi})} = \sum_{k=1}^{n} \chi_k \mathbf{h}(k;n) \qquad \text{with} \qquad \chi_k = \frac{\varepsilon_k - \gamma_k}{2} \tag{2.56}$$

The remainder of the payoff matrix, $\mathbf{A}^{(\mathrm{pp})}$, describes pure player–player interactions, in which both players have an equal influence on the outcome.

$$\mathbf{A}^{(\mathrm{pp})} = \mathbf{A}^{(\mathrm{co})} + \mathbf{A}^{(\mathrm{cy})} \tag{2.57}$$

The coordination-type component $\mathbf{A}^{(\mathrm{co})}$ is the symmetric part of pure player–player interactions, and it is composed of elementary coordinations $\mathbf{d}(k,l;n)$ between each

distinct strategy pair (k,l) with strength ν_{kl}. The corresponding payoff matrix is symmetric, and its entries add up to zero in each of its rows and columns.

$$\mathbf{A}^{(\mathrm{co})} = \sum_{1\le k<l\le n} \nu_{kl}\mathbf{d}(k,l;n) \qquad \text{with} \qquad \nu_{kl} = -\frac{1}{2}\left[A_{kl}^{(\mathrm{pp})} + A_{lk}^{(\mathrm{pp})}\right] \tag{2.58}$$

Last but not least, the cyclic dominance game component $\mathbf{A}^{(\mathrm{cy})}$ is given by the anti-symmetric part of $\mathbf{A}^{(\mathrm{pp})}$. It can easily be expanded in terms of the elementary cyclic dominance games $\mathbf{C}(1,k,l;n)$ of strategy 1. In this case the expansion coefficient are simply the appropriate entries of the payoff matrix component $\mathbf{A}^{(\mathrm{cy})}$. (The remaining elementary cyclic dominance games could be also be used instead with different expansion coefficients.) The cyclic dominance game component can only be present in games with at least three available strategies.

$$\mathbf{A}^{(\mathrm{cy})} = \sum_{1<k<l\le n} \zeta_{kl}\mathbf{C}(1,k,l;n) \qquad \text{with} \qquad \zeta_{kl} = \frac{1}{2}\left[A_{kl}^{(\mathrm{pp})} - A_{lk}^{(\mathrm{pp})}\right] \tag{2.59}$$

The only game component whose presence prevents the existence of a potential is the cyclic dominance component $\mathbf{A}^{(\mathrm{cy})}$. The potential of a game without such a component can simply be written as

$$\mathbf{V} = \mathbf{A}^{(\mathrm{sd})} + \left(\mathbf{A}^{(\mathrm{sd})}\right)^{T} + \mathbf{A}^{(\mathrm{co})} \tag{2.60}$$

in terms of its payoff matrix components, which means that potential games that only differ in their average or cross-dependent components have the same potential associated with them.

2.4 Examples

2.4.1 General two-strategy games

A general two-strategy matrix game is described by a general 2×2 payoff matrix that can be written as

$$\mathbf{A}^{(2\times 2)} = \begin{pmatrix} R & S \\ T & P \end{pmatrix}. \tag{2.61}$$

In the language traditionally employed in the study of social dilemma situations [35, 49, 50] (including the prisoner's dilemma of Sec. 2.1.1), R is the players' reward for mutual cooperation, T is the temptation to defect, S is the betrayed sucker's payoff, and P is the punishment for mutual defection. This interpretation is best suited to describe a

prisoner's dilemma, in which these payoffs are ordered such that $T > R > P > S$, but becomes less fitting in other situations, as we will later see.

The decomposition of the payoff matrix [36, 45] yields

$$\begin{aligned}\mathbf{A}^{(2\times 2)} =& \frac{R+T+S+P}{4}\mathbf{m}(2) + \frac{R-P}{4}\left[\mathbf{f}(1;2) - \mathbf{f}(2;2)\right] + \\ &+ \frac{S-T}{4}\left[\mathbf{h}(1;2) - \mathbf{h}(2;2)\right] + \frac{R+P-S-T}{4}\mathbf{d}(1,2;2).\end{aligned} \tag{2.62}$$

This result tells us that R promotes coordination in general through $\mathbf{d}(1,2;2)$ and coordination on strategy 1 in particular through $\mathbf{f}(1;2)$ but also discourages coordination on strategy 2 through $\mathbf{f}(2;2)$, assuming $R > 0$. P plays a similar role but prefers defection instead of cooperation. S supports anticoordination, but conversely also drives players towards coordination on strategy 1 in a hierarchical way through $\mathbf{h}(1;2)$ while suppressing coordination on strategy 2 through $\mathbf{h}(2;2)$. T acts in a very similar way but changes the roles of the strategies.

All two-strategy matrix games are potential games, because of the lack of 2×2 cyclic dominance payoff matrices. From the decomposition Eq. (2.62) one can straightforwardly determine the game's potential matrix, which up to an additive constant is given by the matrix

$$\mathbf{V}^{(2\times 2)} = \begin{pmatrix} R-T & 0 \\ 0 & P-S \end{pmatrix}. \tag{2.63}$$

Local maxima (locality here is meant row- and columnwise) correspond to the pure Nash equilibria of the game. Based on the structure of the potential matrix, we can distinguish four game classes with different Nash equilibrium sets [45].

In the first case, mutually choosing strategy 1 is the game's only Nash equilibrium, and the payoff parameters fulfill the condition $R - T > 0 > P - S$, which is equivalent to both $R > T$ and $S > P$ being true. Similarly, coordination on strategy 2 becomes the sole Nash equilibrium if $T > R$ and $P > S$. In fact, these two game classes can easily be transformed into each other by simply switching the labels of the strategies, so in the following we will assume $R > P$ without any loss of generality. Notice, however, that the game having only one Nash equilibrium does not necessarily mean that players could not possibly achieve higher payoffs by switching their strategies to the other non-Nash equilibrium coordinated strategy profile. If the coordinated Nash equilibrium has the higher payoff (i.e., $R > T$ and $S > P$ and $R > P$), then the game is called a harmony game. On the other hand, when the Nash equilibrium and the higher payoff coordinated strategy profile do not coincide (i.e., $T > R > P > S$), the players face the prisoner's dilemma. In this case, the hierarchical game components are stronger and prefer a different coordinated strategy arrangement than their external benefit counterparts. It

is worth mentioning that if $T + S$ is higher than $2R$, then the players can achieve the highest per capita average payoff by following an anticoordinated strategy arrangement in both the harmony and prisoner's dilemma games. In a single shot game this gives one of the players less payoff than the Nash equilibrium coordinated strategy profile would. In a repeated game, however, the players gain the highest total payoff by alternately playing strategies $(1, 2)$ and $(2, 1)$.

The two coordinated strategy profiles can also both be Nash equilibria at the same time if $R > T$ and $P > S$. This is called a stag hunt game based on a story described by Jean-Jacques Rousseau in his Discourse on Inequality [51]. Two hunters can individually choose to hunt a stag or a hare. They can both surely catch a hare by themselves, but have to work together in order to successfully take a stag. Of course, the stag, even when shared, is worth more than the hare. We may again assume $R > P$ without any loss of generality, thus designating hunting stag strategy 1 and hunting hare strategy 2. T accounts for the difference between hunting for hare alone or in competition. S is the lone stag hunter's payoff. The payoff dominant Nash equilibrium, hunting stag together does not necessarily have the highest potential, and other equilibrium selection criteria (e.g., risk dominance) may also prefer hunting hare.

Finally, when $T > R$ and $S > P$, the two anticoordinated strategy profiles are the game's two pure Nash equilibria. This is characteristic of hawk–dove games [16, 52]. (This game is also known as the snowdrift game [53] or the chicken game [15, 35].) The two players contest a valuable resource and in doing so can employ one of two strategies. 'Hawk' strategists (in our case strategy 2) are aggressive and willing to fight over the resource, while 'doves' are peaceful. As a result, hawks will scare off doves and take the resource worth T. We denote the dove's payoff by S. Two doves, on the other hand, will divide the resource and both take shares worth $R < T$. A hawk confronting another hawk will either win and take the resource or lose and sustain severe injuries in the fight, and thus on average stands to gain $P < S$ amount of payoff. We may further assume without any loss of generality that $R > P$, or exchange the labels of the two strategies otherwise. Even though the two anticoordinated Nash equilibria have equal potential they do not provide equal payoffs to the two players, one of them will earn more than the other.

Figure 2.1 puts the above classification in a nutshell [45]. Dashed lines separate the four quadrants of the parameter space with differing Nash equilibria: the prisoner's dilemma region (PD quadrant), the hawk–dove region (HD quadrant), the harmony game region (H quadrant), and the stag hunt region (SH quadrant). The smileys indicate the structure of the game's Nash equilibria, white and black smileys correspond to players following strategy 1 and strategy 2, respectively. If the faces are next to each other, the

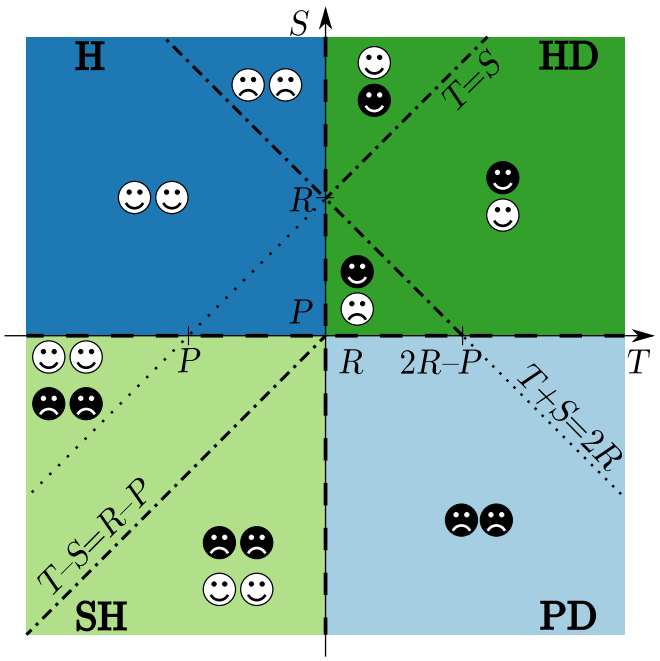

FIGURE 2.1. Classification of 2×2 matrix games based on their pure Nash equilibria and player contentment when $R > P$ is assumed. For a detailed explanation of the used notations, see the main text on page 22. This is the slightly modified version of a figure that originally appeared in Ref. [45].

players receive equal payoffs (like in the PD and H quadrants), the better performing strategy is drawn above the other one otherwise (e.g., in the hawk-dove game). If there are multiple different Nash equilibria, the one with the higher potential is drawn above the other, as in the stag hunt game case. A face smiles when it represents a 'content' player, that is, someone who receives more payoff than his opponent, or when at least the equilibrium provides the two players with the possible highest total payoff, or in other words, when at least their community as a whole is the best off it can be. In the figure, dash-dotted lines indicate changes in player contentment within game classes; the lines are dotted where no such change occurs. Across the $T - S = R - P$ line, different strategy profiles maximize the potential, causing a change in contentment if higher potential strategy arrangements are preferred. Above the $T + S = 2R$ line anti-coordination provides the highest total payoff and thus coordination leads to discontent. Along the $T = S$ line the hierarchical components vanish; below it external benefit and hierarchical components both benefit strategy 1; above it they push players in opposite directions: external benefit components still promote choosing strategy 1, but the hierarchical components prefer picking strategy 2.

Unhappy faces point to social dilemmas where individual interests represented by Nash equilibria and the value of the potential clash with societal interests represented by the total payoff of the two players. In all four game classes, we can identify some kind of a social dilemma in Figure 2.1. In the harmony game the social dilemma arises

when the coordination component of the game actually describes anticoordination. In a hawk–dove game, however, the opposite is true; the dilemma is caused by the presence of a proper coordination component with positive strength. The prisoner's dilemma is always a social dilemma situation, because the hierarchical component of the game is stronger than its external benefit component and the two components incentivize choosing different strategies. The stag hunt game does not inherently pose a social dilemma, because it always has a payoff dominant Nash equilibrium. In this case the concurrence of two Nash equilibria is what can cause the dilemma. Certain solution concepts (also called refinements of the Nash equilibrium in the literature) may favor the lower payoff Nash equilibrium. For example, as Figure 2.1 shows, the payoff dominant equilibrium does not necessarily have the highest potential.

2.4.2 Voluntary prisoner's dilemma

The voluntary prisoner's dilemma extends the usual prisoner's dilemma by giving players a third option, choosing not to take part in the game [54–56]. This third strategy is usally referred to as the loner strategy. If at least one of the two players picks the loner strategy, both players receive σ payoff. The game's payoff matrix then reads

$$\mathbf{A}^{(\mathrm{VPD})} = \begin{pmatrix} R & S & \sigma \\ T & P & \sigma \\ \sigma & \sigma & \sigma \end{pmatrix}. \tag{2.64}$$

The linear decomposition of the matrix [44] leads to the following expansion:

$$\begin{aligned} \mathbf{A}^{(\mathrm{VPD})} =& \frac{R+T+S+P+5\sigma}{9}\mathbf{m}(3)+ \\ &+\frac{S-T}{6}\left[\mathbf{h}(1;3)-\mathbf{h}(2;3)+\mathbf{C}(1,2,3;3)\right]+ \\ &+\frac{4R+T+S-2P-4\sigma}{18}\left[\mathbf{f}(1;3)+\mathbf{d}(1,3;3)\right]+ \\ &+\frac{4P+T+S-2R-4\sigma}{18}\left[\mathbf{f}(2;3)+\mathbf{d}(2,3;3)\right]+ \\ &+\frac{4P+4R-5S-5T+2\sigma}{18}\mathbf{d}(1,2;3)+\frac{4\sigma-R-T-S-P}{9}\mathbf{f}(3;3). \end{aligned} \tag{2.65}$$

Clearly, this game has a much richer elementary game content than the traditional prisoner's dilemma of the previous example. The shared game components are present with different expansion coefficients, and the new components involve the loner strategy in multiple different ways. Thus the decomposition of the matrix reveals that the loner strategy is far from being neutral. Beside having an external game component, it also shares a coordination component with both other strategies, and—perhaps more

importantly—a cyclic game component is introduced as well that prevents the existence of a potential in the voluntary prisoner's dilemma. Furthermore, this cyclic dominance component and the hierarchical components, which are responsible for the social dilemma aspect of the game, are inseparable in this game, as their strengths are proportional to each other. In an evolutionary game theoretic context, however, it is exactly this cyclic dominance component that maintains diversity and ensures the survival of cooperative behavior [32, 57, 58].

Chapter 3

Evolutionary potential games and statistical physics

Chapter 2 deals with the decomposition of single-shot two-player matrix games mostly within the confines of classical noncooperative game theory, where players are assumed to be individualistic, self-interested, pursuing well-defined preferences, rational, and also aware of the rationality of their opponents, their awareness of this awareness, and so on ad infinitum. Classical game theory, however, cannot give an adequate description of all decision situations. One such example is the backward induction paradox related to repeated social dilemmas, like the iterated prisoner's dilemma [17, 32, 33, 59]. In a finitely repeated social dilemma, classical game theory dictates that both players should play a subgame perfect Nash equilibrium, which requires the fulfilment of the equilibrium criterion for the remainder of the game at every stage. This includes the subgame that consists of the last iteration of the social dilemma, where players should definitely mutually defect as this is the single-shot game's sole Nash equilibrium. With the last game's outcome now fixed, it follows from the same argument that the players should do the same in the penultimate game as well, which in turn implies the same for the game before that, and then the one before that, and so on. In conclusion, this backward induction tells self-interested rational players to always defect in a finite iterated prisoner's dilemma. In spite of that, real people in real psychoeconomic experiments still do cooperate [40, 60, 61]. This means that real people are not as rational and well-informed as classical game theory demands them to be. Evolutionary game theory tries to extend the classical description toward bounded rationality by loosening the assumption of the players' decision making being perfectly rational. This puts a special emphasis on the dynamics of decision making, because players are no longer capable of immediately anticipating the decisions of their opponents. Typically we assume players to take a trial-and-error approach to figuring out an optimal strategy in this situation and try to

find dynamical strategy update rules that hopefully emulate the important aspects of real human behavior [32, 62]. The importance of population dynamics is clearly highlighted by the application of game theory to evolution as it naturally replaces utility with Darwinian fitness [16].

This chapter introduces one such update rule, the so-called logit rule. What makes the logit rule interesting is that it establishes a connection between the evolutionary game theory of potential matrix games and the classical spin models of statistical physics. In the following, we highlight the critical points of this correspondence and present some of the concepts and methods of statistical physics that can be employed in the study of potential matrix games whose strategy updates are controlled by the logit rule.

3.1 Spatial evolutionary matrix game models on lattices

In the following, we will consider spatial evolutionary game models of a specific structure: Players are located at the sites of a finite two-dimensional square lattice of $N = L \times L$ sites with periodic boundary conditions, so that all players have $z = 4$ nearest neighbors on the lattice. Neighboring players repeatedly and simultaneously play the same matrix game defined by the same $n \times n$ payoff matrix $\mathbf{A}$. In a single round of the game, the player at site x uses the same strategy, $\mathbf{s}_x$ against all z of her opponents. The players do not keep an account of their past winnings, they are only interested in their total payoff based on the games they play in a single round, which in the case of player x is

$$u_x(\mathbf{s}_x, \mathbf{s}_{-x}) = \sum_{\delta_x} \mathbf{s}_x \cdot \mathbf{A}\mathbf{s}_{x+\delta_x}, \tag{3.1}$$

where δ_x runs over the nearest neighbor sites of player x. After each round a randomly chosen player revises her strategy according to the so-called logit rule introduced in the next section.

This setup can of course be generalized in almost all of its aspects. The underlying square lattice can be replaced by lattices of different dimensionality and geometry [63–66], complex network structures [32, 67–71] with inhomogeneous coordination number distributions, or even adaptive networks [72, 73] that also evolve in time. The pair interaction games need not be symmetric [74–76] and can also vary from player to player [77, 78] or lose their matrix form altogether, for example, to accomodate games with a continuum of available strategies [79] or group interactions [80] that cannot be reduced to a sum of pair interactions. The strategy update rule that dictates the time evolution of the system can be changed as well [62, 81, 82].

3.1.1 The logit rule

The logit or log-linear rule [5, 83–85] is a probabilistic strategy update rule that assigns the following probability $w(\mathbf{s}_x \to \mathbf{s}'_x)$ to player x changing her strategy from $\mathbf{s}_x$ to $\mathbf{s}'_x$:

$$w(\mathbf{s}_x \to \mathbf{s}'_x) = \frac{\mathrm{e}^{u_x(\mathbf{s}'_x,\mathbf{s}_{-x})/K}}{\sum\limits_{\mathbf{s}''_x} \mathrm{e}^{u_x(\mathbf{s}''_x,\mathbf{s}_{-x})/K}}. \tag{3.2}$$

This formula exponentially favors choosing strategies that promise higher payoffs under the assumption that remaining players maintain their strategy choices, but takes into account the promised payoffs attenuated by the noise level parameter K.

This interpretation of K is justified by the asymptotic behavior of $w(\mathbf{s}_x \to \mathbf{s}'_x)$ in both the $K \to 0$ and $K \to \infty$ limits. Let

$$\hat{u}_x(\mathbf{s}_{-x}) = \max_{\mathbf{s}'_x} u_x(\mathbf{s}'_x, \mathbf{s}_{-x}) \tag{3.3}$$

denote the highest payoff player x can achieve in a fixed strategy environment $\mathbf{s}_{-x}$ and

$$\mathrm{BR}(\mathbf{s}_{-x}) = \left\{\mathbf{s}'_x \mid u_x(\mathbf{s}'_x, \mathbf{s}_{-x}) = \hat{u}_x(\mathbf{s}_{-x})\right\} \tag{3.4}$$

be the set of player x's best response strategies for which this maximal payoff obtains. Using these notations and expanding its numerator and denominator, we can reformulate $w(\mathbf{s}_x \to \mathbf{s}'_x)$ and evaluate its $K \to 0$ limit as

$$w(\mathbf{s}_x \to \mathbf{s}'_x) = \frac{\mathrm{e}^{[u_x(\mathbf{s}'_x,\mathbf{s}_{-x})-\hat{u}_x(\mathbf{s}_{-x})]/K}}{\sum\limits_{\mathbf{s}''_x} \mathrm{e}^{[u_x(\mathbf{s}''_x,\mathbf{s}_{-x})-\hat{u}_x(\mathbf{s}_{-x})]/K}} \xrightarrow[K\to 0]{} \begin{cases} \frac{1}{|\mathrm{BR}(\mathbf{s}_{-x})|} & \text{for } \mathbf{s}'_x \in \mathrm{BR}(\mathbf{s}_{-x}) \\ 0 & \text{otherwise.} \end{cases} \tag{3.5}$$

This means that when K vanishes, the logit rule becomes the best response update rule that randomly picks one of the strategies that provide the best payoff in a fixed strategy environment and thus emulates self-interested rational behavior.

On the other hand, in the opposite $K \to \infty$ limit the logit update probabilities are

$$w(\mathbf{s}_x \to \mathbf{s}'_x) \xrightarrow[K\to\infty]{} \frac{1}{n_x}, \tag{3.6}$$

where n_x is the total number of strategies available to player x. So for very high values of K the logit rule represents a completely uninformed strategy choice, an adequate unbiased action when all information regarding the game is drowned out by excessive noise.

The most important feature of the logit strategy update rule is that it drives potential game systems into a so-called Gibbs state [36, 83], a probability distribution over the space of strategy configurations, in which the probability $p(\mathbf{s})$ of finding the system in configuration $\mathbf{s}$ is given by

$$p(\mathbf{s}) = \frac{1}{Z} \mathrm{e}^{U(\mathbf{s})/K}. \tag{3.7}$$

Here $U(\mathbf{s})$ is the potential of the whole system derived from the potential $\mathbf{V}$ of the pair interaction matrix $\mathbf{A}$,

$$U(\mathbf{s}) = \frac{1}{2} \sum_{x} \sum_{\delta_x} \mathbf{s}_x \cdot \mathbf{V}\mathbf{s}_{x+\delta_x}, \tag{3.8}$$

and Z is simply a normalization factor given by a sum over all configurations

$$Z = \sum_{\mathbf{s}} \mathrm{e}^{U(\mathbf{s})/K}. \tag{3.9}$$

These Gibbs states are the only stationary distributions of the system, and they are also translation-invariant. Furthermore, the weak limit points of Gibbs state sequences along which $K \to 0$ are stationary distributions for the best-response strategy update rule and are concentrated on the pure strategy Nash equilibria of the multiplayer game [83].

3.1.2 Equivalence to classical spin models

Our evolutionary game model coincides with a general classical spin model described in the canonical ensemble [83, 86]. Individual players correspond to spins, and their strategies to spin states. The negative potential of the game plays the role of the spin system's Hamiltonian, since players aim to maximize their payoff, while in physics the energy of the system is minimized. In particular, coordination-type and external benefit game components correspond to spin–spin interactions and external magnetic fields, respectively. Hierarchical game components also contribute to the magnetic-field-like part of the potential, but they have no impact on the total payoff of the community due to their zero-sum property. The Gibbs state describing the game system's equilibrium is identical to the Boltzmann distribution used in statistical physics, the noise-level parameter K acts just like temperature, and the normalization factor Z is the partition function. All of the above correspondences hinge on the choice of the logit strategy update rule, which is essentially a version of the Glauber dynamics used in Monte Carlo simulations, and thus satisfies the detailed balance condition.

Consequently, the concepts and methods of statistical physics can also be applied to the spatial evolutionary game theoretic model introduced in Section 3.1. The next section

gives an overview of two such methods that can be used to explore the macroscopic behavior and properties of these model systems.

Models that fit the general spin model framework on the basis of similar analogies can be found in a diverse range of research topics beyond the statistical physical description of magnetism and game theoretic models, which includes, without any claim to comprehensiveness, lattice-gas models [87], the modeling of economies and financial markets [88–91], opinion dynamics [92–94], social segregation [95–97], spatial population dynamics in ecology [98], and disease propagation [99].

3.2 Methods

3.2.1 Monte Carlo simulations

The Monte Carlo simulation [100, 101] or importance sampling method originally proposed by Metropolis et. al in Ref. [102] is a technique used in statistical physics to calculate ensemble averages of observables as time averages of a properly chosen Markov process. As we have seen in the previous section, our game theoretic model is exactly such a Markov process for its analogous spin model. This means that the utility of the Monte Carlo method in the investigation of logit-rule-driven evolutionary potential games is two-fold: In addition to giving exact experimental access to the model via computer simulations, it also lets us estimate the equilibrium properties of the system.

The experimental aspect of the Monte Carlo method can shine a light on the dynamical details of the microscopic behavior of the system. It allows us to directly observe the evolution of spatial patterns in the distribution of strategies, possibly including domain formation processes or the emergence of self-organizing structures. Many of these phenomena are also closely related to the macroscopic properties of the system, and as a result their analysis can bolster other methods probing equilibrium behavior. For example, the direction and the velocity of interfacial fronts between domains can be indicative of the stability of competing ordered phases.

The logit dynamics picks subsequent strategy profiles with a probability proportional to their Boltzmann factor, and as a result the evolutionary process actually samples the equilibrium probability distribution of strategy configurations. This means that the equilibrium expectation values of observable macroscopic quantities can also be evaluated as time averages over an infinite sequence of strategy profiles generated by the logit evolutionary process. We can formalize this the following way for a general

configuration dependent quantity $Q(\mathbf{s})$:

$$\overline{Q} = \sum_{\{\mathbf{s}\}} Q(\mathbf{s}) p(\mathbf{s}) = \langle Q \rangle = \lim_{T\to\infty} \langle Q \rangle_T = \lim_{T\to\infty} \frac{1}{T} \sum_{t=0}^{T} Q\left[\mathbf{s}(t)\right]. \tag{3.10}$$

Here we introduced a handful of notations: $\overline{Q}$ is the equilibrium expectation value of the quantity Q in the Boltzmann distribution, and $\langle Q \rangle_T$ is its time average over the course of the first T time steps of the process. Obviously, exactly calculating $\overline{Q}$ becomes prohibitively hard for large populations, and precisely evaluating $\langle Q \rangle$ is impossible due to the infinite number of required iterations. The latter, however, can be approximated by $\langle Q \rangle_T$ when T is sufficiently high.

The efficacy of this estimation can be improved by modifying the averaging technique to circumvent certain adverse properties of the dynamics. Since individual logit strategy updates only affect single sites, consequent strategy configurations are highly correlated. As a result, using measurements separated by a sufficiently high number of steps (after which correlations can be assumed negligible or significantly small) to estimate averages is one such possible improvement method. This effectively redefines the elementary step of the Monte Carlo process. Henceforth, by a Monte Carlo step we will refer to N subsequent logit strategy revisions by randomly chosen players, so that during one Monte Carlo step all players get one chance on average to update their strategy, and thus allows any configuration to possibly evolve into any other. For similar reasons, it is also worth discarding data points belonging to the first t_t (called pre-thermalization time) Monte Carlo steps to compensate for the initial state not being representative of thermal equilibrium.

In the vicinity of continuous phase transitions, relaxation times, correlation lengths, and fluctuations diverge, which also affect the results provided by the Monte Carlo method. Increasing relaxation times (critical slowing down) demand longer pre-thermalization and sampling times to provide accurate results. Once correlation lengths become comparable to the linear size L of the system, finite-size effects dominate the system's behavior. These can be dampened by increasing the system size, or even exploited by the finite-size scaling approach.

3.2.2 Mean-field and pair approximations

Cluster variation methods in general give an approximate description of a system as a patchwork of uncorrelated clusters, and then estimate thermodynamic functions via a variational extremum principle using the probabilities of finding the clusters in certain

configurations [32, 103–107]. Here we only introduce the two simplest of these methods, the mean-field and pair approximations.

The mean-field approximation employs one-site probabilities $p_1(i)$ of finding strategy i at any of the sites of the translation-invariant lattice system, which we can also interpret as the frequency ρ_i of i-strategists in the population. These probabilities are, of course, normalized so that

$$\sum_{i=1}^{n} p_1(i) = 1. \tag{3.11}$$

In the canonical ensemble the Helmholtz free energy $\Phi = U + K\mathcal{S}$ of the game model is maximal. Here U is the expectation value of the potential of the system, $\mathcal{S}$ denotes its Gibbs entropy, and K is the noise-level parameter.[1] These quantities are estimated at the level of mean-field approximation by the following expressions:

$$U = \sum_{\{\mathbf{s}\}} U(\mathbf{s})p(\mathbf{s}) \approx U^{(1)} = \frac{Nz}{2} \sum_{i} p_1(i)V_{ij}p_1(j), \tag{3.12}$$

$$\mathcal{S} = \sum_{\{\mathbf{s}\}} p(\mathbf{s}) \ln p(\mathbf{s}) \approx \mathcal{S}^{(1)} = -N \sum_{i} p_1(i) \ln p_1(i). \tag{3.13}$$

The maximization problem of $\Phi^{(1)} = U^{(1)} + K\mathcal{S}^{(1)}$ can be approached in multiple ways. The direct numerical approach reduces the maximization problem to solving a set of coupled partial differential equations. The normalization constraint Eq. (3.11) can be taken into account by adding an additional term to the free energy via a Lagrange multiplier Λ to get

$$\begin{aligned} \Psi^{(1)} &= \Phi^{(1)} + \Lambda \left[\sum_{i=1}^{n} p_1(i) - 1 \right] = \\ &= \frac{Nz}{2} \sum_{i,j=1}^{n} p_1(i)V_{ij}p_1(j) - NK \sum_{i=1}^{n} p_1(i) \ln p_1(i) + \Lambda \left[\sum_{i=1}^{n} p_1(i) - 1 \right]. \end{aligned} \tag{3.14}$$

Now the local extremal points of $\Phi^{(1)}$ satisfying the normalization constraint are the stationary points of $\Psi^{(1)}$ as a function of probabilities $p_1(i)$ and Lagrange multiplier Λ, that is, the following equations obtain:

$$\begin{aligned} \frac{\partial \Psi^1}{\partial p_1(i)} &= 0 \qquad \forall i \in \{1, \ldots, n\}, \\ \frac{\partial \Psi^1}{\partial \Lambda} &= 0. \end{aligned} \tag{3.15}$$

[1] In statistical physics the free energy is given by $F = E - T\mathcal{S}$, where E is the energy and T is the temperature of the system, and it is minimal in equilibrium in the canonical ensemble. In the game theoretical analogy, however, E is replaced by $-U$, and thus Φ plays the role of $-F$.

Solving these equations may yield multiple local maxima solutions for a fixed value of K, indicating the presence of competing metastable equilibrium states.

The other approach to determining equilibrium one-site probabilities exploits the underlying dynamics [108–110]. Starting from any arbitrary strategy frequency distribution, we can calculate the rate of change for all $p_1(i)$ based on the logit rule and the assumption that the strategies at neighboring sites are independently drawn from the same strategy distribution at the mean-field approximation level. These 'equations of motion' are of the form

$$\frac{\delta p_1(i)}{\delta t} = \sum_{\substack{j\neq i \\ j=1}}^{n} p_1(j) w^{(1)}(j \to i) - \sum_{\substack{k\neq i \\ k=1}}^{n} p_1(i) w^{(1)}(i \to k) \tag{3.16}$$

for each available strategy i. Here the rates $w^{(1)}(i \to j)$ are the expected probabilities of a random player changing his strategy from i to j during a Monte Carlo step δt,

$$w^{(1)}(i \to j) = \sum_{k,l,r,v=1}^{n} p_1(k) p_1(l) p_1(r) p_1(v) \frac{\mathrm{e}^{\left[V_{jk}+V_{jl}+V_{jr}+V_{jv}\right]/K}}{\sum_q \mathrm{e}^{\left[V_{qk}+V_{ql}+V_{qr}+V_{qv}\right]/K}}. \tag{3.17}$$

The resulting dynamic equation system can be solved numerically using the Euler method, for example.

The pair approximation method takes a very similar approach but instead of one-site probabilities it has two-site probabilities of finding possible i–j strategy pairings on neighboring sites at its center, which we will denote by $p_2(i,j)$ following our earlier notation. These probabilities should be consistent with the previous one-site probabilities. When the original lattice system has rotational and translational symmetry, this means satisfying

$$\sum_{j=1}^{n} p_2(i,j) = \sum_{j=1}^{n} p_2(j,i) = p_1(i) \tag{3.18}$$

for each strategy i , as well as the normalization condition

$$\sum_{i,j=1}^{n} p_2(i,j) = \sum_{i=1}^{n} p_1(i) = 1. \tag{3.19}$$

At the pair approximation level the free energy of the system reads

$$\begin{aligned} \Phi^{(2)} =& U^{(2)} + T\mathcal{S}^{(2)} = \frac{Nz}{2} \sum_{i,j=1}^{n} V_{ij} p_2(i,j) + \\ & - 2NK \sum_{i,j=1}^{n} p_2(i,j) \ln p_2(i,j) + (z-1)NK \sum_{i=1}^{n} p_1(i) \ln p_1(i). \end{aligned} \tag{3.20}$$

With the above in mind, both the direct numerical and the dynamical [108–110] solution methods mentioned above can be developed for the pair approximation as well.

The pair approximation method can provide asymptotically exact results for an appropriate connectivity structure, namely, large randomly generated z-regular graphs, which are locally tree-like and similar to the Bethe lattice [111, 112].

In the following chapters, we apply the above described methods to some simple combinations of the elementary games introduced in Chapter 2 in order to study their basic properties and critical behavior.

Chapter 4

Elementary coordination-type games

In the traditional coordination game [26–28, 35, 113] two players each have to pick one of two available strategies. If they both choose the same strategy, they both receive one unit of payoff, regardless of which strategy they happen to coordinate on. Should they fail to coordinate, they both lose the same amount. The corresponding payoff matrix is

$$\mathbf{d}(1,2;2) = \begin{pmatrix} 1 & -1 \\ -1 & 1 \end{pmatrix}. \tag{4.1}$$

When this matrix defines nearest neighbor interactions in a multiagent game whose strategy updates are governed by the logit rule, the game model is equivalent to the zero-field Ising model [86, 114–116].

The general n-strategy elementary coordination game extends this with $n-2$ further available strategy choices which all provide zero payoff regardless of the opponent's strategy. In the following, we will call such strategies neutral, but they are also referred to as invisible states in the statistical physics literature [117–125]. They are also similar to the loner strategy in the voluntary prisoner's dilemma (Section 2.4.2) and provide the players with $n-2$ distinguishable ways to opt out of playing the coordination game. Similarly, neutral strategies can be thought of as vacancies or inert, non-interacting states in the physical interpretation. Without loss of generality, we may assign the coordinated strategies to the first two and the neutral strategies to the last $n-2$ strategy labels and

write the general elementary coordination game's payoff matrix as

$$\mathbf{d}(1,2;n) = \begin{pmatrix} 1 & -1 & 0 & \cdots & 0 \\ -1 & 1 & 0 & \cdots & 0 \\ 0 & 0 & 0 & \cdots & 0 \\ \vdots & \vdots & \vdots & \ddots & \vdots \\ 0 & 0 & 0 & \cdots & 0 \end{pmatrix}. \tag{4.2}$$

Elementary coordination games are the simplest potential games that actually describe proper player–player interactions and generate the space of games that describe pure coordinations or anticoordinations. This chapter gives an overview of the basic macroscopic properties of the elementary coordination game when played on a square lattice by multiple players whose strategy updates are governed by the logit rule using the methods described in Chapter 3.

4.1 Mean-field approximation

In the mean-field approximation, as described in Section 3.2.2, the free energy density of the elementary coordination game is given by

$$\begin{aligned} \varphi^{(1)} = \frac{1}{N}\Phi^{(1)} &= \frac{z}{2}\sum_{i,j=1}^{n} p_1(i) d_{ij}(1,2;n) p_1(j) - K\sum_{i=1}^{n} p_1(i)\ln p_1(i) = \\ &= \frac{z}{2}[p_1(1) - p_1(2)]^2 - K\sum_{i=1}^{n} p_1(i)\ln p_1(i) \end{aligned} \tag{4.3}$$

as a function of the one-site probabilities of finding each strategy at a randomly chosen site [112]. Solving Eqs. (3.15) numerically yields two kinds of competing states that locally maximize free energy in the space of mean-field strategy distributions. Two sets of representative solutions are plotted in Figures 4.1 and 4.2.

When the noise level is high, the system evolves into a disordered state in which all strategies are chosen by equal shares of the population, so all ρ_i equal $1/n$. As the temperature K is lowered, this state eventually loses its stability at a strategy number–dependent critical noise level $K_c^{(1)}(n)$, and the system exhibits an order-disorder phase transition. This is signaled by the spontaneous breaking of the Ising-type symmetry of the two coordinated strategies in the equilibrium state. Below $K_c^{(1)}(n)$, the share of agents following one of the two coordinated Ising strategies increases as the temperature decreases. From now on, we will assign label 1 to this majority strategy. The frequencies of the remaining strategies all follow the opposite trend and diminish when the noise

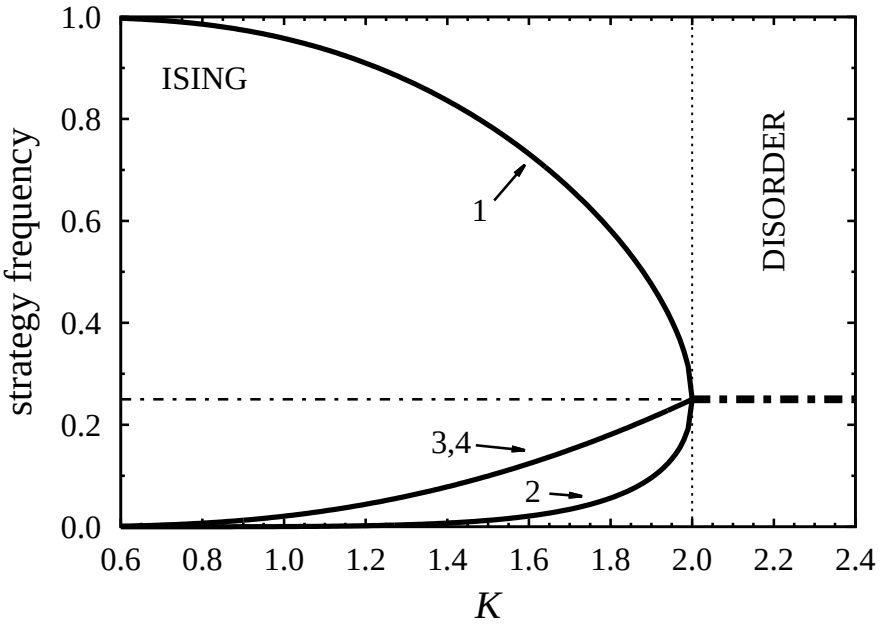

FIGURE 4.1. Strategy frequencies in the two competing metastable equilibrium states as functions of noise-level in the elementary coordination game with a total of $n = 4$ strategies, as predicted by the mean-field approximation. The state with the highest free energy is plotted with a thicker line.

level is lowered. The neutral strategies retain their symmetry and are chosen by more players than the minority Ising strategy, strategy 2. In the low noise limit, as K goes to 0, the Ising state becomes homogeneous and approaches the corresponding ground state, in which $\rho_1 = 1$.

As Figures 4.1, 4.2, and 4.3 suggest, it is not only the critical temperature $K_c^{(1)}(n)$ that depends on the number of neutral strategies but also the order of the phase transition. As long as n is low enough, the transition remains continuous, just like in the Ising model without any neutral strategies. This is illustrated by Figure 4.1, where $n = 4$, and the difference in the frequencies of the coordinated strategies vanishes smoothly at the critical point. In the $n = 10$ case shown in Figure 4.2, however, the equilibrium strategy frequencies (plotted with thick lines) are discontinuous functions of K, so the phase transition is of the first order.

The details of this change in the order of the phase transition can be explored analytically. Exploiting the symmetry and normalization properties of the numerical solutions, we can reduce the number of independent variables in the variational free energy of Eq. (4.3) to just two. If we choose them to be

$$a = \frac{\rho_1 - \rho_2}{2} \qquad \text{and} \qquad b = \frac{n-2}{2}\left(\frac{1}{n} - \rho_3\right) \tag{4.4}$$

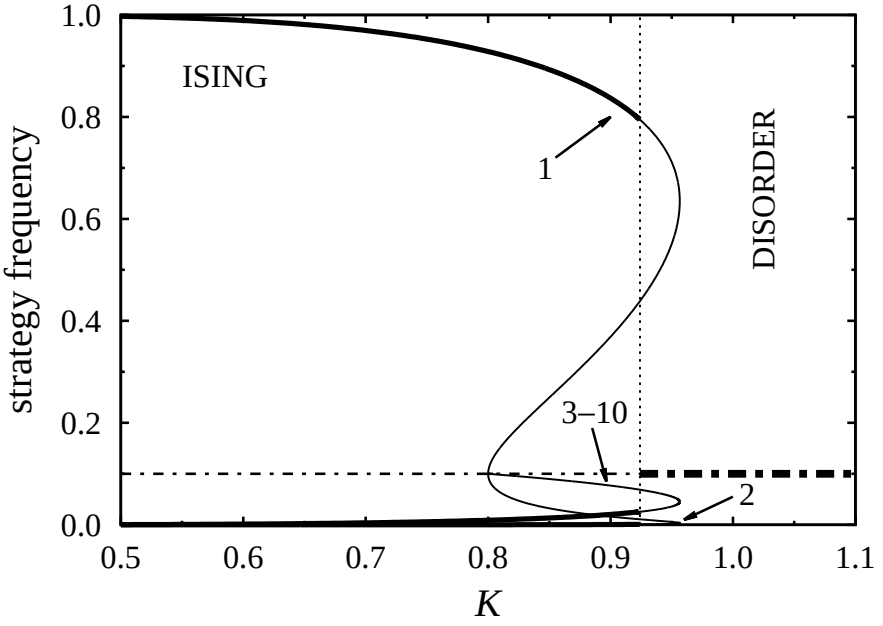

FIGURE 4.2. Strategy frequencies in the mean-field approximated $n = 10$-strategy elementary coordination game plotted against K. Thick lines correspond to the stable equilibrium state.

in terms of the strategy frequencies, then the free energy density can be written as

$$\begin{aligned}\varphi^{(1)} = 2za^2 - (n-2)\frac{K}{n}\left[1-\frac{2n}{n-2}b\right]\ln\left[1-\frac{2n}{n-2}b\right] + \\ -\frac{K}{n}\left[1+(a+b)n\right]\ln\left[1+(a+b)n\right] - \frac{K}{n}\left[1+(b-a)n\right]\ln\left[1+(b-a)n\right],\end{aligned} \tag{4.5}$$

and equilibrium states satisfy $\partial\varphi^{(1)}/\partial a = 0$ and $\partial\varphi^{(1)}/\partial b = 0$ simultaneously. The second equation can be rearranged to read

$$a^2 = \frac{n(n-4)}{(n-2)^2}b^2 + \frac{2}{n-2}b, \tag{4.6}$$

which in turn can be plugged into the first equation, reducing it to a single variable, b. $a_{\mathrm{D}} = b_{\mathrm{D}} = 0$ is a trivial solution that corresponds to the disordered state with $\rho_i = 1/n$ for all strategies. Further analysis reveals that this solution ceases to be a local maximum location of the free energy when

$$K < K_{\mathrm{c}}^{(1\mathrm{c})}(n) = \frac{2z}{n}. \tag{4.7}$$

Near this critical point, both a and b are small and positive when the phase transition is continuous, which can be exploited to derive an approximate solution describing the

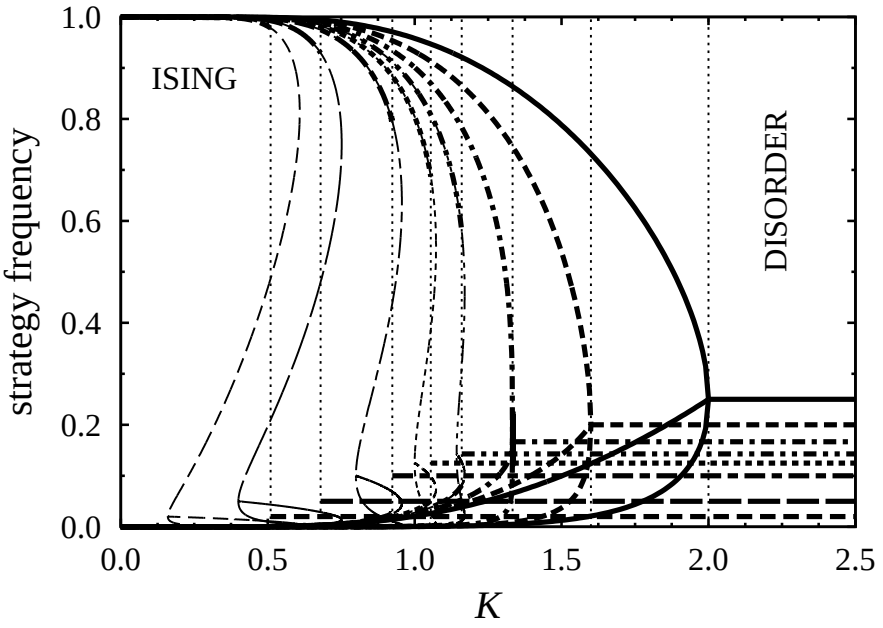

FIGURE 4.3. Mean-field strategy frequencies for elementary coordination games with $n = 4, 5, 6, 7, 8, 10, 20$, and 50 strategies (from right to left).

ordered phase close to $K_{\mathrm{c}}^{(1\mathrm{c})}(n)$. To leading order the solution is given by

$$a_{\mathrm{I}} \approx \sqrt{\frac{2}{n-2} b_{\mathrm{I}}} \qquad \text{and} \qquad b_{\mathrm{I}} \approx \begin{cases} \frac{3}{2z}\frac{n-2}{n-6}\left[K - K_{\mathrm{c}}^{(1\mathrm{c})}(n)\right] & \text{for } n \neq 6 \\ \sqrt{\frac{5}{3z}\left[K_{\mathrm{c}}^{(1\mathrm{c})}(n) - K\right]} & \text{for } n = 6. \end{cases} \tag{4.8}$$

These results imply that for $n \leq n_{\mathrm{th}}^{(1)} = 6$ the mean-field approximated square-lattice elementary coordination game undergoes a continuous phase transition at a critical temperature $K_{\mathrm{c}}^{(1)}(n) = K_{\mathrm{c}}^{(1\mathrm{c})}(n) = 2z/n$, similar to the $n = 4$ case shown in Figure 4.1. The quantities a and b are both order parameters for this transition, in the sense that their value is non-zero in the ordered phase and vanishes in the disordered state. Eq. (4.8) also predicts that their algebraic behavior in the vicinity of the transition point is characterized by critical exponents $\beta = 1/2$ and $\beta' = 1$ when $n < 6$, and $\beta = 1/4$ and $\beta' = 1/2$ when $n = 6$. The numerical results support all of these findings, as shown by Figure 4.3.

In the opposite case, when $n > n_{\mathrm{th}}^{(1)}$, the behavior of the solution changes, a and b only provide sensible, real valued strategy frequencies above $K_{\mathrm{c}}^{(1\mathrm{c})}(n)$, not below it. This is illustrated by the thin solid lines in Figure 4.2. The numerically obtained solutions of the free energy maximization problem indicate that this behavior is accompanied by the presence of a first-order phase transition. This 'backward curving' branch of the plot describing the strategy frequencies does not play a role in the equilibrium behavior of the system, because it never maximizes the free energy of the system. Consequently,

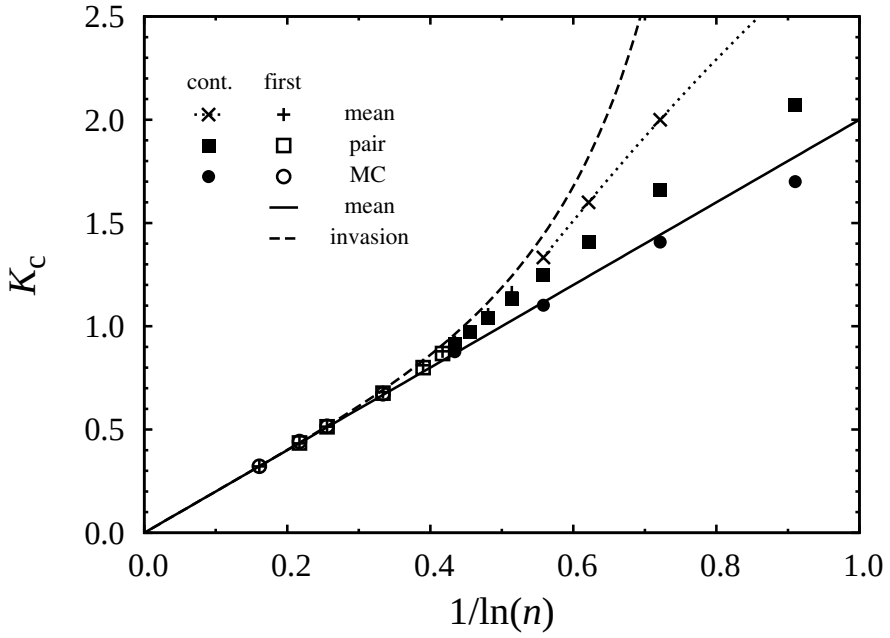

FIGURE 4.4. Comparison of critical temperatures in the square-lattice elementary coordination game obtained using different approximation methods and Monte Carlo simulations.

first-order transitions occur above $K_c^{(1c)}(n)$, that is, $K_c^{(1)}(n) > K_c^{(1c)}(n)$ when $n > n_{th}^{(1)}$. Furthermore, it also means that the approximate analytic solution does predict the presence of the first-order phase transition, but it does not describe the stable equilibrium state of the system near the transition point. The existence of these metastable states does, however, suggest the possibility of undercooling-related and hysteresis-related phenomena in elementary coordination games.

The numerical analysis of the mean-field approximated model reveals that the critical temperature of the phase transition is a monotonically decreasing function of the number of neutral strategies. (It is plotted with crosses and plusses in Figure 4.4 for continuous and first-order transitions, respectively.) Continuous transitions are correctly identified and located by the analytical solution presented in the previous paragraphs, $K_c^{(1)}(n)$ is indeed given by $K_c^{(1c)}(n) = 2z/n$ (the dotted line in Figure 4.4).

We can also derive an approximating analytic formula for the first-order transition temperatures. The numerical results show that as n is increased, the critical temperature decreases, while the share of the majority Ising strategy the transition leads to increases. (Figure 4.3) So for large n, the transition occurs approximately between a completely disordered phase with $\rho_i = \frac{1}{n}$ for all strategies and a completely ordered state with $\rho_1 = 1$ and $\rho_i = 0$ for the remaining $n-1$ strategies. In the completely ordered state $\mathcal{U} = 2N$ and the entropic term of the free energy vanishes, whereas in the completely disordered phase $\mathcal{U}^{(1)} = 0$ and $\mathcal{S}^{(1)} = N \ln n$ in the mean-field approximation. The

disordered phase gains stability when the entropic free energy of the disordered phase exceeds the potential of the ordered phase, that is, when $2N < KN \ln n$. This places the phase transition at approximately

$$K_{\mathrm{c}}^{(1\mathrm{f})}(n) = \frac{2}{\ln n}. \tag{4.9}$$

As expected, this approximation only proves to be effective for large n. This is confirmed by Figure 4.4, where the solid line corresponds to $K_{\mathrm{c}}^{(1\mathrm{f})}(n)$, and first-order transition temperatures for the mean-field approximated model are represented by plusses. We find that $K_{\mathrm{c}}^{(1\mathrm{f})}(n)$ in general underestimates the mean-field first-order transition temperatures.

The central idea of the above large-n approximation also provides a possible explanation for the observed change in the order of the model's phase transition. Adding more and more neutral strategies to the system increases the free energy of the disordered state at all temperatures through increasing its dominant entropic component. On the other hand, the presence of additional neutral strategies does not directly contribute to the potential of the ordered phase, nor does it significantly increase its entropy at low temperatures, due to the highly homogenized nature of the ordered state. As a result, the increased entropy content extends the stability region of the disordered phase, lowering the critical temperature of the phase transition. Eventually, the stabilizing effect of the entropy puts the nearly completely ordered state in direct competition with the disordered state, which leads to the emergence of a first-order transition in the system. So-called high entropy alloys [126–128], materials composed of at least five different principal metal elements in roughly equal proportions, seem to exhibit a similar entropy-based stabilization of solid-solution phases, which potentially induce desirable properties.

4.2 Pair approximation

The pair approximation improves on the mean-field approach by considering two-site probabilities and taking nearest-neighbor correlations into account. The corresponding expression for the free energy density reads

$$\begin{aligned}\varphi^{(2)} = \frac{1}{N}\Phi^{(2)} = \frac{z}{2}\sum_{i,j=1}^{n} d_{ij}(1,2;n)p_2(i,j) + \\ - 2K\sum_{i,j=1}^{n} p_2(i,j)\ln p_2(i,j) + (z-1)K\sum_{i=1}^{n} p_1(i)\ln p_1(i),\end{aligned} \tag{4.10}$$

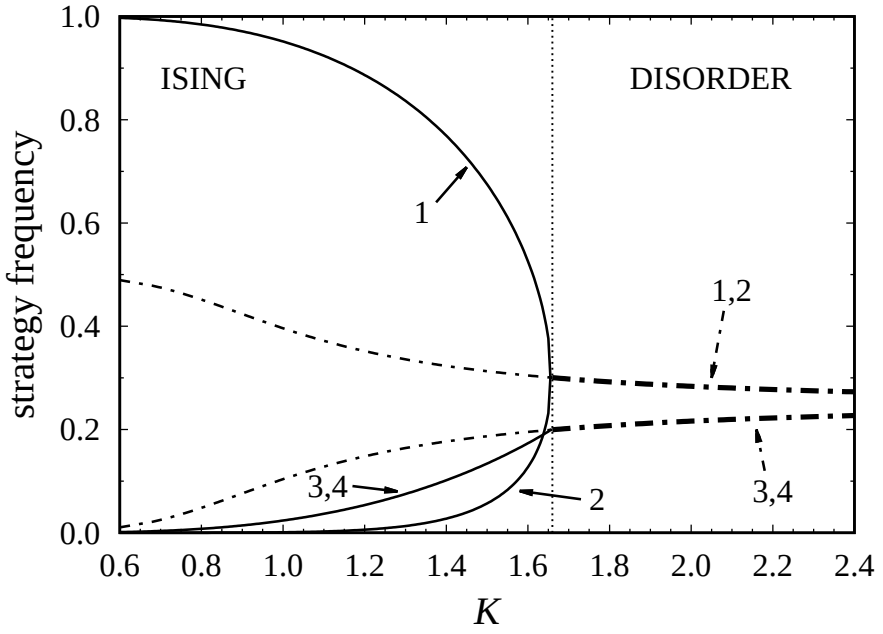

FIGURE 4.5. Strategy frequencies in the pair approximated $n = 4$ elementary coordination game.

where the one-site probabilities $p_1(i)$ are normalized and consistent with the two-site probabilities through the compatibility conditions in Eqs. (3.18) and (3.19) due to the translational and rotational symmetry of the system.

Again, just like in the mean-field approximation, we can derive equations for the equilibrium states that can be solved numerically. This approach again yields two types of solutions, one ordered and stable in a low-temperature regime, and another with roughly equal strategy frequencies that characterizes the system at higher temperatures. The ordered phase breaks the symmetry of the coordinated strategies, and may be formed by either of the two degenerate ordered equilibrium states. For the sake of simplicity, we will assign strategy label 1 to the majority strategy in the ordered phase.

The results of this pair approximation approach are qualitatively quite similar to those provided by the mean-field approximation method. For low enough n (e.g., $n = 4$ pictured in Figure 4.5), the transition between the ordered and disordered phases is continuous, while high-n (e.g., $n = 20$ shown in Figure 4.6) versions of the model exhibit a first-order phase transition.

However, we can see a marked difference from the mean-field solution in the structure of the disordered phase. The disordered state is only completely disordered in the $K \to \infty$ limit. When K is finite, the two coordinated strategies are chosen more frequently than the neutral ones, without breaking the symmetry of the payoff matrix. As K is lowered, the gap between the frequencies of coordinated and neutral strategies increases, until eventually the neutral strategies disappear in the $K \to 0$ limit, though this happens

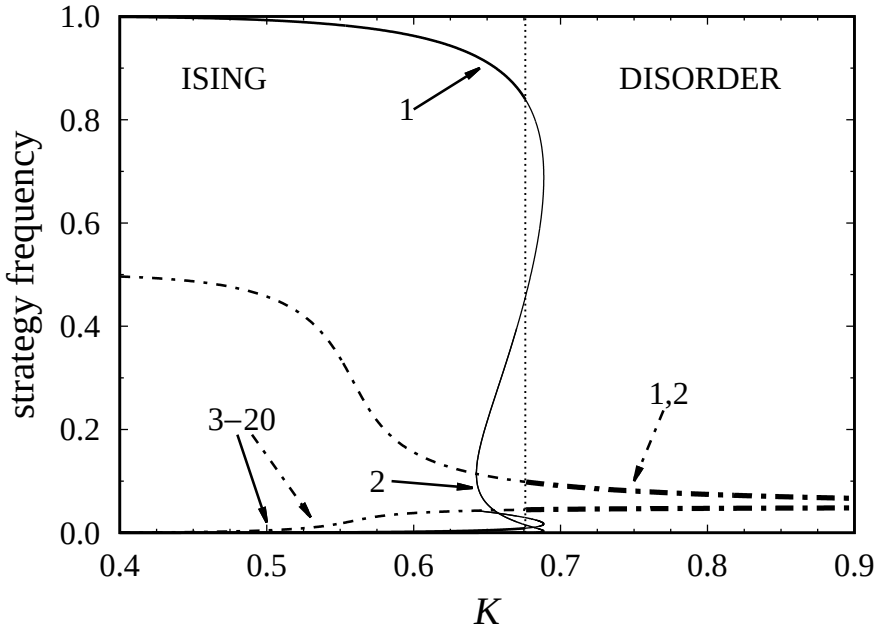

FIGURE 4.6. First-order phase transition in the pair approximated elementary coordination game with $n = 20$ strategies.

deep in the ordered phase, where the disordered state is already unstable. This partial ordering is a direct manifestation of the pair correlations introduced by the pair approximation that do not simply prefer having more of one of the coordinated strategies as the mean-field model, but actually rewards having matching coordinated strategies on neighboring sites. Another resulting change in comparison with the mean-field approximation is that in the close vicinity of continuous phase transitions the frequency of the minority coordinated strategy can be higher than the frequency of neutral strategies even in the ordered phase.

It is still true in the pair approximated model that the critical temperature is a monotonically decreasing function of the number of neutral strategies. Numerically evaluated critical temperatures are shown in Figure 4.4 for some values of n. The pair approximated critical temperature $K_c^{(2)}(n)$ is always lower than its mean-field approximated counterpart $K_c^{(1)}(n)$ for any fixed n, but they become very close to each other as soon as the mean-field phase transition becomes discontinuous. The pair approximated model requires a higher number of neutral strategies to possess a first-order transition, namely more than $n_{\text{th}}^{(2)} = 10$.

4.3 Monte Carlo simulations

We also carried out Monte Carlo simulations in order to verify the qualitative predictions of the mean-field and pair approximations and measure quantities like the critical

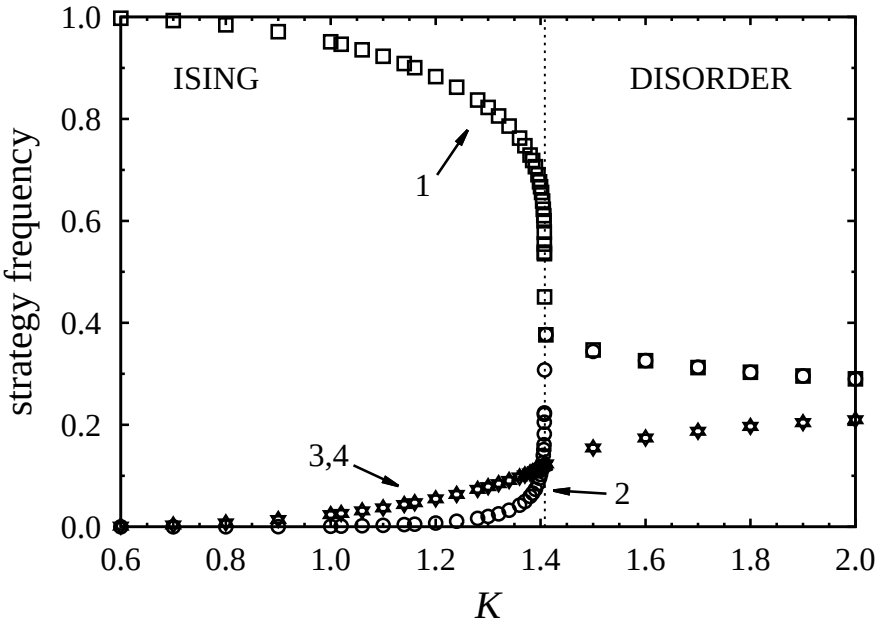

FIGURE 4.7. Monte Carlo simulated strategy frequencies in the continuous phase transition in the elementary coordination game with $n = 4$ strategies.

temperature and critical exponents in an experimental realization of the square-lattice elementary game. To dampen finite-size effects, we imposed periodic boundary conditions and the size of the simulated system and sampling and pre-thermalization times were increased in the vicinity of the phase transition. The linear size varied from 300 to 1000 sites, while both the sampling and pre-thermalization times ranged from 10^4 to 10^5 Monte Carlo steps. Furthermore, to speed up the thermalization process, we started the simulations in the ordered phase from a prepared, fully ordered initial state, while simulation runs were started from a randomized initial state in the disordered phase.

The noise level dependence of the equilibrium strategy frequencies (shown in Figures 4.7 and 4.8 for $n = 4$ and 20) reveals that the matching qualitative predictions of the mean-field and pair approximations for the system's behavior are indeed correct. The Monte Carlo simulation data confirm the presence of an order-disorder transition and the low-temperature breaking of the symmetry of the two coordinated strategies. The critical points of the transitions turn out to be lower than those predicted by the mean-field and pair approximations. On the other hand, we also find that these estimates become more and more accurate the larger n is, as demonstrated by Figure 4.4. The data also corroborate the change in the order of the phase transition. If the number of available strategies is at most the approximate threshold value of $n_{\rm th}^{\rm (MC)} \approx 27$, the data indicate (see Fig. 4.9) a continuous transition, while the transition seems to be of the first order when the number of strategies is above it [112].

We find a similar change in the critical exponents of the transitions, as illustrated

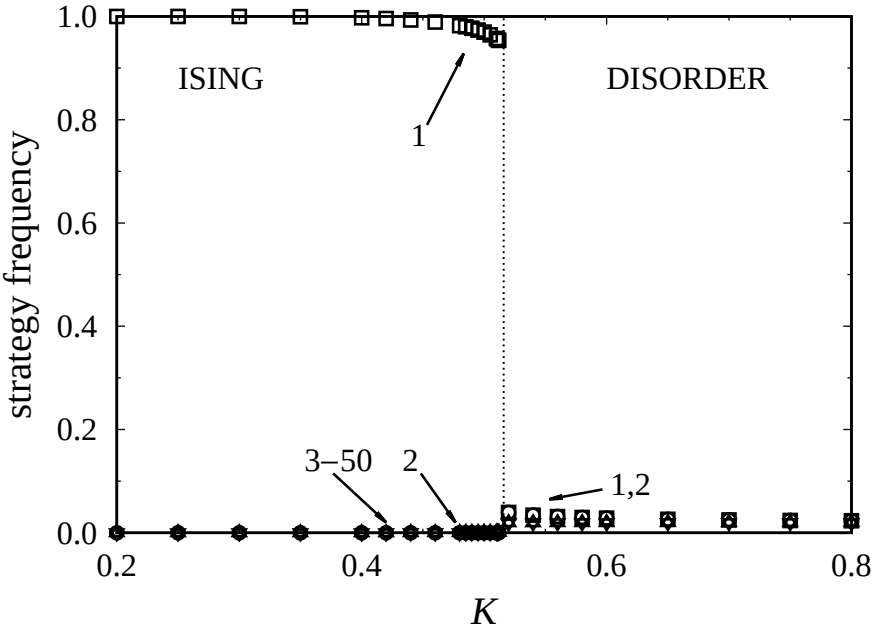

FIGURE 4.8. Strategy frequencies in the Monte Carlo simulated $n = 50$ elementary coordination game.

by Figure 4.10. On the log-log plot of the Ising magnetization-like order parameter $\rho_1 - \rho_2$ against the normalized distance of the noise level from the critical point $[K_c(n) - K]/K_c(n)$, simulation data for low enough n collapse onto the same straight line in the vicinity of the critical point, which line coincides with Onsager's exact solution [129] to the two-dimensional square-lattice Ising model. This suggests that the continuous transitions belong to the Ising universality class. However, we also find that the higher n is the closer K has to be to the critical point for the Ising-type behavior to manifest itself, making it more and more time-consuming to validate using Monte Carlo simulations due to growing critical slowing down and finite-size effects. Nevertheless, as Figure 4.10 shows, we still find that the order parameter seemingly follows algebraic behavior near the critical point for higher strategy numbers and even above n_{th} in our simulation results, that is,

$$\rho_1 - \rho_2 \propto [K_c(n) - K]^{\beta}, \tag{4.11}$$

but the exponent β is no longer equal to 1/8 that characterizes the Ising model, but it seems to decrease with n when n is large enough. Such a variation in β with the model's defining parameter could, on one hand, be an essential feature of the model, like it is of the Potts [130] and Ashkin–Teller [86] models. On the other hand, it could also be explained by the enhancement of the entropy effect of the neutral strategies as their number increases, which—just like finite-size effects—decreases the correlation length, and our simulation temperatures not being sufficiently close to the critical point. Of course, these two possible explanations are not mutually exclusive, so the observed n-dependence of β could be the result of a combination of both of them.

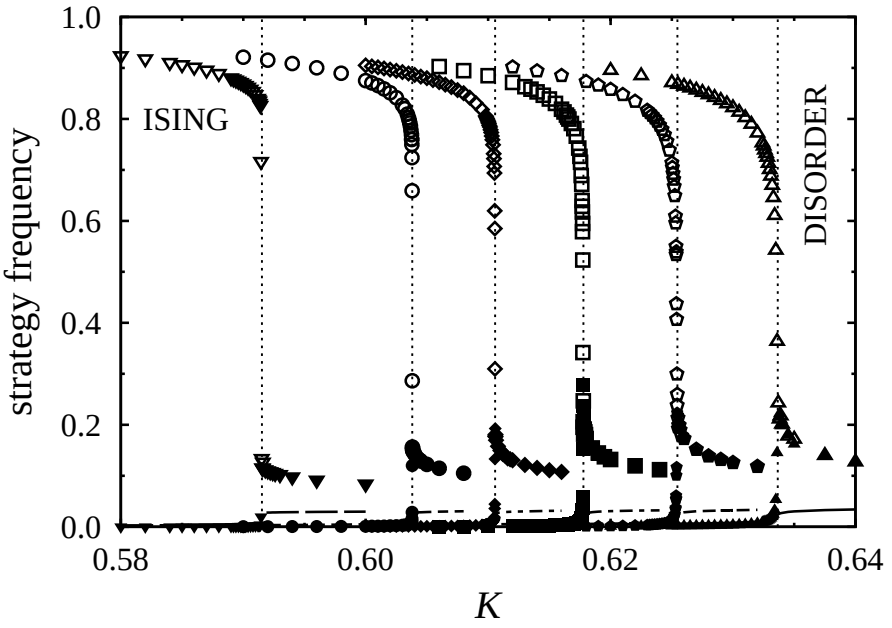

FIGURE 4.9. Comparison of the phase transitions of the $n = 24$, 25, 26, 27, 28, and 30 (from right to left) elementary coordination games.

As we will later see in Chapter 5, elementary coordination games can be considered as special cases of the Blume–Capel model. This analogy confirms the validity of our findings, which are in excellent agreement with the existing literature. This includes providing further evidence of the elementary coordination game having a continuous phase transition that belongs to the Ising universality class when $n \leq n_{\text{th}} = 27$ and a first-order transition otherwise. This also suggests that the slight variation of β in our simulation data is caused by the entropy effect, at least when the transitions are continuous.

The other potential order parameter suggested by the mean-field analysis, the quantity b in Eq. (4.4), turns out to not be an order parameter for the unapproximated system, as both the pair approximation and simulation results show that it does not vanish in the disordered phase. This is a direct consequence of the asymmetry between coordinated and neutral strategies and a manifestation of the game's preference for having matching coordinated strategy pairs on neighboring sites. In the disordered phase, the increase in the system's potential that could be realized by breaking the symmetry of the coordinated strategies is evidently not high enough to offset the loss this process would cause in the entropic term of the free energy, but having a slightly, symmetrically higher amount of both coordinated strategies than neutral strategies still produces a net gain in the free energy over the completely disordered phase. The gap between the frequencies of the coordinated and neutral strategies is a decreasing function of K and vanishes as $K \to \infty$, because the entropic term of the free energy is proportional to the system's temperature, unlike the potential term that does not directly depend on K.

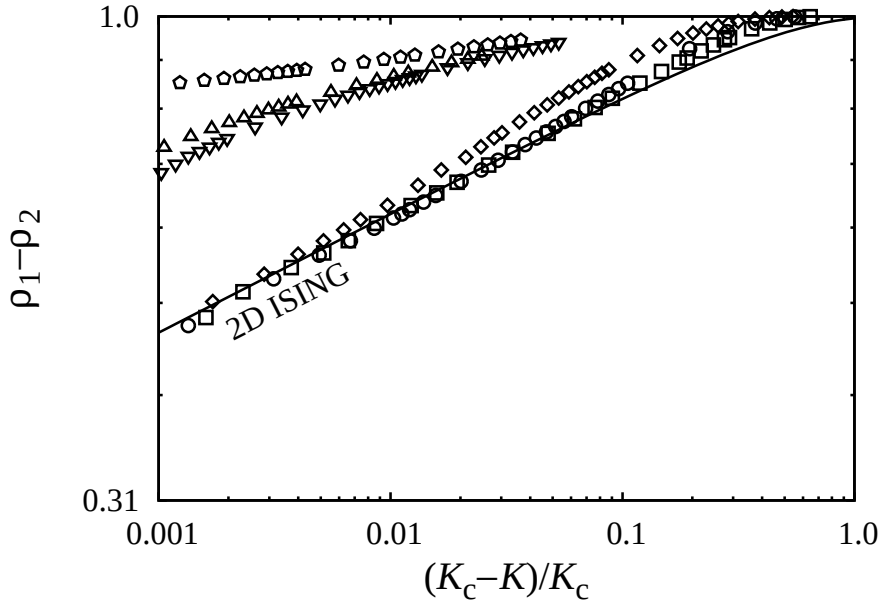

FIGURE 4.10. Log-log plots of the order parameter of different elementary coordination games. The squares, circles, diamonds, downward and upward pointing triangles, and pentagons correspond to Monte Carlo simulation data for games with $n = 4$, 6, 10, 20, 25, and 50 strategies respectively. The solid line shows Onsager's exact result [129] for the two-dimensional square-lattice Ising model.

4.4 Microscopic behavior

The Monte Carlo simulation method also allows us to examine the microscopic details of the dynamics. A strategy configuration of the system can be easily visualized by assigning different colors to different strategies and coloring a square lattice—whose sites represent the players—accordingly. The movies generated by the dynamics reveal the mechanics of ordering and some interesting pattern formation in the spatial distribution of the strategies. Furthermore, we will see that observing the time evolution of the system can also help develop an approximation method for the critical temperature based on the invasion velocities along interfaces separating domains.

As we have seen earlier in this chapter, the system evolves toward an ordered state if the noise level is below the critical point. If we start the system from a randomized initial state (Figure 4.11a), we can see all important stages of how such an ordered state is formed. At first, the system is obviously disordered, with at most a few neighboring sites occupied by players playing the same coordinated strategy, and these islands are surrounded by a sea of neutral strategies, especially if n is high. Because of the positive payoff provided by coordination, these islands are more likely to grow than shrink, and through this domain-growing process larger domains of both coordinated strategies are

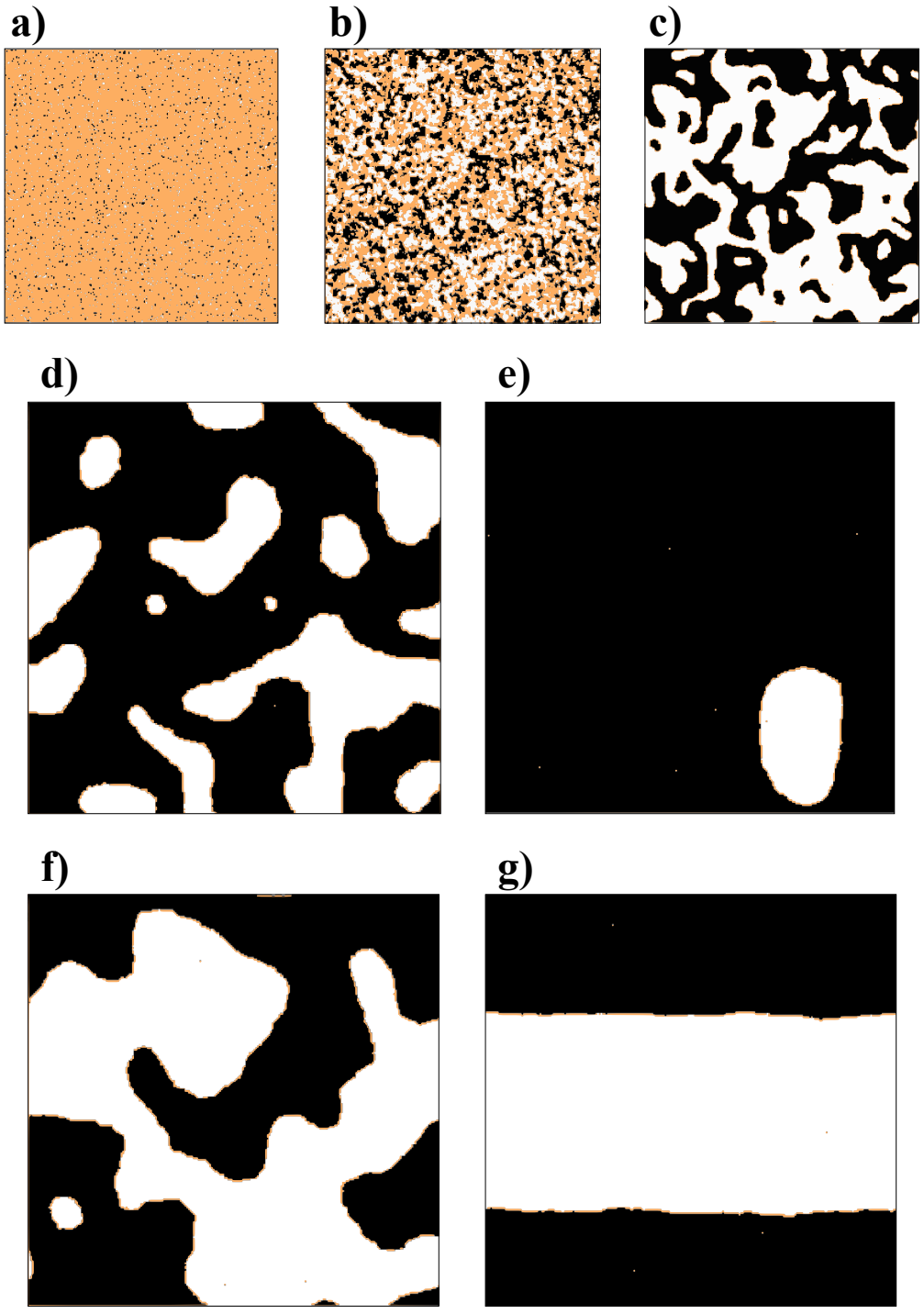

FIGURE 4.11. Snapshots of the domain growth process described on page 47, in the $n = 50$ elementary coordination game $[K_c^{(\mathrm{if})}(50) \approx 0.517]$ at $K = 0.3$. Black and white sites are occupied by players following the two coordinated strategies and players at orange (gray) sites play one of the neutral strategies. Panels a) through c) show the emergence of the domain structure. In panels d) and e), the black coordinated domain percolates in both directions of the square lattice and eventually takes over the whole system. In another simulation run, however,—pictured in panels f) and g)—there are two opposing coordinated domains that both percolate in only one direction and eventually evolve into a striped structure.

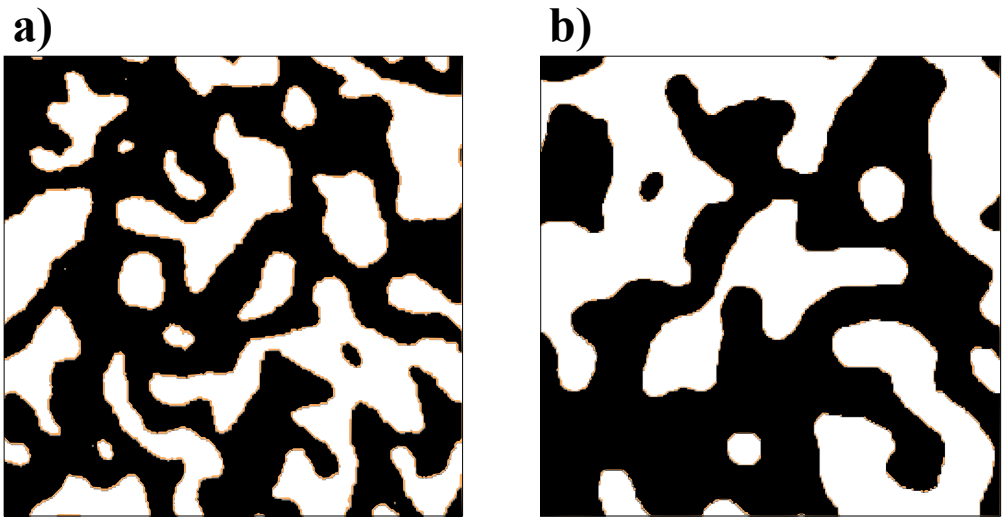

FIGURE 4.12. Two snapshots of Monte Carlo simulated $n = 50$ elementary coordination games taken at a) $K = 0.3$ and b) $K = 0.2$. Neutral separating monolayers between different coordinated domains recede to corners when the temperature is below $K^{(\mathrm{ml})}(50) \approx 0.258$.

formed. The domains keep growing into the mixed sea of interchangeable neutral strategies, which in turn becomes thinner and thinner (Figure 4.11b) between the domains, until it eventually disappears (Figure 4.11c) as neighboring domains of the same coordinated strategy merge or becomes a neutral monolayer wall that separates differently coordinated domains. For lower temperatures, deep within the ordered phase, these monolayers recede into corner-like interfaces, as pictured in Figure 4.12b. On the other hand, the separating neutral monolayers remain present between opposing domains if the temperature is higher, like in Figure 4.12a. In either case, domains formed by the same strategies keep merging, while the domain walls keep randomly moving, smoothing and straigthening out the domain walls to decrease losses along interfaces, until finally one of the domains percolates and engulfs all other domains (Figures 4.11d and 4.11e). Sometimes the system may get stuck for a long time in a striped or faceted metastable configuration where two large opposing domains remain in the system, as shown in Figures 4.11f and 4.11g. Similar phenomena can also be observed in Monte Carlo simulations of the Ising model for single-spin-flip Glauber dynamics [131–133].

Due to the probabilistic nature of the logit strategy update rule, the domains are never perfectly coordinated at any finite temperature, and point defects may appear with a temperature-dependent probability. These point defects are responsible for the incomplete homogenization of the system at finite temperatures, but they also drive domain-growing and domain-merging processes by initiating the invasion of one domain by another. The increased rate of defect generation also prevents the nucleation process from forming domains in the disordered phase. In the bulk, point defects are generally short-lived at low temperatures because players can gain a relatively high increase in payoff if

they return to coordination with four neighbors. At the edge of a domain, however, the losses of defectors become smaller, so they are more likely to appear, shift the domain wall, and thus make neighboring players more likely to defect. In fact, if one of the players along a straight domain wall defects, then their two (now opposing) neighbors along the edge will choose any strategy with the same probability—should they be given the opportunity—because they have the same number of neighbors following opposing coordinated strategies, so the defect will likely grow if the temperature and the number of available neutral strategies is high. This is also why a neutral monolayer separating two opposing coordinated domains can be relatively stable if the temperature is high enough.

Based on the above observations, we can estimate the critical temperature of the system and the temperature above which separating monolayers are present by calculating and comparing certain domain growth probabilities. Moreover, the simulations suggest that the most relevant changes occur at step-like vertical and horizontal interfaces, so we can reasonably assume that simply comparing invasion velocities along such interfaces is sufficient for obtaining good approximations. Below the critical temperature, when the number of neutral strategies is high, coordinated domains first have to invade a disordered domain mostly made up of interchangeable neutral strategies. Figure 4.13a illustrates a horizontal step-like interface separating such coordinated and disordered domains. At this step, the probability of the coordinated domain expanding to site x is

$$w(\mathbf{s}_x \to \mathbf{s}_{x,1}) = \frac{\mathrm{e}^{2/K}}{\sum_{\hat{\mathbf{s}}_x} \mathrm{e}^{u_x(\hat{\mathbf{s}}_x)}}, \tag{4.12}$$

whereas the probability of the expansion of the neutral domain to site y is the probability of the player at site y switching to any one of the $n-2$ neutral strategies, which is

$$\sum_{j=3}^{n} w(\mathbf{s}_y \to \mathbf{s}_{y,j}) = \frac{n-2}{\sum_{\hat{\mathbf{s}}_y} \mathrm{e}^{u_y(\hat{\mathbf{s}}_y)}}. \tag{4.13}$$

Notice that the denominators of the two expressions are equal, because site x and site y are surrounded by the same set of neighboring strategies. If we neglect the possibility of either the player at site x or the player at site y switching to the other coordinated strategy—the lower the noise level and the higher n is, the lower the probability of these transitions becomes—we may conclude that the ordered coordinated domain will expand at the expense of the mixed neutral domain when

$$w(\mathbf{s}_x \to \mathbf{s}_{x,1}) > (n-2) w(\mathbf{s}_y \to \mathbf{s}_{y,3}), \tag{4.14}$$

that is, when $\mathrm{e}^{2/K} > (n-2)$, while the disordered phase prevails in the opposite case.

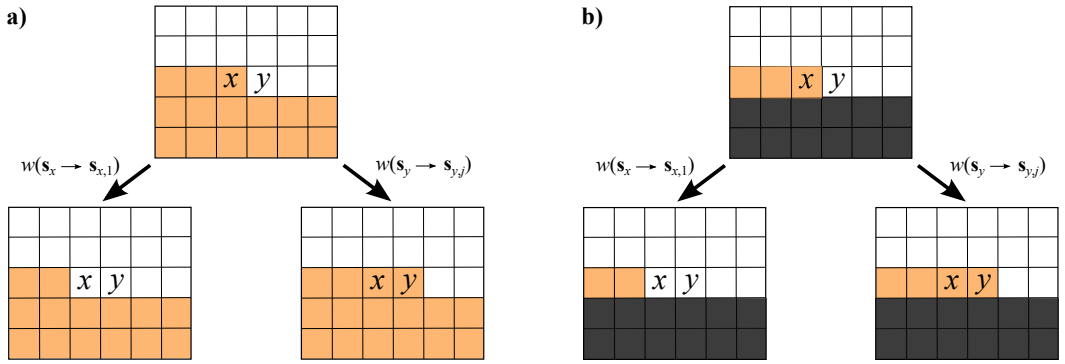

FIGURE 4.13. Proposed interface types in the elementary coordination game for the invasion-velocity-based estimation of the critical temperature of a) the order-disorder phase transition and b) the stability of the neutral monolayers separating opposing coordinated domains. White and black squares represent players following the two coordinated strategies, while players at orange (gray) sites play one of the neutral strategies.

At the critical point of the order-disorder phase transition neither growth direction is preferred to the other by the system, so the two probabilities are equal to each other. This yields the following approximate formula for the critical temperature:

$$K_{\mathrm{c}}^{(\mathrm{if})}(n) \simeq \frac{2}{\ln(n-2)}. \tag{4.15}$$

Comparison with Monte Carlo simulation data reveals (see Figure 4.4) that this is indeed an asymptotically good approximation of the critical temperature for large n.

The stability of separating monolayers between opposing coordinated domains can also be analyzed in a similar way by checking whether a 'half' separating neutral layer (Fig. 4.13b) is more likely to grow or shrink. The probability of the layer growing by one site is again formally given by Eq. (4.13), though the terms in the denominator are different due to the changed strategy configuration of the neighboring sites. The probability of the layer receding is

$$w(\mathbf{s}_x \to \mathbf{s}_{x,1}) = \frac{\mathrm{e}^{1/K}}{\sum_{\hat{\mathbf{s}}_x} \mathrm{e}^{u_x(\hat{\mathbf{s}}_x)}}, \tag{4.16}$$

and we again neglect the role of less probable transitions to the other coordinated strategy. Comparing the two probabilities yields a strategy number dependent characteristic temperature

$$K^{(\mathrm{ml})}(n) \simeq \frac{1}{\ln(n-2)} = \frac{1}{2} K_{\mathrm{c}}^{(\mathrm{if})}(n). \tag{4.17}$$

Above this temperature, separating neutral monolayers will expand and coat horizontal and vertical domain walls in the ordered phase, while in the opposite case the monolayers recede to the corners of the domains. This prediction is again confirmed by Monte Carlo simulations of elementary coordination games with a large number of neutral strategies.

4.5 Potts models with invisible states

Refs. [117–125] study a very similar model family called Potts models with invisible states and report very similar results regarding a change in the order of the transition as the number of invisible states is increased. They take the usual q-state Potts model [130, 134], whose payoff matrix in our game theoretic framework is the $q \times q$ unit matrix, and extend it with r neutral strategies, the same way as the traditional coordination game $\mathbf{d}(1,2;2)$ is extended to the n-strategy elementary coordination game $\mathbf{d}(1,2;n)$. For $q=2$, the Potts model becomes equivalent to the Ising model defined by $\mathbf{d}(1,2;2)$ up to a payoff-shifting irrelevant component. It turns out, however, that the irrelevant component has a non-negligible role in this situation, as its extension with neutral strategies significantly changes the elementary game content of the irrelevant component. For example, when we add a single neutral strategy, the resulting payoff matrix has more elementary coordination components than just one, and the original coordination's strength is changed as well:

$$\mathbf{P}(q=2,r=0) = \begin{pmatrix} 1 & 0 \\ 0 & 1 \end{pmatrix} = \frac{1}{2}\mathbf{m}(2) + \frac{1}{2}\mathbf{d}(1,2;2), \tag{4.18}$$

$$\mathbf{P}(2,1) = \begin{pmatrix} 1 & 0 & 0 \\ 0 & 1 & 0 \\ 0 & 0 & 0 \end{pmatrix} = \frac{4}{9}\mathbf{m}(3) - \frac{1}{3}\mathbf{f}(3;3) + \frac{4}{9}\mathbf{d}(1,2;3) + \frac{1}{9}\left[\mathbf{d}(1,3;3) + \mathbf{d}(2,3;3)\right].$$

Consequently, elementary coordination games and the two-state Potts model with additional invisible states are not equivalent to each other, even though they can be obtained by extending equivalent models with neutral strategies.

In light of this, it may seem somewhat surprising how similar their properties turn out to be. The $q=2$ Potts model with invisible states also changes the order of its phase transition as the number of invisible states increases [117–119] (Refs. [120, 121] provide a rigorous proof), its critical temperature is a monotonically decreasing function of the number of available states and also vanishes asymptotically as $\frac{2}{\ln(q+r)}$ [124]. Even the threshold number of states separating continuous and first-order transitions is very similar: in the mean-field approximation $r_{\text{th}}^{(1)} = 3$ [117] (or more precisely, after generalization to non-integer strategy numbers $r_{\text{th}}^{(1)} \approx 3.65$ [123, 124]), while on a Bethe lattice with $z=4$ neighbors $r_{\text{th}}^{(2)} = 9$ [123], which both translate to total strategy numbers very close to their elementary coordination game counterparts $n_{\text{th}}^{(1)} = 6$ and $n_{\text{th}}^{(2)} = 10$. All these similarities hint at the robustness of the entropy effect of introducing neutral strategies that extends the disordered phase's region of stability.

Chapter 5

Interplay of elementary coordination and self-dependent components

Some of the simplest complex matrix games in terms of elementary game content are the combinations of the elementary coordination game of Chapter 4 and self-dependent games that retain the interchangeability of the coordination component's $n-2$ neutral strategies. The two simplest ways such a self-dependent component can be introduced are defined in relation to the symmetry of the coordinated strategies: the introduced self-dependent component may either break or respect that symmetry [135]. The corresponding payoff matrices are of the form

$$\mathbf{A}' = \mathbf{d}(1,2;n) + h'\mathbf{e}(1;n), \tag{5.1}$$

$$\mathbf{A}'' = \mathbf{d}(1,2;n) + h''\left[\mathbf{e}(1;n) + \mathbf{e}(2;n)\right], \tag{5.2}$$

where h' and h'' are the strengths of the symmetry-breaking and symmetry-retaining self-dependent components, respectively. These are both potential games, and their potential matrices are

$$\mathbf{V}' = \mathbf{d}(1,2;n) + h'\mathbf{f}(1;n), \tag{5.3}$$

$$\mathbf{V}'' = \mathbf{d}(1,2;n) + h''\left[\mathbf{f}(1;n) + \mathbf{f}(2;n)\right], \tag{5.4}$$

using the notations introduced in Chapter 2. As we have seen in Chapter 3, it is a game's potential that determines its equilibrium state and properties when strategy updates are governed by the logit rule, so any other games with the same potential will behave in essentially the same way while potentially providing different payoffs.

In this chapter, we discuss the macroscopic properties of the two composite games mentioned above, played on a square lattice and governed by the logit strategy update rule. First, however, let us take a look at purely self-dependent games which, together with the results reported in Chapter 4, will allow us to identify interplay effects between the self-dependent and the coordination-type components.

5.1 Self-dependent games

A purely self-dependent game with n available strategies has a payoff matrix of the general form

$$\mathbf{A}^{(\mathrm{sd})} = \sum_{k=1}^{n} \varepsilon_k \mathbf{e}(k;n), \tag{5.5}$$

that is, it has the same entries in each of its rows. The elements of the corresponding potential matrix are given by

$$V_{ij}^{(\mathrm{sd})} = \varepsilon_i + \varepsilon_j. \tag{5.6}$$

We call these games self-dependent precisely because the payoffs of the players are not affected by the strategy choices of their opponents. Consequently, the logit strategy update rates do not depend on the actual configuration of the system either, they are constant, and directly give the equilibrium one-site probabilties ρ_i of finding strategy i at any site. On a regular network with coordination number z, these probabilities read

$$\rho_i = \frac{\mathrm{e}^{z\varepsilon_i/K}}{\sum_k \mathrm{e}^{z\varepsilon_k/K}}. \tag{5.7}$$

As we have seen earlier in Secion 3.1.1, this tends to the uniform distribution over all n strategies as K goes to infinity and to another uniform distribution over strategies with maximal ε_i strength in the opposite low-temperature limit of $K \to 0$. Moreover, ρ_i is a monotonically decreasing function for strategies with maximal ε_i as a function of K, but it monotonically increases for all other strategies.

Specifically, these probabilities for the self-dependent games that are of interest in this chapter are

$$\rho_1 = \frac{\mathrm{e}^{zh'/K}}{\mathrm{e}^{zh'/K} + (n-1)} \qquad \text{and} \qquad \rho_i = \frac{1}{\mathrm{e}^{zh'/K} + (n-1)} \quad \text{for } i > 1 \tag{5.8}$$

in the game $h'\mathbf{e}(1;n)$ and

$$\rho_1 = \rho_2 = \frac{\mathrm{e}^{zh''/K}}{2\mathrm{e}^{zh''/K} + (n-2)} \qquad \text{and} \qquad \rho_i = \frac{1}{2\mathrm{e}^{zh''/K} + (n-2)} \quad \text{for } i > 2 \tag{5.9}$$

when the payoff matrix is $h''\,[\mathbf{e}(1;n)+\mathbf{e}(2;n)]$ [135].

5.2 The symmetry-breaking game

Adding a self-dependent component to the elementary coordination game in the way prescribed by Eq. (5.1) has somewhat different effects on the system and its phase transition depending on the number of available strategies and the sign and strength of the self-dependent game component [135].

In the mean-field approximation, the free energy density of the game system is given by

$$\varphi^{(1)} = \frac{z}{2}[p_1(1)-p_1(2)]^2 + zh'p_1(1) - K\sum_{i=1}^{n} p_1(i)\ln p_1(i) \tag{5.10}$$

from which we can derive a set of equations for an approximation of the equilibrium one-site probabilities of finding players following each strategy. Their numerical solutions predict the following changes in the system's behavior with respect to the elementary coordination game considered in Chapter 4.

When $n \leq n_{\text{th}}^{(1)}$ and the elementary coordination game undergoes a continuous phase transition, its extension with a symmetry-breaking self-dependent component abolishes the phase transition (see Figure 5.1a). It still remains true that the system is homogeneously ordered in the low-temperature limit and completely disordered in the high-temperature limit, but the transition becomes smooth.

If $h' > 0$, strategy 1 is the most and strategy 2 is the least frequent, and neutral strategies are followed by equal shares of the population at all finite noise levels. Notice that in the pure elementary coordination game either strategy 1 or strategy 2 could form the thus twice degenerate ordered phase, which is not the case when $h' \neq 0$. The frequency of strategy 1 monotonically decreases from 1 to $1/n$ as the temperature is increased from 0 to infinity, while the frequencies of the remaining strategies monotonically increase from 0 and tend to $1/n$ from below.

On the other hand, setting $h' < 0$ reverses the order of the strategy frequencies, because in this case strategy 2 offers the highest average payoff. As a result, the frequency of strategy 2 is a monotonically decreasing function of the temperature that goes to 1 in the low-temperature limit, while this time strategy one has the lowest frequency that monotonically increases with temperature. The frequency of the neutral strategies remains between the frequencies of the coordinated strategies, but it ceases to be a monotonic function of the noise level, because it surpasses its asymptotic $K \to \infty$ limit of $1/n$ at a finite noise level. This is explained by the fact that the self-dependent component of the

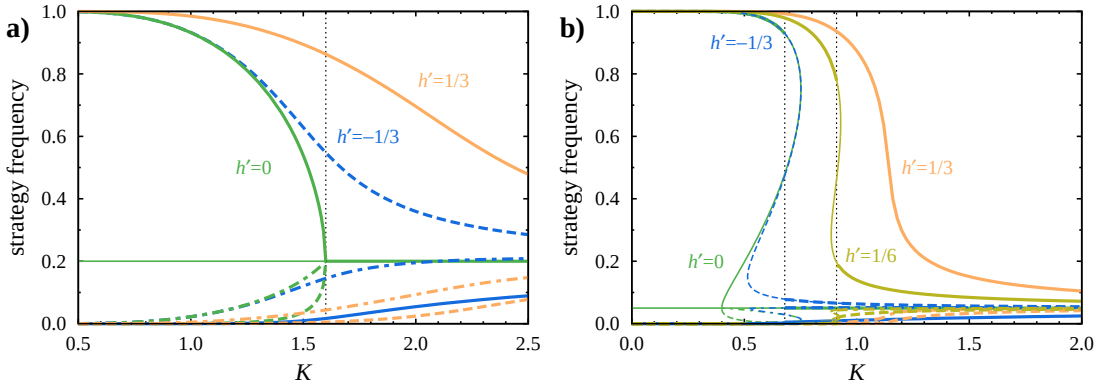

FIGURE 5.1. Strategy frequencies in the mean-field approximated $n = 5$ elementary coordination game with a symmetry-breaking self-dependent component. Different colors correspond to different values of the h' strength parameter; solid, dashed, and dash-dotted lines represent the frequencies of strategy 1, strategy 2, and the neutral strategies, respectively. Stable states are drawn with thick lines.

game only penalizes the choice of the first strategy when h' is negative. This means that in the high-temperature limit, when the effects of spontaneous coordination are suppressed, the self-dependent component of the game should determine the asymptotics, which would suggest that strategies with maximal ε_i (in the present case all strategies except strategy 1) have frequencies that tend to $1/n$ from above, while remaining frequencies approach $1/n$ from below. The actual asymptotics of the game are of course also affected by the interplay between the self-dependent and coordination components: The increase in the number of 2-strategists induced by the self-dependent component also increases their payoff through the coordination component which further boosts the number of 2-strategists and discourages choosing strategy 1.

In the $n > n_{\text{th}}^{(1)}$ case, the first-order phase transition exhibited by the elementary coordination game is not necessarily abolished by the introduction of the symmetry-breaking self-dependent component, as can be seen in Figure 5.1b. In fact, the transition only vanishes when h' is above a positive critical value h'_{c}. In the low-temperature limit the system is homogeneously ordered and players coordinate on strategy 1. As the temperature is increased, the share of 1-strategists decreases, while the number of players following the other strategies increases, and again $\rho_1 > \rho_i = \rho_j > \rho_2$ holds at all temperatures for all $i, j > 2$; the strategy frequencies are again smooth, monotonical, and tend to $1/n$ in the $K \to \infty$ limit, like in the previously discussed lower n case.

Most of the above-mentioned properties remain true for $0 < h' < h'_{\text{c}}$ except for the smoothness of the strategy frequencies: The system still undergoes a first-order phase transition if the self-dependent component is not strong enough, though some of its characteristics do change. In this case, the transition occurs between two branches of the same locally smooth multivalued function, as opposed to the $h' = 0$ elementary

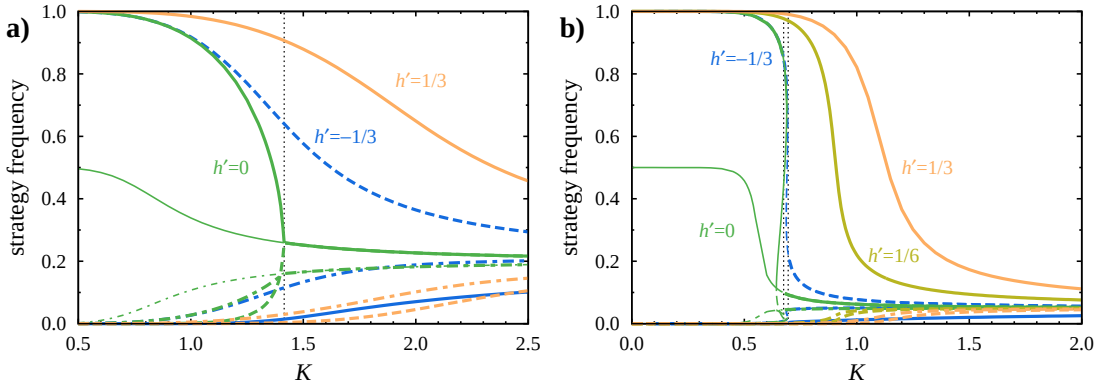

FIGURE 5.2. Pair approximated strategy frequencies in the $n = 20$ game defined by the payoff matrix $\mathbf{A}'$ in Eq. (5.1). For an explanation of what the lines represent, see the caption to Figure 5.1.

coordination game, whose transition happens between two states that are not analytically connected. The presence of the self-dependent component also changes the critical temperature of the transition, which becomes higher as h' is increased.

The $h' < 0$ game is similar to the previous $0 < h' < h'_c$ system in that it possesses a similar first-order transition. The chief difference, just like in the $n < n_{\text{th}}^{(1)}$ case, is that due to the punishment meted out through the self-dependent component to players following strategy 1, the numerical order of the strategy frequencies is inverted, and strategy 2 is chosen most frequently at all temperatures. The non-monotonicity of the frequency of neutral strategies can be observed in this case as well. In this regime, the critical temperature only changes very slightly, it increases if the magnitude of $h' < 0$ is increased.

As the data plotted in Figure 5.2 illustrate, the pair approximation analysis of the game defined by the payoff matrix $\mathbf{A}'$ also results in the same qualitative findings as those obtained using the mean-field approach above.

5.3 The symmetry-retaining game

The symmetry-retaining version of the game defined by the payoff matrix $\mathbf{A}''$ in Eq. (5.2) deviates from its constituent elementary game in a more uniform way than its symmetry-breaking counterpart $\mathbf{A}'$. It turns out that tuning h'' can change the order of the phase transition or even abolish it completely, regardless of the number of available strategies [135]. This section discusses the macroscopic equilibrium properties of this game based on results obtained within the framework of the mean-field approximation method. Figure 5.3a shows the mean-field approximated equilibrium strategy frequencies for the $n = 5$-strategy version of the game. For different n, we find qualitatively similar

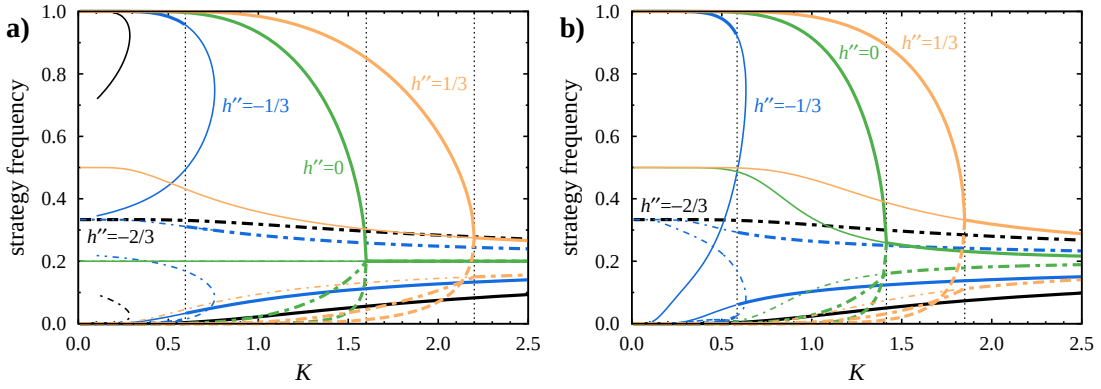

FIGURE 5.3. Strategy frequencies in a) the mean-field approximated and b) pair approximated $n = 5$ elementary coordination game with an added self-dependent component that retains the symmetry of the coordinated strategies, whose payoff matrix is given by Eq. (5.2). Line types and colors were chosen the same way as in Figure 5.1.

solutions. Furthermore, these findings are also supported by the pair approximation method, as suggested by Figure 5.3b.

When h'' is above a threshold value h''_c, the system possesses a continuous phase transition. Above a critical temperature, the system is in a disordered state, in which the two coordinated strategies are followed by equal shares of the population. In the mean-field approximation, the disordered phase is accurately described by the equilibrium state of the self-dependent component of the game, whose strategy frequencies are given by Eq. (5.9). Accordingly, this disordered state tends to a uniform distribution of strategies as K goes to infinity, while either the coordinated or neutral strategies vanish in the opposite $K \to 0$ limit, depending on the sign of h''. As the temperature of the system is lowered below the critical temperature, however, the disordered phase loses its stability, the symmetry of the two coordinated strategies is spontaneously broken in a continuous manner, and an ordered phase is formed. As before, we will again use strategy label 1 for the majority and 2 for the minority coordinated strategy in the ordered phase, without any loss of generality. The frequency of the majority coordinated strategy goes to 1 in the low noise limit, while the remaining strategies vanish. In essence, the system is very similar to the $n < n_{\text{th}}$ elementary coordination game, even if n is actually higher than n_{th}. Consequently, the lower bound of this parameter regime, h''_c is determined by n, and we find that the higher n is, the higher h''_c becomes. The critical temperature of the phase transition is also an increasing function of h'', as can be seen in Figure 5.4.

As a generalization of the case of the elementary coordination game and Eq. (4.7), the stability analysis of the disordered state in the mean-field approximation leads to a formula for the critical temperature of the system's continuous phase transitions in the

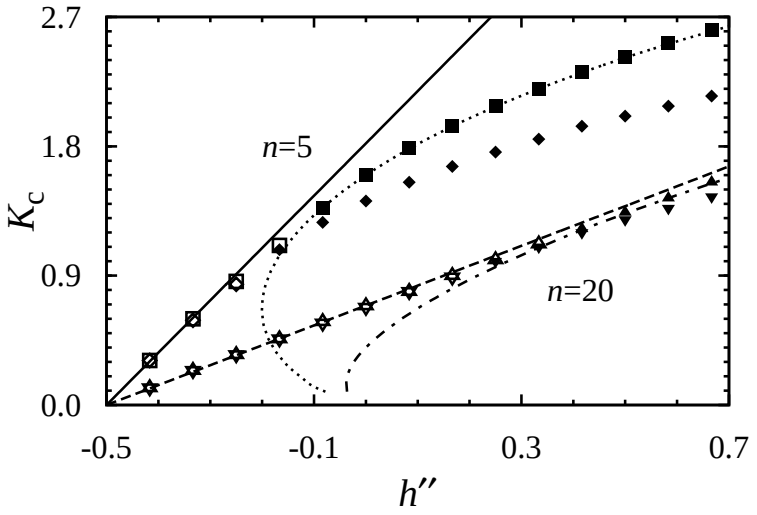

FIGURE 5.4. Critical temperatures in the game defined by the payoff matrix $\mathbf{A}''$ in Eq. (5.2) as a function of the strength h'' of the self-dependent component for $n = 5$ and 20 available strategies, mean-field (pair) approximation results are represented by boxes (diamonds) and upward (downward) pointing triangles, respectively. Continuous transitions are indicated by filled symbols. Solutions of the implicit formula Eq. (5.11) for the critical temperature of the continuous transition are drawn with dotted and dash-dotted lines. The solid and dashed lines correspond to the results of the invasion front velocity method [Eq. (5.12)].

following implicit form:

$$K_{\mathrm{c}}^{(1\mathrm{c})}(h'',n) = 2z\rho_1[K_{\mathrm{c}}^{(1\mathrm{c})}(h'',n)] = 2z\frac{\mathrm{e}^{zh''/K_{\mathrm{c}}^{(1\mathrm{c})}(h'',n)}}{2\mathrm{e}^{zh''/K_{\mathrm{c}}^{(1\mathrm{c})}(h'',n)}+(n-2)}. \tag{5.11}$$

When the strength of the self-dependent component is set below h''_{c} but still exceeds another critical value h''_{f}, the system's behavior resembles that observed in the $n > n_{\mathrm{th}}$ elementary coordination game. An order-disorder phase transition can still be observed, but it is of the first order instead of being continuous. Otherwise, most macroscopic properties of the phases are carried over from the $h'' > h''_{\mathrm{c}}$ game to this parameter region. For example, the numerical order and the asymptotics of the equilibrium strategy frequencies in both the high- and low-temperature limit remain the same, and increasing h'' is still accompanied by an increase in the critical temperature of the phase transition.

Exploiting the similarity of the symmetry-retaining game to the elementary coordination game, the critical temperature of first-order transitions can again be estimated using the invasion front method introduced in Section 4.4. Comparing invasion velocities for the step-like neutral-coordinated interface pictured in Figure 4.13 yields the following

approximation:

$$K_{\mathrm{c}}^{(\mathrm{if})}(h'', n) \simeq \frac{2 + 4h''}{\ln(n-2)}, \tag{5.12}$$

which is analogous to and generalizes the result in Eq. (4.15). As Figure 5.4 shows, this approximation again proves better the deeper the system is inside the first-order transition regime, that is, the higher n and the lower h'' is.

For h'' below h''_{f}, the coordinated ordered phase loses its stability at all temperatures to the disordered phase (described by Eq. (5.9) in the mean-field approximation), which in turn abolishes the phase transition. With this in mind, h''_{f} is the strength of the self-dependent component for which the potential of the ordered and disordered phases is equal in the low-temperature $K \to 0$ limit. In the ordered phase this means uniform coordination with an average potential of $\mathcal{U}/N = z/2 + zh''$. The low-temperature limit of the disordered phase depends on the sign of h''. When it is positive, the disordered state is dominated by coordinated strategies, and the potential goes to $\mathcal{U}/N = zh''$, which is clearly lower than its counterpart in the ordered phase. Conversely, there are only neutral strategies in the disordered state, so the average potential is $\mathcal{U}/N = 0$. Comparison with the ordered state yields $h''_{\mathrm{f}} = -1/2$, regardless of n or z, and valid for the system without using any kind of approximation.

5.4 Bunching of neutral strategies

The results presented in the previous section show remarkable similarity to those obtained in the elementary coordination game of Chapter 4, with the opposite of the self-dependent component's strength $-h''$ seemingly playing a similar role to the number of available strategies n.

To shed light on the precise nature of this similarity, let us first bunch together the $n-2$ interchangeable neutral strategies of the payoff matrix $\mathbf{A}''$ [for a definition see Eq. (5.2)] and determine the payoff matrix of the corresponding three-strategy game $\widetilde{\mathbf{A}}''_{n-2}$. We can write the logit strategy update rates [Eq. (3.2)] for $\mathbf{A}''$ in the following way:

$$w(\mathbf{s}_x \to \mathbf{s}'_x) = \frac{\mathrm{e}^{[d_x(\mathbf{s}'_x, \mathbf{s}_{-x}) + zh'']/K}(\delta_{1,\mathbf{s}'_x} + \delta_{2,\mathbf{s}'_x}) + (1 - \delta_{1,\mathbf{s}'_x} - \delta_{2,\mathbf{s}'_x})}{\mathrm{e}^{[d_x(1,\mathbf{s}_{-x}) + zh'']/K} + \mathrm{e}^{[d_x(2,\mathbf{s}_{-x}) + zh'']/K} + (n-2)}, \tag{5.13}$$

where $\delta_{i,j}$ denotes Kronecker's delta, $d_x(\mathbf{s}'_x, \mathbf{s}_{-x})$ is the total payoff of player x in the elementary coordination game $\mathbf{d}(1, 2; n)$ when playing strategy $\mathbf{s}'_x$ in surrounding strategy environment $\mathbf{s}_{-x}$, and we exploited the linearity of combining payoff components, the self-dependent property of $h''[\mathbf{e}(1; n) + \mathbf{e}(2; n)]$, and the neutrality of strategies 3 through n. Bunching the neutral strategies together involves replacing the $n-2$ neutral

strategies with a single strategy $\tilde{3}$ whose logit rate is equal to the total rate of choosing any one of the original neutral strategies, while keeping the coordinated strategies, their payoffs, and switching rates the same. Because of the neutrality of the replaced strategies, the latter condition can easily be satisfied by simply truncating the payoff components that contribute to the subgame defined by the coordinated strategies, that is, replacing $\mathbf{d}(1,2;n)$ and $h''[\mathbf{e}(1;n)+\mathbf{e}(2;n)]$ with $\mathbf{d}(1,2;3)$ and $h''[\mathbf{e}(1;3)+\mathbf{e}(2;3)]$ respectively. This leaves

$$\widetilde{w}(\widetilde{\mathbf{s}}_x \to \tilde{3}) = \sum_{\mathbf{s}_x=3}^{n} w(\mathbf{s}_x \to \mathbf{s}'_x) = \frac{n-2}{\mathrm{e}^{[\widetilde{d}_x(1,\widetilde{\mathbf{s}}_{-x})+zh'']/K} + \mathrm{e}^{[\widetilde{d}_x(2,\widetilde{\mathbf{s}}_{-x})+zh'']/K} + (n-2)} \tag{5.14}$$

to be satisfied, which boils down to the condition

$$\mathrm{e}^{\widetilde{u}_x(\tilde{3},\widetilde{\mathbf{s}}_{-x})/K} = n-2 = \mathrm{e}^{\ln(n-2)} \tag{5.15}$$

that prescribes a self-dependent component paying $K\ln(n-2)/z$ to $\tilde{3}$-strategists. Here $\widetilde{u}_x$ and $\widetilde{d}_x$ are the payoff functions of $\widetilde{\mathbf{A}}''_{n-2}$ and the three-strategy elementary coordination game. Of course, we may also shift the payoffs of the game by adding an arbitrary irrelevant component, for instance $-[K\ln(n-2)/z]\mathbf{i}(3)$, which leads to the bunched three-strategy equivalent payoff matrix

$$\widetilde{\mathbf{A}}''_{n-2} = \mathbf{d}(1,2;3) + \left[h'' - \frac{\ln(n-2)}{z}K\right][\mathbf{e}(1;3)+\mathbf{e}(2;3)]\,. \tag{5.16}$$

This is also an elementary coordination game with a symmetry-retaining self-dependent component in the mold of $\mathbf{A}''$ with just a single available neutral strategy and a self-dependent component whose strength depends on the temperature K of the system. In fact, it is exactly the temperature-dependent part (and that alone) that emulates the presence of $n-2$ neutral strategies by bunching them together. In other words, the extension of any n-strategy game by k neutral strategies that is played on a z-regular network can be reduced to the truncated $(n+1)$-strategy version of the game with an additional temperature-dependent self-dependent component $\widetilde{h}''_k\mathbf{e}(n+1;n+1)$, where

$$\widetilde{h}''_k = \frac{\ln k}{z}K. \tag{5.17}$$

5.5 Equivalence to the Blume–Capel model

Bunching the neutral strategies in the symmetry-retaining game $\mathbf{A}''$ allows us to directly connect it to an established model of statistical physics, the zero-field Blume-Capel model.

The zero-field Blume–Capel model [136–139] is defined [140] by the spin-1 Hamiltonian

$$\mathcal{H} = -\sum_{\langle ij \rangle} \sigma_i \sigma_j + \Delta \sum_i \sigma_i^2, \tag{5.18}$$

where the spin variables σ_i take on one of the values $+1$, -1, or 0, the parameter Δ is called crystal-field coupling, and $\langle ij \rangle$ indicates summation over nearest neighbor pairs of sites. This model translates to the game theoretic model defined by the payoff matrix

$$\mathbf{A}^{(\mathrm{BC})} = \begin{pmatrix} 1 - 2\frac{\Delta}{z} & -1 - 2\frac{\Delta}{z} & -\frac{\Delta}{z} \\ -1 - 2\frac{\Delta}{z} & 1 - 2\frac{\Delta}{z} & -\frac{\Delta}{z} \\ -\frac{\Delta}{z} & -\frac{\Delta}{z} & 0 \end{pmatrix} \tag{5.19}$$

if spin states $+1$, -1, and 0 are mapped onto strategies 1, 2, and 3, respectively. This game is potential-equivalent to

$$\widetilde{\mathbf{A}}^{(\mathrm{BC})} = \mathbf{d}(1,2;3) - \frac{\Delta}{z}\left[\mathbf{e}(1;3) + \mathbf{e}(2;3)\right], \tag{5.20}$$

which has the same structure as the bunched payoff matrix $\widetilde{\mathbf{A}}''_{n-2}$. As a result, any elementary coordination game with a symmetry-retaining self-dependent component can be mapped onto the Blume–Capel model by setting

$$\Delta = K \ln(n-2) - z h''. \tag{5.21}$$

The bunching mechanism also allows us to actually realize elementary coordination games with non-integer strategy numbers. Our previously presented results can also be extended to these games by simply considering n as a continuous variable and assuming analyticity in n.

The Blume–Capel model hosts two stable phases, as shown by its phase diagram in Figure 5.5. One of them is a ferromagnetic, ordered phase characterized by the alignment of either $+1$ or -1 spin states, which corresponds to coordination on either of the first two strategies of the corresponding game $\widetilde{\mathbf{A}}^{(\mathrm{BC})}$. The other, paramagnetic phase is either completely disordered at high temperatures or dominated by the 0 spin state at low temperatures and high crystal fields. The transition between the two phases is continuous and belongs to the Ising universality class in the former case, but it is of the first order in the latter case [136–140].

The parametrization Eq. 5.21 of the bunched game $\widetilde{\mathbf{A}}''_{n-2}$ traces a straight line in the two-dimensional parameter space of the Blume–Capel model for any fixed n and h'' as the system's temperature K is changed, and the model's phase transitions occur when the line intersects the Blume–Capel phase boundary (see Figure 5.5 for examples).

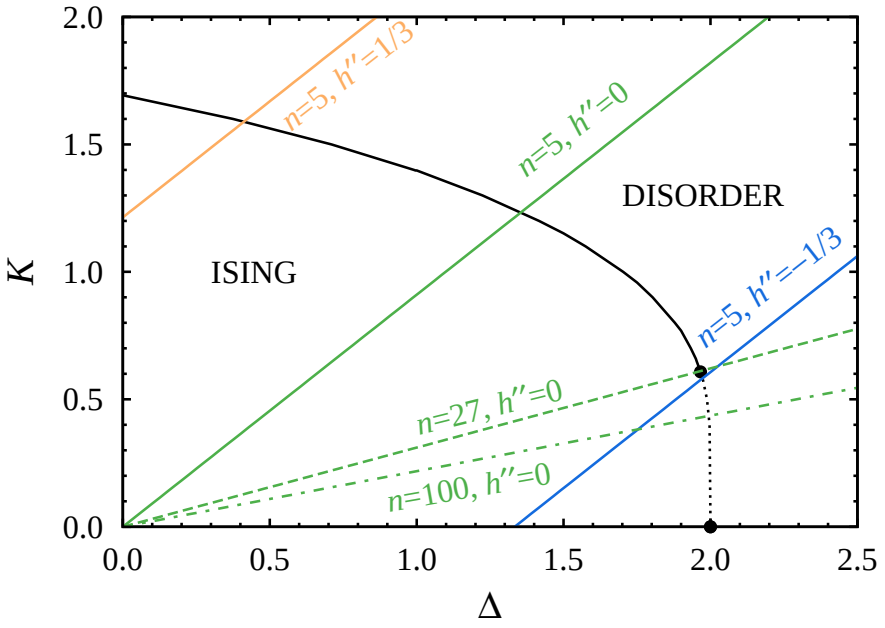

FIGURE 5.5. Comparison of the $\widetilde{\mathbf{A}}''_{n-2}$ bunched elementary coordination game to the phase diagram of the Blume–Capel model on the square lattice. The black lines indicate the phase boundary of the Blume–Capel model between its Ising-ordered and disordered phase, transitions across the solid part of the curve are continuous and belong to the Ising universality class, while transitions across the dotted line are of the first-order. The colored lines trace Δ as a function of the temperature K for different $\widetilde{\mathbf{A}}''_{n-2}$ models. Different line types and line colors correspond to different value of n and h'', respectively. The data used to draw the phase boundary were taken from Ref. [140], which compiles results from Refs [140–144].

Comparison with the phase diagram reveals that increasing the number of strategies n decreases the slope of the line, which generally drives the system towards the first-order transition regime and decreases the critical temperature. Conversely, the strength of the self-dependent component h'' determines the intersect of the parameter line, which means that for high h'' the phase transition is continuous and expected to belong to the Ising universality class. For lower h'', the transition may be of the first order, and for sufficiently low h'' ($h'' < -1/2$) the line does not intersect the phase boundary for any positive K, which means that the system exhibits no phase transition. All of these qualitative findings are in excellent agreement with those reported in Chapters 4 and 5 and Refs. [112, 135].

The value of n_{th}, the highest number of strategies for which the elementary coordination game still possesses a continuous phase transition, can also be estimated by exploiting the equivalence of the bunched elementary coordination game to the Blume–Capel model. In the Blume–Capel model, the continuous and first-order segments of the phase boundary are separated by a tricritical point, which is approximately located at $\Delta_{\mathrm{t}} = 1.966$, $K_{\mathrm{t}} = 0.608$ [140]. Since elementary coordination games are represented by straight lines that go through the origin of the Blume–Capel model's parameter space, the line

separating $n \leq n_{\mathrm{th}}$ and $n > n_{\mathrm{th}}$ elementary coordination games has to pass through both the origin and the tricritical point. Thus, after plugging $h'' = 0$ and the coordinates of the tricritical point into Eq. (5.21), we get

$$n_{\mathrm{th}} = \left\lfloor \mathrm{e}^{\Delta_{\mathrm{t}}/K_{\mathrm{t}}} + 2 \right\rfloor = 27. \tag{5.22}$$

The invisible states of the extended Potts model from Section 4.5 can also be bunched together in a similar way. For the $q = 2$ Ising version of the model, this also leads to an established model of statistical physics, the Blume–Emery–Griffiths model [117, 123, 124, 145, 146].

Chapter 6

Maximally nonoverlapping coordination games

In Chapters 4 and 5 games with a single elementary coordination component were discussed. An obvious next step in a systematic investigation of the interplay between different game components is the examination of games composed of multiple elementary coordinations. Of course, there are numerous different ways to combine coordination games when the number of available strategies is high. In this chapter, we study a highly specific set of games we call maximally nonoverlapping coordination games. These games have an even $n = 2m$ number of strategies and are made up of m elementary coordinations whose coordinated strategies do not overlap, that is, each strategy is involved in only one of the constituent elementary coordinations. The choice of these models is motivated by two considerations. First, we may reasonably expect the interplay between nonoverlapping components to have a more comprehensible effect than games with more complex structures. For example, we will see that at the mean-field approximation level a composite game essentially boils down to a competition between its nonoverlapping components, and deviations from this predicted behavior in simulation results may indicate more subtle interplay effects. Second, we can also expect that the presence of neutral strategies in a general game has a very similar entropic effect to the one observed in the elementary coordination game and otherwise only obfuscates other interplay effects; in "maximal" games without neutral strategies, however, these effects should be much more prominent and easier to identify.

The payoff matrix of a general maximally nonoverlapping coordination game [147] made up of m elementary coordinations can be written as

$$\mathbf{A}^{(m)} = \sum_{i=1}^{m} \mathbf{d}(2i-1, 2i; 2m) \tag{6.1}$$

after an appropriate relabeling of the strategies. Since it is a purely coordination-type game, its potential and payoff matrices are identical.

In this chapter, we first analyze the properties of maximally nonoverlapping coordination games at the mean-field approximation level. The rest of the chapter concentrates on analytic and Monte Carlo simulation results for the four-strategy or two-Ising-pair version of the game, its connection to established models of statistical physics, and its critical properties, and then moves on to comparatively discuss the six-strategy version of the game.

6.1 Mean-field approximation

The mean-field approximated free energy of the general m-Ising-pair maximally coordinated nonoverlapping coordinated game is given by

$$\varphi^{(1)} = \frac{z}{2}\sum_{i=1}^{m}[p_1(2i-1) - p_1(2i)]^2 - K\sum_{j=1}^{2m} p_1(j)\ln p_1(j). \tag{6.2}$$

Under the normalization constraint, the possible competing equilibrium states of the system satisfy the stationary point equations Eq. (3.15), which can be solved numerically. Figure 6.1a shows solutions found for the $m = 4$-Ising-pair, eight-strategy game.

When the temperature is high, we find only one solution, the totally disordered state, in which players choose their strategy according to the uniform distribution, that is, the one-site probabilities $p_1(i)$ are all equal to $1/n$ for all strategies. As a result, both the expected average payoff and the potential vanish in the disordered state.

At lower temperatures, m other types of solutions emerge. (See Figure 6.1.) In contrast to the disordered state, these all break some of the symmetries of the strategies. More precisely, they each break the symmetry of a different number of the m coordinated strategy pairs while keeping the pairs themselves interchangeable. So in the $2^k\binom{m}{k}$-times degenerate state that breaks the symmetry of k pairs, for example, k of the $2m$ strategies that belong to different elementary coordination components are present in the system with equal and higher frequencies than they are in the disordered state, while the ratios of players following their coordinated counterparts are also equal to each other but fall below $1/n$. The frequencies of the remaining $2(m-k)$ strategies also drop equally, albeit to a smaller extent than the frequencies of the minority strategies. As their symmetry remains unbroken, these $(m-k)$ coordinated pairs do not contribute to the potential term of the free energy, so they effectively become neutral. In the low-temperature $K \to 0$ limit, the one-site probability distribution $p_1(i)$ tends to a uniform

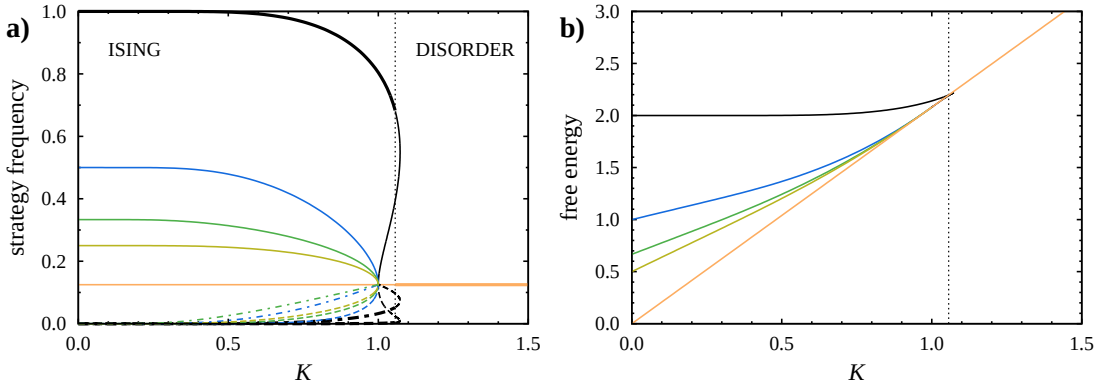

FIGURE 6.1. Competing equilibrium states in the mean-field approximated eight-strategy maximally nonoverlapping coordination game. Panel a) and panel b) show their strategy frequencies and free energy, the five different colors correspond to the five competing states: the black, blue, green, and yellow (progressively lighter) curves belong to the states that break the symmetry of one, two, three, and four of the coordinated pairs, respectively, while the orange (lightest) lines stand for the disordered state. In panel a), the frequencies of majority, neutral, and minority strategies are represented by different line types. Thick lines highlight the stable state with the highest free energy.

distribution over the k majority strategies, and consequently the state's average free energy goes to $\frac{z}{2k}$, so the less pair symmetries the state breaks, the higher its limiting free energy becomes.

It turns out that the order of the free energies of the different symmetry-breaking states remains the same in the whole low-temperature regime (see Figure 6.1), and the stable equilibrium state breaks the symmetry of only one of the coordinated strategy pairs. Consequently, the frequencies of the remaining $2m-2$ strategies are all equal, which reduces the free energy expression in Eq. (6.2) to the one in Eq. (4.3) that is the mean-field approximated free energy of the $\mathbf{d}(1,2;2m)$ elementary coordination game. Accordingly, the state itself is also identical to the mean-field approximated ordered state of $\mathbf{d}(1,2;2m)$. In a nutshell, the two models are mean-field equivalent, and the results and predictions regarding the general behavior and the phase trasitions of the model reported in Section 4.1 also apply to maximally nonoverlapping coordination games.

In the following, we will show, through the examples of the two- and three-Ising-pair games, that this equivalence does not extend to the experimental Monte Carlo realizations of these systems and highlight some of their differences, mostly focusing on their critical properties.

6.2 The two-Ising-pair game

The four strategy maximally nonoverlapping game is a combination of two elementary, Ising-type coordination games that do not share any of their coordinated strategies and reward coordination equally [147]. This description applies to three different-looking payoff matrices:

$$\mathbf{A}^{(2)} = \mathbf{d}(1,2;4) + \mathbf{d}(3,4;4) = \begin{pmatrix} 1 & -1 & 0 & 0 \\ -1 & 1 & 0 & 0 \\ 0 & 0 & 1 & -1 \\ 0 & 0 & -1 & 1 \end{pmatrix}, \tag{6.3}$$

$$\mathbf{d}(1,3;4) + \mathbf{d}(2,4;4) = \begin{pmatrix} 1 & 0 & -1 & 0 \\ 0 & 1 & 0 & -1 \\ -1 & 0 & 1 & 0 \\ 0 & -1 & 0 & 1 \end{pmatrix}, \tag{6.4}$$

$$\mathbf{d}(1,4;4) + \mathbf{d}(2,3;4) = \begin{pmatrix} 1 & 0 & 0 & -1 \\ 0 & 1 & -1 & 0 \\ 0 & -1 & 1 & 0 \\ -1 & 0 & 0 & 1 \end{pmatrix}. \tag{6.5}$$

The first of these in Eq. (6.3) is of course the "canonical" maximally nonoverlapping payoff matrix defined by Eq. (6.1). The other two payoff matrices can easily be transformed into the first one by simply exchanging the labels of strategies 2 and 3 in Eq. (6.4) and 2 and 4 in Eq. (6.5), so the games defined by the three payoff matrices are clearly equivalent to each other.

Both of the "noncanonical" payoff matrices are used in the literature of statistical physics to introduce the model called the four-state clock model [134, 148, 149], which uses equidistantly spaced angles $\theta = \frac{2\pi i}{n}$ ($i = 1,\ 2,\ 3,$ or $n = 4$) to characterize possible spin orientations and derives from them the nearest neighbor interaction energy $-\cos(\theta_x - \theta_y)$.

Importantly, the four-strategy clock model is equivalent to a system made up of two identical independent uncoupled Ising models with dimensionless coupling coefficients of $1/2$ [148]. In fact, this equivalence relation is a special case of a more general connection involving the so-called Ashkin–Teller model and a coupled double Ising-type model.

The Ashkin–Teller model [150] is defined by the payoff matrix

$$\mathbf{A}^{(\mathrm{AT})} = \begin{pmatrix} \varepsilon & \varepsilon' & \varepsilon'' & \varepsilon''' \\ \varepsilon' & \varepsilon & \varepsilon''' & \varepsilon'' \\ \varepsilon'' & \varepsilon''' & \varepsilon & \varepsilon' \\ \varepsilon''' & \varepsilon'' & \varepsilon' & \varepsilon \end{pmatrix}. \tag{6.6}$$

In terms of elementary games, it can also be written as

$$\begin{aligned} \mathbf{A}^{(\mathrm{AT})} = (\overline{\varepsilon} - \varepsilon')[\mathbf{d}(1,2;4) + \mathbf{d}(3,4;4)] + (\overline{\varepsilon} - \varepsilon'')[\mathbf{d}(1,3;4) + \mathbf{d}(2,4;4)] + \\ + (\overline{\varepsilon} - \varepsilon''')[\mathbf{d}(1,4;4) + \mathbf{d}(2,3;4)] + \overline{\varepsilon}\mathbf{m}(4), \end{aligned} \tag{6.7}$$

a linear combination of the three forms of the four-strategy maximally nonoverlapping coordination game and the irrelevant game, where we introduced the shorthand notation

$$\overline{\varepsilon} = \frac{\varepsilon + \varepsilon' + \varepsilon'' + \varepsilon'''}{4} \tag{6.8}$$

for the mean of the four defining parameters of the Ashkin–Teller payoff matrix.

Alternatively, the configurations of the Ashkin–Teller model can be represented by introducing two independent Ising spins ($T_x, S_x = \pm 1$) at each site and mapping the two-spin states $(+,+)$, $(+,-)$, $(-,+)$, and $(-,-)$ to strategies 1, 2, 3 and 4, respectively [86, 148, 151, 152]. In this representation, the potential of the pair interaction between players x and y is given by

$$U_{xy} = J_0 + J' S_x S_y + J'' T_x T_y + J_4 S_x S_y T_x T_y, \tag{6.9}$$

where $J_0 = \overline{\varepsilon}$ simply shifts the potential of all configurations, $J' = (\varepsilon + \varepsilon' - \varepsilon'' - \varepsilon''')/4$ and $J'' = (\varepsilon - \varepsilon' + \varepsilon'' - \varepsilon''')/4$ are Ising coupling coefficients in the two spin sectors, and the fourth term couples these Ising models via a four-spin interaction of strength $J_4 = (\varepsilon - \varepsilon' - \varepsilon'' + \varepsilon''')/4$. It may not seem evident in this two-layer Ising spin formulation of the model, but the permutation symmetry of the parameters in the Ashkin–Teller form Eq. (A.2) also implies that the model is invariable under permutations of the parameters J', J'', and J_4 [153]. For a maximally nonoverlapping coordination game, two of the parameters ε', ε'', and ε''' are equal to each other and $\overline{\varepsilon}$, which results in one of the J parameters vanishing that—by the symmetry mentioned above—means that the four-spin interaction term is missing and the two Ising spin sectors are decoupled. The general Ashkin–Teller model is expected to have two phase transitions that coalesce into a single transition when the middle two of the model's defining ε parameters are equal [153–155], which implies that the two-Ising-pair model has only one phase transition.

In Ref. [150] Ashkin and Teller develop a self-duality relation for the model defined by the payoff matrix $\mathbf{A}^{(\mathrm{AT})}$ that then they apply to the special case $\varepsilon' = \varepsilon'' = \varepsilon'''$ equivalent to the four-state Potts model [130, 134] to determine its critical temperature. The very same method can also be used to calculate the critical temperature of the four-strategy maximally nonoverlapping coordination game. In Appendix A, we summarize the relevant results of Ashkin and Teller and rederive a duality relation for the two-Ising-pair coordination game $\mathbf{A}^{(2)}$ already mentioned in Refs. [134, 152]. This relation combined with Kramers and Wannier's argument presented in Refs. [156, 157] gives the critical temperature

$$K_{\mathrm{c}}(2) = \frac{1}{\ln(\sqrt{2}+1)} \approx 1.1346. \tag{6.10}$$

This result coincides with the critical temperature of the two-Ising-pair coordination game's constituent 1/2-strength Ising models [134, 152]. Moreover, it also concurs with the critical temperature reported for the four-state clock model in Ref. [158], which is the product of a different duality-based approach.

By changing the signs of all payoffs, we get an anticoordination version of the game. In this case the above-mentioned duality argument breaks down. On bipartite lattices, however, like the square lattice in question, this anticoordinated system can easily be mapped onto its coordinated counterpart, by exchanging the labels of the anticoordinated strategy pairs on one of the sublattices. This means that two-Ising-pair anticoordinated systems, too, undergo the same type of phase transition, and form sublattice ordered structures under $K_{\mathrm{c}}(2)$. In fact, we can further generalize this result using essentially the same argument: all games made up solely of m non-overlapping, same-strength (either coordinated or anticoordinated) $n = 2m$-strategy elementary coordination games are equivalent to their all-coordinated m-Ising-pair coordination game counterparts on any bipartite lattice.

The existence of the single continuous transition and the value of the critical temperature $K_{\mathrm{c}}(2)$ as derived from the Ashkin–Teller duality relation are also corroborated by our Monte Carlo simulation data [147] presented in Fig 6.2 that place the transition at $K_{\mathrm{c}}^{(\mathrm{MC})}(2) = 1.135(1)$. The temperature dependence of the strategy frequencies is qualitatively similar to the prediction provided by the mean-field approximation. Below the critical temperature the system spontaneously breaks the symmetry of just one of the two coordinated strategy pairs. The lower the temperature is, the more players follow the majority strategy, and in the low-temperature $K \to 0$ limit the system becomes homogeneous, completely ordered. Unlike the mean-field equivalent elementary coordination game (see Fig. 4.7), the two-Ising pair game is completely disordered at all temperatures above the critical temperature, not just in the $K \to \infty$ limit, owing to the higher symmetry of its payoff matrix.

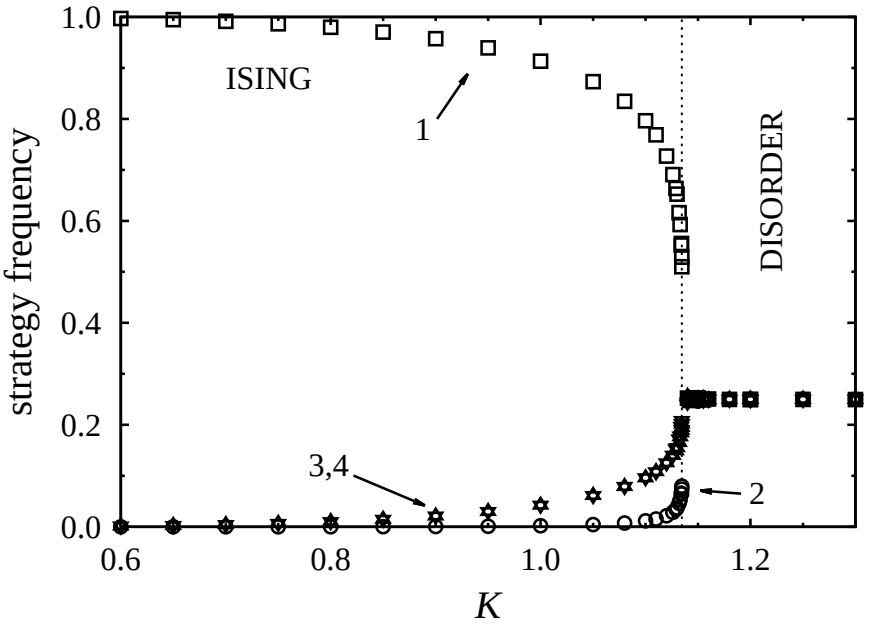

FIGURE 6.2. Continuous phase transition in the two-Ising-pair game, Monte Carlo simulated strategy frequencies.

We extracted critical exponents from the Monte Carlo data to characterize the critical behavior of the phase transition. The results are summarized by Fig. 6.3. Based on the mean-field analysis in Sec. 4.1, we looked at the temperature dependence of the following two order parameters, which are both naturally generalized to arbitrary m-Ising-pair games:

$$M_1(m) = \rho_1 - \rho_2, \tag{6.11a}$$

$$M_2(m) = 1 - 2m\rho_3 = 1 - 2m\rho_j \qquad \text{for } j > 3. \tag{6.11b}$$

The reciprocal relations that give the strategy frequencies as functions of these order parameters are

$$\rho_1 = \frac{1}{2m}\left[1 + (m-1)\,M_2(m) + mM_1(m)\right], \tag{6.12a}$$

$$\rho_2 = \frac{1}{2m}\left[1 + (m-1)\,M_2(m) - mM_1(m)\right], \tag{6.12b}$$

$$\rho_j = \frac{1}{2m}\left[1 - M_2(m)\right] \qquad \text{for } j \geq 3. \tag{6.12c}$$

The first order parameter, $M_1(m)$, is the usual Ising or elementary coordination-type order parameter, while the other, $M_2(m)$, is related to the remaining strategies that are present in the system with equal frequencies. In these definitions, we tacitly assumed strategy 1 to be the majority strategy in the ordered phase and strategy 2 to be its coordinated pair. Both order parameters vanish in the disordered phase and go to 1 as

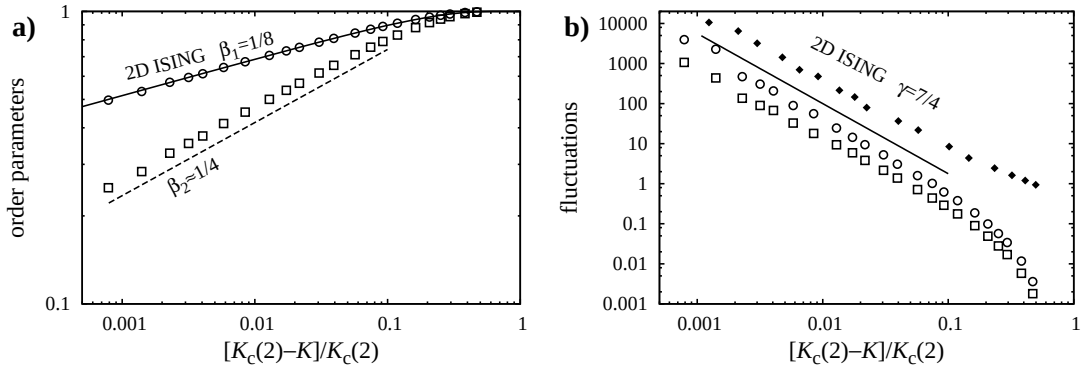

FIGURE 6.3. Log-log plots of the order parameters [panel a)] and fluctuations [panel b)] in the square-lattice two-Ising-pair game. $M_1(2)$ and $\chi_1(2)$ are represented by circles, squares correspond to $M_2(2)$ and $\chi_2(2)$, and filled diamonds stand for $\chi'(2)$.

$K \to 0$ and the system becomes homogeneously ordered. They both exhibit power-law-type behavior close to the critical temperature, that is,

$$M_j(m) \propto [K_c(m) - K]^{\beta_j(m)} . \tag{6.13}$$

The existence of two independent order parameters for the system's phase transition is not unexpected considering that general Ashkin–Teller models can have two phase transitions [153–155].

As Fig. 6.3a demonstrates, we find that the order parameter $M_1(2)$ coincides with Onsager's exact results [129] for the Ising model's order parameter $M_1(1)$ as an algebraic function of the normalized relative noise level $[K_c(m) - K]/K_c(m)$ in the ordered phase. As a result, the critical exponent of $M_1(2)$ equals the corresponding exponent of the Ising universality class, that is, $\beta_1(2) = \beta_1(1) = 1/8$, in accordance with the analytical results presented in Ref. [148]. The second order parameter's critical exponent turns out to be higher, approximately $\beta_2^{(\mathrm{MC})}(2) \simeq 1/4$. Interestingly, this reproduces the prediction of the mean-field approximation insofar as estimating $\beta_2(2)/\beta_1(2) = 2$, which was definitely not the case in the mean-field equivalent elementary coordination game, as there $M_2(m)$ is neither an order parameter, since it does not vanish in the disordered phase, nor does it follow a power law close to criticality. Fitting the 13 data points closest to the critical point in Fig. 6.3a yields the estimates $\beta_1^{(\mathrm{f})}(2) = 0.124(1)$ and $\beta_2^{(\mathrm{f})}(2) = 0.247(2)$.

To further explore the critical properties of the two-Ising-pair game, we also measured the fluctuations of the order parameters that are expected to increase following a power law as the temperature approaches its critical value. We evaluated three such quantities,

which for the general m-Ising-pair game are defined by

$$\chi_1(m) = N\left\{\left\langle[\rho_1(t)-\rho_2(t)]^2\right\rangle - [\rho_1-\rho_2]^2\right\}, \tag{6.14a}$$

$$\chi_2(m) = \frac{N}{2m-2}\sum_{i>2}^{n}\left\langle[\rho_i(t)-\rho_i]^2\right\rangle, \tag{6.14b}$$

$$\chi'(m) = \frac{N}{2m}\sum_{i=1}^{2m}\left\langle\left[\rho_i(t)-\frac{1}{n}\right]^2\right\rangle, \tag{6.14c}$$

where the angled braces denote time-averaging and $\rho_i = \langle\rho_i(t)\rangle$ are the estimates of the equilibrium strategy frequencies. $\chi_1(m)$ and $\chi_2(m)$ measure the fluctuations of the two order parameters below the critical temperature, while $\chi'(m)$ quantifies the fluctuations in the disordered phase. The averaging over strategies with equal equilibrium strategy frequencies was introduced in $\chi_2(m)$ and $\chi'(m)$ to improve statistical accuracy. The three quantities diverge following power laws of the form

$$\chi_i \propto |K - K_c(m)|^{-\gamma_i(m)} \tag{6.15}$$

as the temperature approaches its critical value.

In the two-Ising-pair game, specifically, we find that $\gamma_1^{(f)}(2) = 1.85(4)$, $\gamma_2^{(f)}(2) = 1.69(2)$, and $\gamma'^{(f)}(2) = 1.68(3)$ after fitting the 13 data points that are closest to the critical point in Figure 6.3b for each susceptibility χ_i. These values are remarkably close to each other and $\gamma = 7/4$ that is characteristic of the Ising universality class, especially considering the statistical and systemic errors of our Monte Carlo method.

The estimated values of $\beta_1(2)$ and $\gamma_1(2)$ suggest that the correspondence of the two-Ising-pair game and its constituent half-strength Ising models goes beyond the simple coincidence of their critical temperatures and extends to the coincidence of the universality classes of their phase transitions. In the following section, we show that this robustness of Ising-type behavior does not extend to the three-Ising-pair version of the game.

6.3 The three-Ising-pair game

The three-Ising-pair, six-strategy maximally nonoverlapping game's payoff matrix can always be written as

$$\mathbf{A}^{(3)} = \mathbf{d}(1,2;6) + \mathbf{d}(3,4;6) + \mathbf{d}(5,6;6) \tag{6.16}$$

after appropriately relabeling the strategies and rescaling the payoffs.

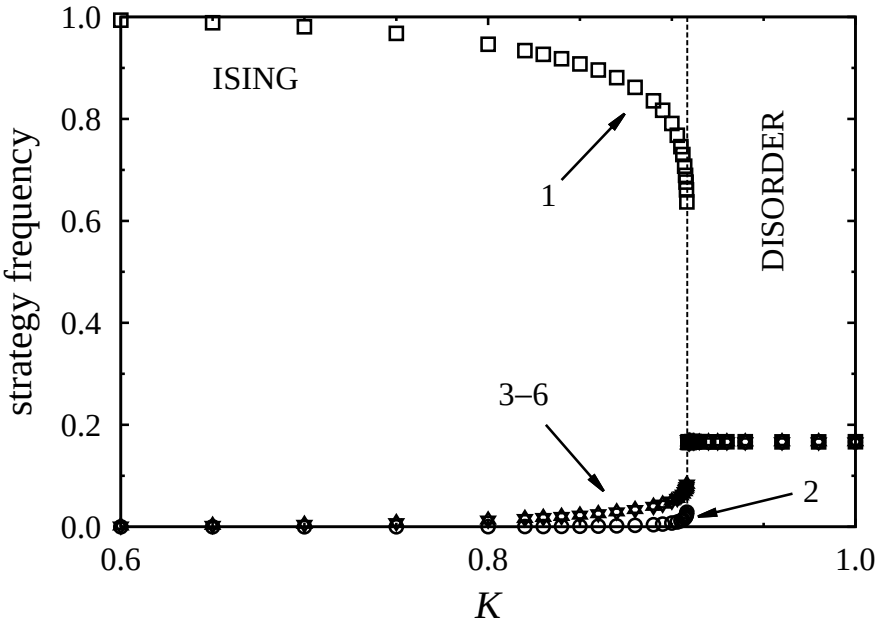

FIGURE 6.4. Monte Carlo simulated strategy frequencies of the three-Ising-pair game.

As illustrated by Fig. 6.4, the temperature dependence of the three-Ising-pair game's strategy frequencies is qualitatively very similar to that found in the two-Ising-pair case, in accordance with the predictions of the mean-field approximation. It exhibits a continuous order-disorder phase transition, whereby a completely disordered phase loses its stability as the temperature is lowered below $K_{\mathrm{c}}^{(\mathrm{MC})}(3) = 0.9084(1)$, accompanied by the spontaneous breaking of the symmetry of just one of the constituent coordinated strategy pairs. This also means that $M_1(3)$ and $M_2(3)$, as defined by Eq. (6.11a) and Eq. (6.11b), are indeed two separate order parameters associated with the same, unique phase transition, which both vanish algebraically as the temperature approaches its critical value from below and go to 1 in the low temperature limit as the system becomes homogeneously ordered.

On closer inspection of the system's critical properties, however, quantitative differences emerge. Fitting the 13 data points of Fig. 6.5 that lie closest to the critical points yields the following estimates: $\beta_1^{(\mathrm{f})}(3) = 0.0745(5)$, $\beta_2^{(\mathrm{f})}(3) = 0.102(1)$, $\gamma_1^{(\mathrm{f})}(3) = 1.33(2)$, $\gamma_2^{(\mathrm{f})}(3) = 1.08(2)$, and $\gamma'^{(\mathrm{f})}(3) = 0.93(2)$. These clearly place the transition outside of the Ising universality class, which is a departure from the two-Ising pair game. Even certain relations between the different exponents cease to hold. The ratio of $\beta_2(3)$ and $\beta_1(3)$ does not match the mean-field prediction, and the three $\gamma(3)$ exponents are definitely not all equal to each other, $\gamma_1(3)$ being larger than the other two, which seem to remain close to each other.

The chief reason that leads to these dissimilarities is probably the subtle difference between the symmetries of the two-Ising-pair and three-Ising-pair payoff matrices. In the

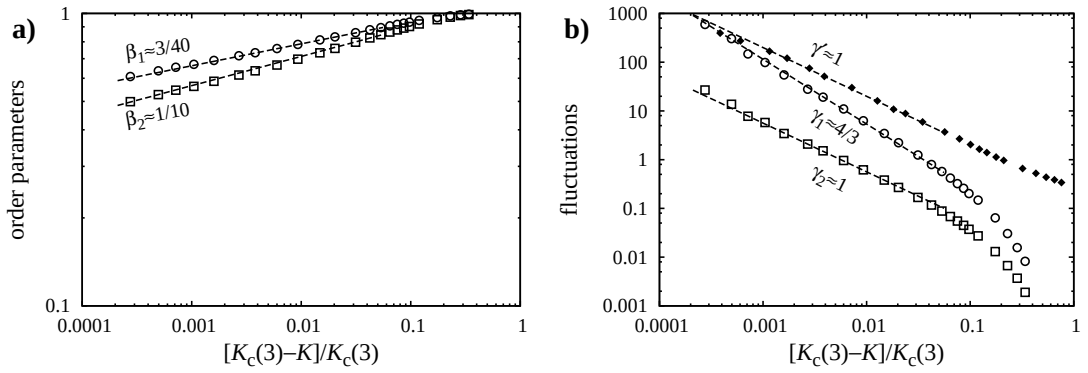

FIGURE 6.5. Critical behavior of the three-Ising-pair game. The notations are the same as in Fig. 6.3.

two-Ising-pair game the two constituent elementary games, $\mathbf{d}(1,2;4)$ and $\mathbf{d}(3,4;4)$, have the same two-element permutation symmetry between each other that connects their coordinated strategy pairs and defines the Ising model. In the three-Ising-pair game, however, the three constituent elementary games, $\mathbf{d}(1,2;6)$, $\mathbf{d}(3,4;6)$, and $\mathbf{d}(5,6;6)$, and the whole game is invariant under their three-element permutations, which is the defining symmetry of the three-state Potts model instead of the Ising model. As mentioned earlier, the ordered phase explicitly breaks the symmetry of one of the Ising symmetric strategy pairs, but also breaks the Potts symmetry of the pairs. Yet the measured critical exponents match neither those of the Ising model nor those of the three-state Potts model, so the transition's universality class must be affected in a nontrivial way by the composition and resulting interplay of the game's elementary components. Nevertheless, it may also be possible to construct further order parameters for the model in such a way that they highlight these underlying symmetries.

Chapter 7

A game of competing Ising and Potts components

This chapter deals with a seemingly more complex game, made up of more elementary coordination components than those discussed previously. Still, we will see that its properties are related to its constituent game components in a more tangible way than what we found in the three-Ising-pair game, for example.

The game's payoff matrix can be described as follows [159]. The first two of its five available strategies define an elementary coordination subgame with the symmetry of the Ising model, whereas the subgame of the remaining three strategies is a pure coordination-type game equivalent to the three-state Potts model, and these two sets of strategies are neutral to each other. The Ising and the Potts subgames are not necessarily of the same strength. We fix the unit of payoffs to be the reward for coordination in the Ising subgame, while α will denote the corresponding Potts payoff. This description is formalized by the payoff matrix

$$\mathbf{A}^{(\mathrm{IP})}(\alpha) = \begin{pmatrix} 1 & -1 & 0 & 0 & 0 \\ -1 & 1 & 0 & 0 & 0 \\ 0 & 0 & \alpha & -\frac{\alpha}{2} & -\frac{\alpha}{2} \\ 0 & 0 & -\frac{\alpha}{2} & \alpha & -\frac{\alpha}{2} \\ 0 & 0 & -\frac{\alpha}{2} & -\frac{\alpha}{2} & \alpha \end{pmatrix} \tag{7.1}$$

that can alternatively be written as

$$\mathbf{A}^{(\mathrm{IP})}(\alpha) = \mathbf{d}(1,2;5) + \frac{\alpha}{2}\left[\mathrm{d}(3,4;5) + \mathrm{d}(3,5;5) + \mathrm{d}(4,5;5)\right] \tag{7.2}$$

in terms of elementary game components.

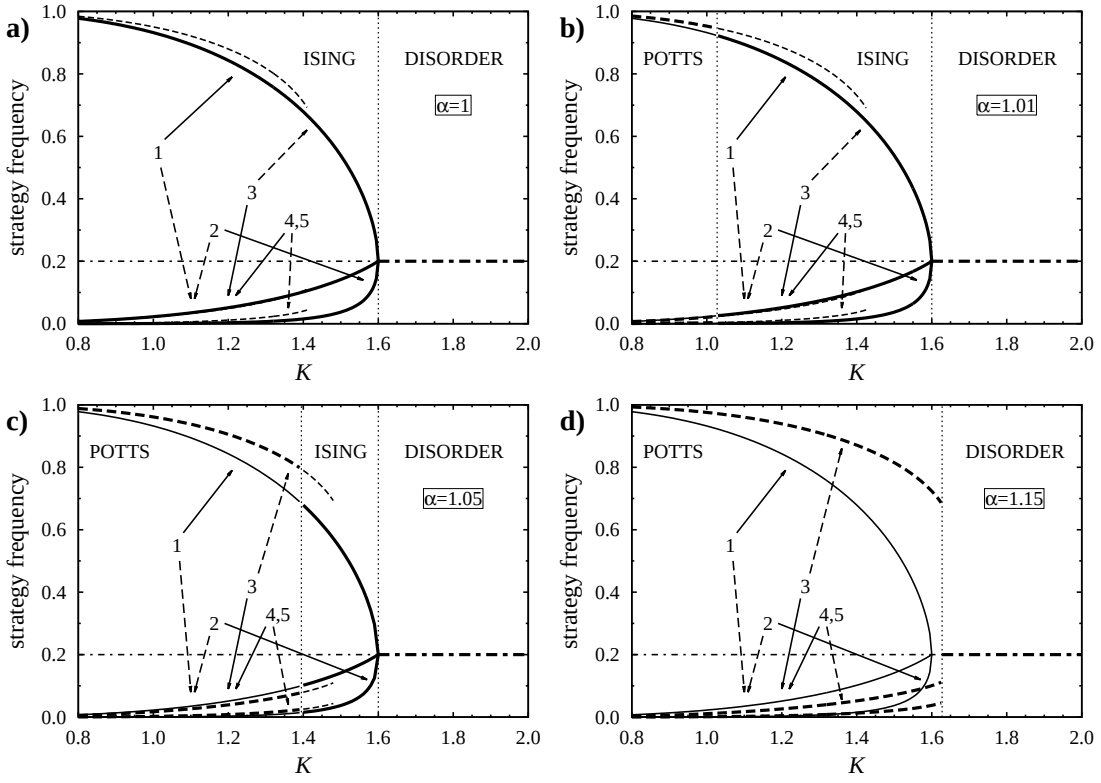

FIGURE 7.1. Strategy frequencies in the mean-field approximated $\mathbf{A}^{(\mathrm{IP})}(\alpha)$ game for different values of α. Solid, dashed, and dash-dotted lines correspond to the Ising-type, the Potts-type, and the disordered states, respectively. Thicker lines indicate the stable equilibrium state with the highest free energy.

The game's preferred Nash equilibria are all players uniformly choosing one of the first two Ising strategies when $\alpha < 1$, one of the three Potts strategies when $\alpha > 1$, and any one of the five strategies when $\alpha = 1$.

7.1 Cluster variation analyses

First, let us briefly survey the most important macroscopic properties of the model at the mean-field approximation level [159]. As we have seen earlier, noninteracting subgame components contribute to separate terms of the mean-field approximated potential, and as a result the fixed point equations Eq. (3.15) of their strategies are only coupled via the normalization constraint. Consequently, after numerically solving the equations, we find that the system's behavior can be effectively described as a direct competition between its constituent Ising and Potts components.

The competing states are shown in Fig. 7.1. As usual, it turns out that the system is completely disordered in the high temperature limit, and order emerges only below a critical point. This time, however, there are two types of ordered states that can

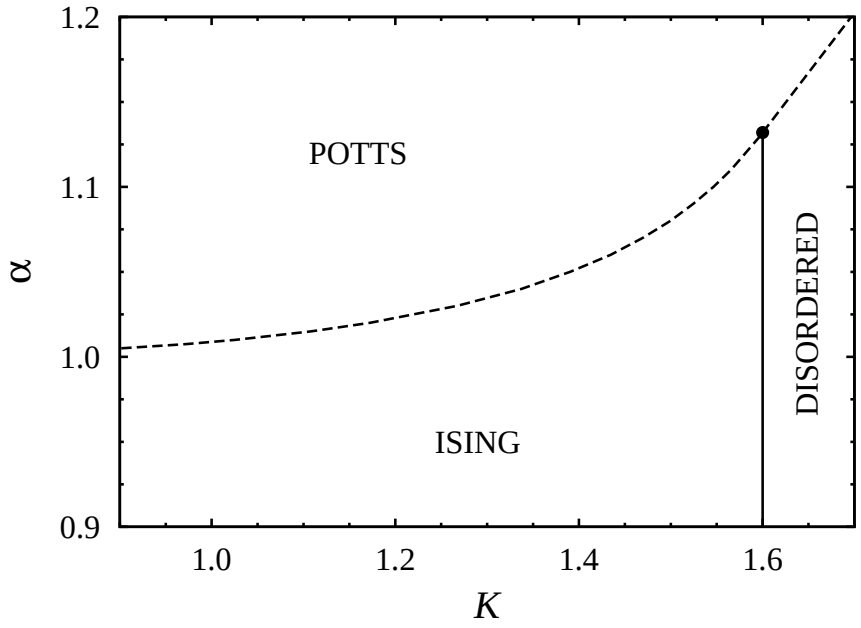

FIGURE 7.2. Mean-field phase diagram of the game of competing Ising and Potts components given by the payoff matrix $\mathbf{A}^{(\mathrm{IP})}(\alpha)$. Solid and dashed lines indicate continuous and first-order phase transitions, respectively.

gain stability. The first of them is the ordered state of the five-strategy elementary coordination game introduced in Sec. 4.1, which we will refer to as the Ising-type state of $\mathbf{A}^{(\mathrm{IP})}$, because it breaks the Ising symmetry of the first two strategies. Conversely, the other ordered state retains this symmetry and breaks the Potts symmetry of the last three strategies instead. The two ordered states are of course twice and three times degenerate. In the following, we will assign strategy labels 1 and 3 to the majority strategies of the Ising- and the Potts-type states, respectively.

At $\alpha = 1$, when the two subgames reward coordination equally, the Ising-type state forms continuously below $K_{\mathrm{I}}^{(\mathrm{mf})} = 2z/n$, where z is the coordination number of the model and $n = 5$ denotes the number of available strategies. In the following, we will assume $z = 4$ to be compatible with an underlying square lattice, which leads to $K_{\mathrm{I}}^{(\mathrm{mf})} = 1.6$. The Potts-type state, on the other hand, appears in a discontinuous manner, as a metastable state of the system, below another critical temperature, $K_{\mathrm{P}}^{(\mathrm{mf})}(\alpha = 1) \simeq 1.413(5)$. Since α is the strength of the Potts component, the critical temperature of the Potts-type state scales proportionally with α as $K_{\mathrm{P}}^{(\mathrm{mf})}(\alpha) = \alpha K_{\mathrm{P}}^{(\mathrm{mf})}(\alpha = 1)$.

Comparing the free energies of the two competing ordered states, we find that the stable equilibrium state of the system may show one of three kinds of temperature dependences for different values of α. The phase diagram in Fig. 7.2 gives an overview. When $\alpha \leq 1$, the Potts-type state cannot gain stability over its Ising-type counterpart, and thus the system becomes equivalent to the five-strategy elementary coordination game. Raising α

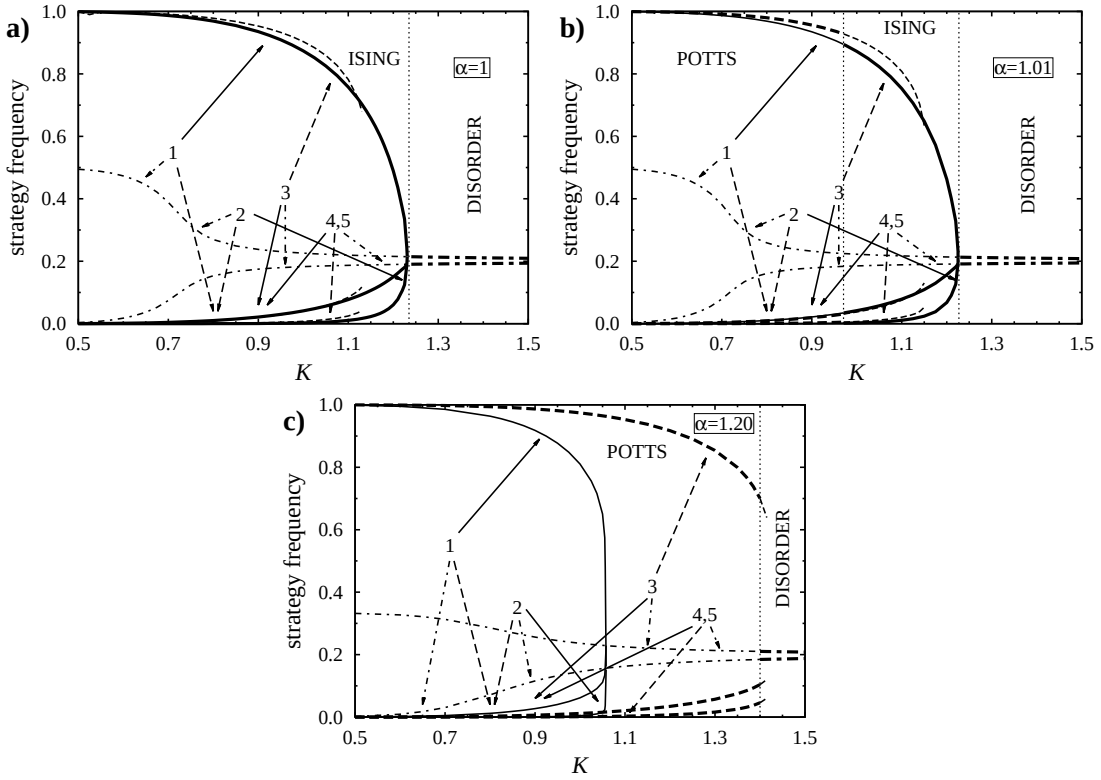

FIGURE 7.3. Competing states in the pair approximated $\mathbf{A}^{\mathrm{IP}}(\alpha)$ game, using the same notations as in Fig. 7.1.

above 1, so that the Potts component provides higher payoffs than the Ising component, leads to the stabilization of the Potts phase in the low-temperature regime. As long as α is lower than the critical value $\alpha_{\mathrm{c}}^{(\mathrm{mf})} = 1.132(5)$, the system exhibits two phase transitions: The continuous order-disorder transition already present for $\alpha \leq 1$ can still be observed at $K_{\mathrm{I}}^{(\mathrm{mf})}$, and the Ising phase and the low-temperature Potts phase are separated by a first-order transition at $K_{\mathrm{I-P}}^{(\mathrm{mf})}(\alpha) \leq K_{\mathrm{P}}^{(\mathrm{mf})}(\alpha)$, which is also an increasing function of α. For $\alpha \geq \alpha_{\mathrm{c}}^{(\mathrm{mf})}$, $K_{\mathrm{P}}^{(\mathrm{mf})}(\alpha) \geq K_{\mathrm{I}}^{(\mathrm{mf})}$ and the Potts-type state has higher free energy for all $K \leq K_{\mathrm{I}}^{(\mathrm{mf})}$ than the Ising-type state, so the Ising phase vanishes. The Potts phase loses its stability to the disordered phase via a first-order transition at $K_{\mathrm{P}}^{(\mathrm{mf})}(\alpha)$. The system acts just like the three-state Potts model's extension with two neutral strategies.

The pair approximation approach [159] leads to qualitatively similar results, as illustrated by Fig. 7.3, with a few differences that are very similar to those found in the elementary coordination game. On the quantitative side, the predicted critical temperatures are lower in the higher-order pair approximation. Qualitatively, the most significant change is in the structure of the disordered state. At the pair approximation level, it is not completely disordered at finite temperatures, but it has an α-dependent structure instead that still respects the symmetries of the payoff matrix. As long as the

system's order-disorder transition occurs between the Ising and the disordered phases (Fig. 7.3a and 7.3b), the frequencies of the two Ising strategies are higher than the frequencies of the other three strategies, and this gap opens up as the temperature is lowered until eventually the Potts strategies vanish in the $K \to 0$ limit. Conversely, the disordered state is characterized by a majority of Potts states when $\alpha > \alpha_{\mathrm{c}}^{(\mathrm{p})}$ (Fig. 7.3c), and the Ising states are squeezed out in the low temperature limit. Notice that this also affects the unstable Ising state, since it changes the way it loses its metastability, including the apparently still continuous transition's now α-dependent location $K_{\mathrm{I}}^{(\mathrm{p})}(\alpha)$.

7.2 Monte Carlo simulation results

We carried out Monte Carlo simulations in order to verify the predictions of the mean-field and pair approximation methods. The simulations were performed on square lattices of linear sizes varying from 400 to $3,000$ sites with thermalization and sampling times ranging from 10^4 to 10^6 Monte Carlo steps. The larger system sizes and longer run times were used closer to the phase transitions to counteract critical slowing down caused by the divergence of fluctuations and relaxation times.

Simulation runs were started from homogeneously pre-ordered Ising-type and Potts-type initial states to steer the system into their finite temperature partially ordered metastable counterparts, which the system can get stuck in for long periods of time even if it is not the stable equilibrium state of the system, allowing us to study both competing phases. In addition to allowing access to metastable states, another advantange of this method is that it significantly reduces the length of the transient domain growing processes preceding the formation of the ordered states, thus increasing the efficiency of the simulation. On the other hand, this exploitation of the metastability of states has a serious drawback as well, as it prevents the identification of the stable equilibrium state.

So, in order to locate phase transitions, we also had to perform more time-consuming simulations that were started from randomized initial states. Figure 7.4 shows the time evolution of strategy frequencies in two such simulations for the same value of α but two different temperatures. At first, the random distribution of strategies seems to favor the two Ising strategies, because their frequencies rise while the number of players following Potts strategies decreases in both cases during the initial nucleation of clusters of like strategies and the subsequent emergence of a domain structure. Following this process, the evolution of the system changes and becomes governed by the movement of these domain walls. In the first case pictured in Figure 7.4a, the Potts domains invade the Ising domain until one of them percolates and eventually engulfs the system. At a higher temperature (Fig. 7.4b), however, the roles are switched, and one of the Ising states takes

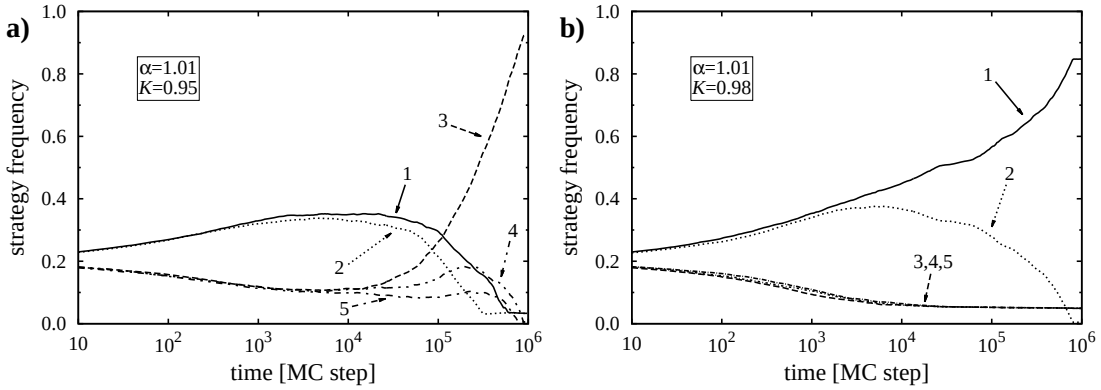

FIGURE 7.4. Time evolution of strategy frequencies in Monte Carlo simulation runs started from random initial states. The simulations were performed on a square lattice of linear size $L = 1,600$. The measured data were smoothed for these graphs by taking averages over time periods ranging from $0.95t$ to $1.05t$ for each time step t in order to suppress fluctuations and get a clearer view of trends.

over the system in a similar fashion. These results concur with the predictions of mean-field and pair approximations regarding the presence of a Potts order to Ising order phase transition.

Results obtained by combining the random initial state and pre-ordered initial state Monte Carlo methods are plotted in Figure 7.5. The qualitative predictions of the mean-field and pair approximations are mostly borne out by the simulation data. For $\alpha \leq 1$ only Ising-type ordering proves stable in the low temperature regime. Conversely, above a critical value $\alpha_c^{(\mathrm{MC})}$ the system's ordered phase is Potts ordered. Interestingly, the simulation data and the predictions of the pair approximation are at odds in this case: The Ising states can still be slightly more frequent than their Potts counterparts in the disordered phase at finite temperatures according to the simulation data (Fig. 7.5c), though for higher values of α (Fig. 7.5d) the pair approximation prediction is recovered. This is especially interesting in conjunction with the fact that the square-lattice three-state Potts model's phase transition is also continuous [130]. More interestingly, the data for $\alpha = 1.1$ hint at the order-disorder transition becoming a continuous transition. When $1 < \alpha < \alpha_c$, both ordered phases can be observed, the Ising phase below, and the Potts phase above the first-order transition temperature $K_{\mathrm{I-P}}^{(\mathrm{MC})}(\alpha)$. On the quantitative side, we again find that the cluster variation methods overestimate critical temperatures, more so when the transition in question is continuous. Moreover, this seems to result in the apparent shrinking of the size of the α parameter region for which both phases may be stable by about one order of magnitude compared to the prediction provided by the mean-field approximation approach.

To characterize the order-disorder phase transitions of the system, we also studied the critical behavior of the system's ordered phases close to the corresponding transition

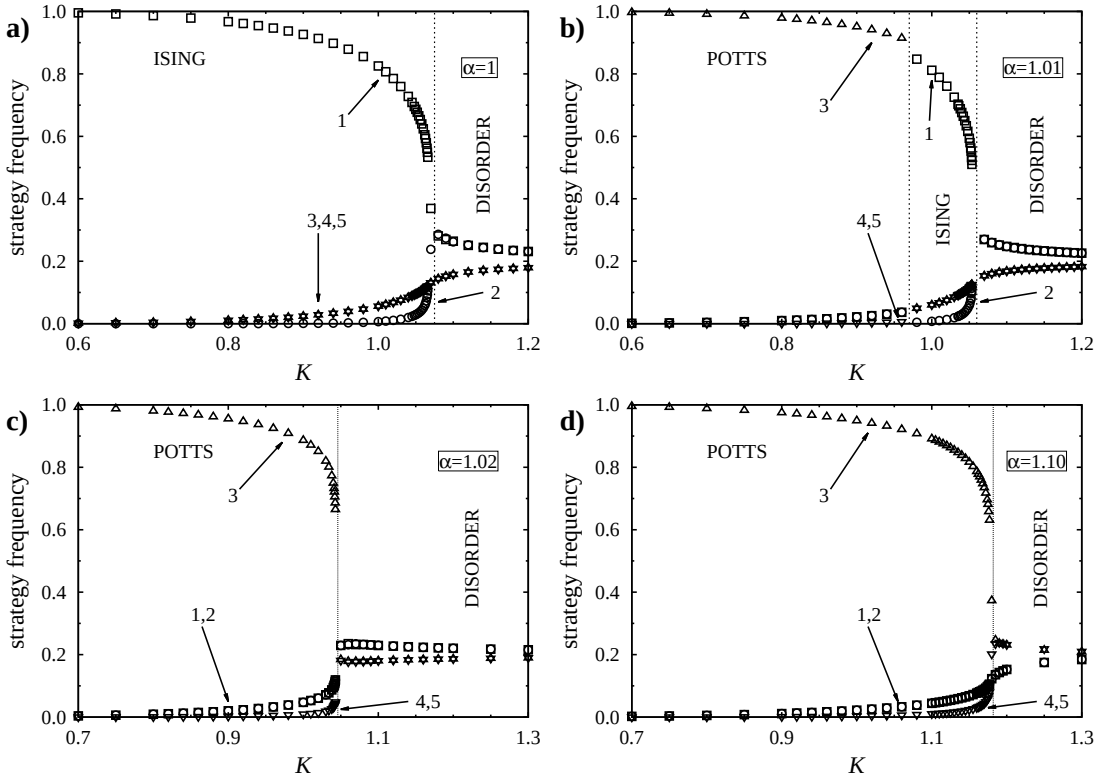

FIGURE 7.5. Monte Carlo simulated strategy frequencies plotted against the system's temperature in the game of competing Ising and Potts components.

temperatures. Specifically, we were interested in two order parameters, one measuring the degree of order for each ordered state. We chose the standard order parameters used in the literature for the constituent subgame models, $\rho_1 - \rho_2$ for the Ising phase [129] and $\rho_3 - (\rho_4 + \rho_5)/2$ for the Potts phase [130, 160]. As Figure 7.6 shows, the Ising order parameter vanishes following a power law approaching the order to disorder transition when $\alpha = 1$ and 1.01, and the Potts order parameter does the same for $\alpha = 1.02$ and 1.1. We estimated the critical exponents of the transitions by fitting algebraic functions to the data points in Figure 7.6 that were closest to their respective transition temperatures. The Ising order parameter's critical exponent turned out to be $\beta_{\mathrm{I}}^{(\mathrm{MC})}(1) = 0.135(10)$ for $\alpha = 1$ with $K_{\mathrm{I}}^{(\mathrm{MC})}(1) = 1.06665(10)$ and $\beta_{\mathrm{I}}^{(\mathrm{MC})}(1.01) = 0.131(10)$ for $\alpha = 1.01$ with $K_{\mathrm{I}}^{(\mathrm{MC})}(1) = 1.05373(10)$, which both are remarkably close to $\beta_{\mathrm{I}} = 1/8$ charateristic of the two-dimensional Ising model [129]. In the $\alpha = 1.1$ case, performing the same calculations for the Potts order parameter yielded $K_{\mathrm{P}}^{(\mathrm{MC})}(1.1) = 1.1777(10)$ and $\beta_{\mathrm{P}}^{(\mathrm{MC})}(1.1) = 0.102(10)$, which is in close agreement with the corresponding critical exponent $\beta_{\mathrm{P}} = 1/9$ of the square-lattice three-state Potts model [130]. The similar Potts order to disorder transition observed at $K_{\mathrm{P}}^{(\mathrm{MC})}(1.02) = 1.0432(10)$ in the $\alpha = 1.02$ version of the model, however, seems to be markedly different with $\beta_{\mathrm{P}}^{(\mathrm{MC})}(1.02) = 0.0754(10)$.

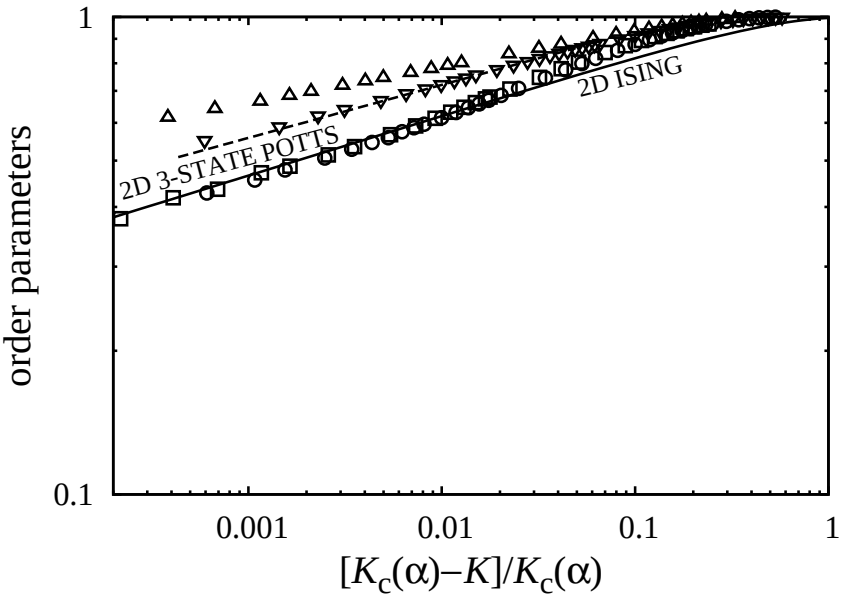

FIGURE 7.6. Log-log plot of the order parameters as a function of relative temperature with respect to the critical point in the $\mathbf{A}^{\mathrm{IP}}(\alpha)$ game. Circles and boxes represent $\rho_1 - \rho_2$ for $\alpha = 1$ and $\alpha = 1.01$, respectively, whereas upward and downward pointing triangles correspond to $\rho_3 - (\rho_4 + \rho_5)/2$ for $\alpha = 1.02$ and $\alpha = 1.10$.

In conclusion, our results suggest that the behavior of the $\mathbf{A}^{\mathrm{IP}}(\alpha)$ game is dominated by its Ising component for $\alpha \leq 1$ and its Potts component for $\alpha > \alpha_{\mathrm{P}}$. In both cases, the system exhibits just a single order-disorder phase transition between an ordered phase that spontaneously breaks the symmetry of the dominant component and a disordered state that has a slight majority of the dominant component's coordinated strategies. Furthermore, the phase transition apparently belongs to the dominant subgame's (i.e., the Ising or the three-state Potts model's) universality class. When $\alpha_{\mathrm{c}} < \alpha < \alpha_{\mathrm{P}}$, we still observe only one order-disorder transition, this time between a Potts-type ordered state and an Ising majority disordered state. It does not seem to belong to either the Ising or the Potts universality class. Finally, for $1 < \alpha < \alpha_{\mathrm{c}}$, both the Ising and the Potts phases become stable, the Potts state below $K_{\mathrm{I-P}}(\alpha)$, the Ising state above it. The order-disorder transition appears to be of the Ising universality class.

At first sight, the stable presence of the Ising phase for $1 < \alpha < \alpha_{\mathrm{c}}$ might seem somewhat counterintuitive, since the Potts-type state provides a higher average payoff. The total dominance of the Ising phase when $\alpha = 1$ is similarly puzzling, because the Potts state still leads to better payoffs (Fig. 7.7) for finite temperatures. (The ground state is five-fold degenerate.) As Figure 7.7 illustrates, it is the entropic term $K\mathcal{S}$ of the free energy that stabilizes the Ising-type state in spite of its lower average payoff. Both ordered states have four minority strategies, but these are distributed differently. The Potts-type state has two minority strategies with higher and two with lower frequencies,

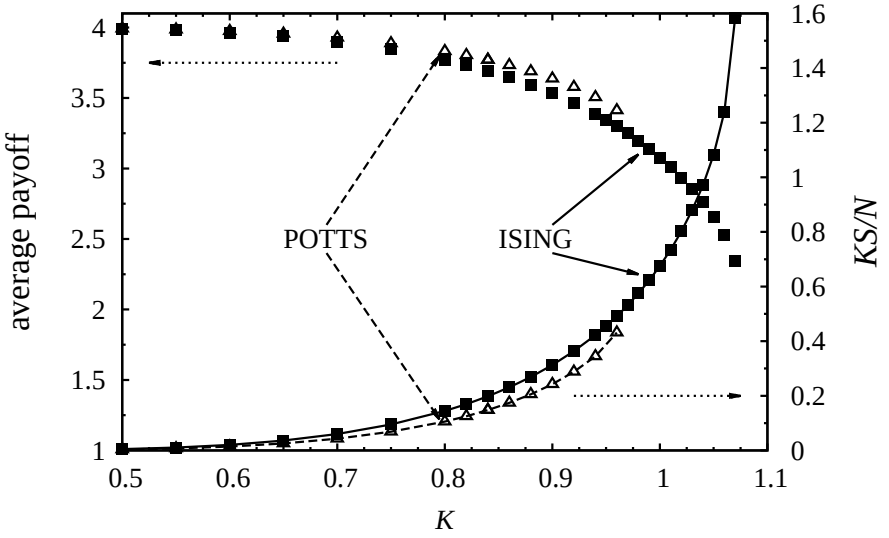

FIGURE 7.7. Comparison of the average payoffs and average entropies of the Ising- and Potts-type states in the Monte Carlo simulated $\mathbf{A}^{\mathrm{IP}}(1)$ game. Filled symbols indicate the stable equilibrium state. The entropies were estimated using the mean-field approximation formula $\mathcal{S}/N = \frac{1}{K}\sum_i \rho_i \ln \rho_i$. Plotted entropy data points are connected by lines.

whereas the same ratio is three to one in the Ising-type state. As a result, the Ising-type state is comparatively less ordered than the Potts-type state. Consequently, its entropy is higher and grows faster as the temperature increases, which in turn means that its free energy also increases faster and becomes higher than that of the Potts-type state, thus becoming the stable equilibrium state. The higher-paying Potts phase not being the stable equilibrium state can be thought of as an entropic social trap situation, wherein the presence of a competing higher-entropy state prevents the community of players from maximizing their total payoff.

Chapter 8

Conclusion

In this thesis, I have given an overview of my recent research into the properties of a handful of logit-rule-driven simple coordination-type games. I have used well-known methods of statistical physics to investigate both the microscopic and macroscopic behavior of these systems ranging from analytical calculations through different approximation methods to Monte Carlo computer simulation techniques. The overarching long-term aim of this continued work is to learn more about the implications and potential utility of the linear decomposition of games into elementary components representing different interaction types, the characteristics of the individual elementary games, and the way the interplay between combinations of multiple game components affect them.

In Chapter 2, I have introduced the game theoretic model family of (two-player, symmetric) matrix games and the concept of their linear decomposition, along with a proposed basis set of games that classifies game components based on their level and symmetry of interactivity. The outcome of an irrelevant game is fixed regardless of the choice of either player. In cross- and self-dependent games players can unilaterally set their opponent's and their own payoffs, respectively, but not the other way around. Coordination-type and cyclic dominance games, on the other hand, define proper player–player interactions wherein both players equally influence each other's winnings, equally sharing in the former, one taking away from the other in the latter. Certain properties directly derive from this decomposition. For example, the presence of a cyclic dominance component precludes the game from having a potential, and social dilemmas are caused by the game containing a strong enough antisymmetric (hierarchical) combination of the cross- and self-dependent components. Moreover, decomposition can help reveal the inherent symmetries between a game's strategies and expose the differences and similarities between games defined by different payoff matrices by making permuting strategy labels more tractable, which is closely related to both tasks: Two payoff matrices that can be

mapped onto each other by such a permutation define the same game, and a symmetry of the game is defined by its payoff matrix being self-equivalent under certain nonidentity strategy label permutations.

Chapter 3 has dealt with the connection between potential games and statistical physics and has briefly introduced some of the latter's concepts and methods that were used in the studies this thesis is based on. When multiple players, who are located at the sites of a lattice or the nodes of a network structure, repeatedly play two-player symmetric potential matrix games with their neighbors and they choose their strategies according to the logit stochastic strategy update rule, the corresponding game theoretic model becomes equivalent to a classical spin model. The players and their available strategies act like spins and the states they can be in, the negative of the game's potential plays the role of the spin model's Hamiltonian, and the noise level parameter of the logit rule is analogous to the temperature of the statistical physical system. Similarly, we can also define the game system's free energy, and combine approximations and the variational principle that this free energy is maximal in the system's equilibrium steady state to predict its properties. The accuracy of these results can be verified by computer simulations—direct realizations of the model, which coincide with the so-called Monte Carlo simulation technique in the spin model context. The original work presented in this thesis concerns such multiplayer square-lattice potential games governed by the logit rule.

Chapter 4 has discussed the simplest potential games describing proper player–player interactions, elementary coordination games. In the general n-strategy version of the game, two of the strategies are coordinated, which means that choosing either of them yields 1 unit of payoff as long as the opponent picks the same strategy, but reduces the players winnings by 1 should their opponent happen to play the other coordinated strategy; the remaining $n - 2$ strategies are neutral, meaning that playing them and playing against them both provide zero payoff. The mean-field and pair approximations both qualitatively agree with Monte Carlo simulation data on the most prominent feature of the elementary coordination game: The system undergoes a phase transition between an ordered phase that breaks the symmetry of the coordinated strategies and a disordered phase, which gains stability above the critical temperature. The higher the number of available strategies n is, the lower this critical temperature becomes, vanishing in the $n \to \infty$ limit approximately as $2/\ln n$. When n is increased above a threshold value n_{th}, the transition changes from being continuous to being of the first order, due to the entropy-based stabilization of the disordered phase. The difference between the frequencies of the two strategies is an order parameter for the transition, and follows a power law as the temperature approaches its critical value from below, with a critical

exponent of 1/8 characteristic of the square-lattice Ising model if the transition is continuous. The system's time evolution from an initially disordered state in the ordered phase generally involves the formation and growth of coordinated domains. Depending on the temperature of the system, the neutral strategies may form a monolayer coating between differently coordinated domains or recede from straight domain walls to domain corners.

In Chapter 5, I have introduced two extensions of the elementary coordination game by combining it with self-dependent components. The first of these models involves a single elementary self-dependent game of strength h' that benefits (or punishes) only one of the two coordinated strategies, thus breaking their symmetry. When $h' \neq 0$, continuous transitions invariably vanish, and the system's low-temperature ordered strategy arrangements morph into a disordered state smoothly as the temperature increases. First-order transitions prove more resilient and remain present for h' below a positive critical value.

The other extended model we have investigated has two self-dependent components—one affecting each coordinated strategy—that are of equal strength h'' so as to preserve the symmetry of the coordinated strategies. Regardless of the number of a available strategies, the model's phase transition is continuous for high enough h'', vanishes when h'' is below $-1/2$, and is of the first order otherwise. The transition temperature is a decreasing function of n, but an increasing function of h''. By bunching together the interchangeable neutral strategies into a single strategy, the system can be transformed into a zero-field Blume–Capel model with temperature-dependent crystal-field coupling. The literature of the Blume–Capel model not only confirms and quantifies the above-mentioned properties of our game model, which were chiefly based on the mean-field and pair approximations, but also reveals that the continuous phase transitions indeed belong to the Ising universality class, as indicated by our Monte Carlo simulation results for the $h'' = 0$, elementary coordination case.

Chapter 6 has concerned certain highly symmetric combinations of multiple elementary coordinations called maximally nonoverlapping coordination games or m-Ising-pair games. The $2m$-strategy version consists of m elementary coordinations in such a way that none of them share any of their coordinated strategies. Although m-Ising pair games are mean-field equivalent to their $2m$-strategy elementary coordination game counterparts, there are some conspicuous differences between the two model families, especially in their critical properties. The present work has highlighted some of them through the examples of the $m = 2$ and $m = 3$ versions of the game. The two-Ising-pair game is equivalent to the four-state clock model—a special case of the Ashkin–Teller model—of statistical physics, which in turn is equivalent to a system made up of two identical

independent uncoupled Ising models. The composite two-Ising-pair game inherits some of its key properties from these constituent Ising models, as its order-disorder phase transition that breaks the symmetry of one of its coordinated pairs occurs at the same critical point, and the transition's magnetization-like order parameter apparently belongs to the Ising universality class. We can derive another order parameter from the other coordinated pair's strategy frequencies that also follows a power law behavior close to the same critical temperature, but has completely different critical exponents. Of the above, the ordered phase's breaking of the symmetry of one coordinated pair and the coexistence of two order parameters for a single phase transition carry over to the three-Ising-pair game, but neither order parameter seems to have Ising-type critical exponents. This is probably related to the fact that the three-Ising-pair game's elementary coordinations are related by Potts-type three-element permutation symmetry instead of the Ising-type exchange symmetry of the two-Ising-pair game's components, though the critical exponents are apparently not of the Potts class either.

Finally, Chapter 7 has explored the features of a five-strategy purely coordination-type game of competing Ising-type and Potts-type subgame components. The system's behavior is controlled by its temperature and the ratio α of the Potts component's reward for coordination to that of the Ising subgame. When the Ising component is at least as strong as the Potts component (i.e., $\alpha \leq 1$), the model exhibits a single continuous Ising-class order-disorder transition between a low-temperature ordered phase that breaks the symmetry of the Ising strategies and a high-temperature symmetry-retaining disordered phase characterized by Ising strategies having higher frequencies than Potts strategies. Conversely, for all α exceeding a threshold value α_{P}, one of the Potts strategies becomes dominant below a critical temperature, and Potts strategies are more frequent than their Ising-type counterparts in the symmetric disordered state that becomes stable above it. In other words, the model's behavior is dominated by its Ising component when α is low enough and by its Potts component when α is high enough. In between, we have found that the system's behavior is more Ising-like for higher and more Potts-like for lower temperatures. Above a threshold value α_{c} the model still only exhibits one phase transition as its temperature varies, but it seems to have nonuniversal critical exponents and occurs between a Potts-like ordered and an Ising-majority disordered phase. Below α_{c} the Ising components influence extends even below the stability region of the disordered state leading to the emergence of an Ising-ordered phase between the disordered and the Potts-ordered phases. As a result, two phase transitions can be observed, a first-order one between the two ordered states and one that is continuous and belongs to the Ising universality class. These alterations of the phase diagram are explained by the higher entropy content of the Ising-type (ordered and disordered) states that give them a competitive edge over their Potts-type counterparts at higher temperatures. This is why the

Ising phase can gain stability over the Potts phase even when it provides lower average and individual payoffs in the $1 < \alpha < \alpha_c$ driving the system into a state reminiscent of a social trap.

For linear payoff matrix decomposition to be a truly useful tool in the analysis of games, it should inform and help us predict a game's behavior based on its payoff matrix in a followable manner. To explore whether this is true, we should not simply look at our different models and what we have learned about them in isolation, but also examine their shared features and how they differ from each other. The most striking commonality between the models treated in this thesis is that under appropriate conditions they all seem to possess an order-disorder phase transition that belongs to the Ising universality class. Based on the evidence of the results reported in this thesis, we may conjecture that the Ising-type critical behavior of the elementary coordination game is robust and remains prominent in potential game models with composite nearest-neighbor interactions as long as the following criteria are satisfied: i) At least one of the components has to be an elementary coordination. ii) It should not be symmetry related to other elementary coordination components of the game, though interchangeability with a single other elementary coordination may be allowed (cf. the Potts model or the m-Ising-pair game). iii) The symmetry of its strategy pairs should not be broken by the game's self-dependent component. iv) It should have a high enough positive expansion coefficient, though it does not necessarily have to be the strongest component. (See the game of competing Ising and Potts components or the h''-extended elementary coordination.) v) The game should not have too many available strategies to avoid the excessive stabilization of the disordered phase. This robustness conjecture could be tested, for example, by conducting a thorough and extensive study of games defined by randomly generated payoff matrices that satisfy or (selectively) break the criteria.

On bipartite networks, such as the square lattice, criterion iv) can be loosened to having a large enough either positive or negative expansion coefficient. Since the nodes of a bipartite network can by definition be divided into two subnetworks such that the network's edges only connect nodes that belong to different subnetworks, any elementary anticoordination can be uniformly transformed into a same strength elementary coordination by simply switching the labels of its originally anitcoordinated strategies on one of the subnetworks. By induction, it follows that games that only differ in the signs of their elementary coordination coefficients are all equivalent to each other on bipartite lattices. For instance, the square-lattice logit-rule-driven elementary anticoordination game, whose payoff matrix is the negative of the elementary coordination game's, is characterized by anticoordinated sublattice ordering in the low-temperature regime, but the corresponding staggered order parameter exhibits the same continuous

Ising-type phase transition at the same critical temperature as the elementary coordination game's order parameter, imitating the correspondence of the ferromagnetic and antiferromagnetic square-lattice Ising models.

Further research into the benefits of the game decomposition approach should, on the one hand, aim to verify and improve our results using more sophisticated and accurate or altogether different methods (e.g., finite-size scaling analysis and different Monte Carlo techniques [100, 101, 140, 161], various renormalization group methods [162–164], high- and low-temperature expansions [165], and ε-expansions [166]) and, on the other hand, should also seek to complement them by studying more differently structured or more complex games, as well as broaden our knowledge of the models treated in this thesis. We have also mostly resticted ourselves to the investigation of models and phenomena at the intersection of game theory and statistical physics, but linear decomposition can, of course, also be employed whenever payoff matrices are involved, including matrix game models that are governed by different dynamical rules or lack a potential [167]. For example, it could help predict the general features of phase portraits in replicator population dynamics models [168]. The basis sets introduced in Chapter 2 may also prove useful for applications beyond game theory, for instance, in the detection of hierarchical and cyclic structures in directed graphs represented by adjacency matrices [44].

New scientific contributions

My main scientific contributions resulting from the research work reported in this thesis can be summarized in the following thesis statements:

1. I have explored the properties of the square lattice, logit-rule-driven elementary coordination game. I have established that as a result of changing the noise level parameter, which is analogous to temperature, the system may undergo an order–disorder phase transition whose order depends on the defining parameter of the model, the number of available neutral strategies. As long as this number remains below a threshold value, the transition is continuous and belongs to the universality class of the two-dimensional Ising model; its is of the first order otherwise. I have determined the threshold value and estimated the critical temperature of the transition. These results were published in Ref. [112]:
   G. Szabó and B. Király, "Extension of a spatial evolutionary coordination game with neutral options," Phys. Rev. E **93**, 052108 (2016).

2. I have extended the model mentioned in thesis statement 1 with a self-dependent component that retains the symmetry of its coordinated strategies. I have established that, in the resulting model, the critical point and the order of the original phase transition may both be changed, or the transition may even be abolished altogether depending on the strength of the self-dependent component. These results were published in Ref. [135]:
   B. Király and G. Szabó, "Evolutionary games with coordination and self-dependent interactions," Phys. Rev. E **95**, 012303 (2017).

3. By consistently bunching the neutral strategies, I have mapped the extended model mentioned in thesis statement 2 onto the Blume–Capel model, thereby verifying the accuracy of my findings on the properties of the model. I have shown that the same mapping can also be used to replace an arbitrary number of neutral strategies in games defined on regular graphs with a single neutral strategy and an additional self-dependent component whose strength depends on the temperature.

4. I have introduced the concept of maximally nonoverlapping coordination games as the family of games that have an even number of available strategies and are made up of a maximal number of elementary coordinations that share none of their coordinated strategies. I have explored the properties of these games in a square-lattice, logit-rule-driven setup. At the mean-field approximation level, a general maximally nonoverlapping coordination game is equivalent to the elementary coordination game with the same number of available strategies, so its ordered phase breaks the symmetry of just one of its coordinated pairs. I have demonstrated this property for the four- and six-strategy versions of the game using Monte Carlo simulations. I have assigned two independent order parameters to their phase transitions and determined their critical exponents. While in the four-strategy model one of the order parameters exhibits Ising-type critical behavior just like the elementary coordination game, the six-strategy game is characterized by different critical exponents because of the different permutation symmetry that connects its coordinated pairs. I have identified the four-strategy model as a special case of the Ashkin–Teller model, the clock model. This correspondence provides analytical underpinning for the model's apparent Ising-type behavior, and it can be used to exactly determine the critical temperature of the model's phase transition via a duality relation. These results were published in Ref. [147]:
   B. Király and G. Szabó, "Evolutionary games combining two or three pair coordinations on a square lattice," Phys. Rev. E **96**, 042101 (2017).

5. I have studied a square-lattice, logit-rule-driven model of competing Ising- and Potts-type subgame components. I have shown that even though the system generally exhibits a single order-disorder phase transition, in the vicinity of which the system's critical behavior corresponds to that of the subgame that provides higher payoffs, Ising-type behavior can still be stabilized by entropy effects close to the critical point when the Potts-type subgame is only slightly stronger. In this case an additional, first-order transition can also be observed between the two competing ordered phases. These results were published in Ref. [159]:
B. Király and G. Szabó, "Entropy affects the competition of ordered phases," Entropy **20(2)**, 115 (2018).

Appendix A

Derivation of the two-Ising-pair game's critical temperature

In this appendix, an analytical formula for the critical temperature of the two-Ising-pair game defined by the payoff matrix

$$\mathbf{A}^{(2)} = \Delta\varepsilon \begin{pmatrix} 1 & -1 & 0 & 0 \\ -1 & 1 & 0 & 0 \\ 0 & 0 & 1 & -1 \\ 0 & 0 & -1 & 1 \end{pmatrix} \tag{A.1}$$

is derived following the method used in Ref. [150] for another special case of the Ashkin–Teller model. First, we give a brief summary of the notations and general results of Ref. [150], and then apply them to the two-Ising-pair game.

In the game theoretic framework used throughout this thesis, the general Ashkin–Teller model is defined by the payoff matrix

$$\mathbf{A}^{(\mathrm{AT})} = \begin{pmatrix} \varepsilon & \varepsilon' & \varepsilon'' & \varepsilon''' \\ \varepsilon' & \varepsilon & \varepsilon''' & \varepsilon'' \\ \varepsilon'' & \varepsilon''' & \varepsilon & \varepsilon' \\ \varepsilon''' & \varepsilon'' & \varepsilon' & \varepsilon \end{pmatrix}, \tag{A.2}$$

and its partition function is given by

$$\mathcal{Z} = \sum_{\{\mathbf{s}\}} \sum_{\langle v,w \rangle} \exp\Big(\mathbf{s}_v \cdot \mathbf{A}^{(\mathrm{AT})} \mathbf{s}_w \Big), \tag{A.3}$$

where the first summation runs over all possible strategy configurations and the second summation is taken over all distinct nearest neighbour pairs.

$$\exp\left(\frac{\varepsilon}{K}\right) = u + x + y + z \tag{A.4a}$$

$$\exp\left(\frac{\varepsilon'}{K}\right) = u - x + y - z \tag{A.4b}$$

$$\exp\left(\frac{\varepsilon''}{K}\right) = u - x - y + z \tag{A.4c}$$

$$\exp\left(\frac{\varepsilon'''}{K}\right) = u + x - y - z \tag{A.4d}$$

By expanding the second summation and introducing a set of auxiliary functions through Eqs. (A.4a)–(A.4d), we can rewrite the partition function as

$$\mathcal{Z} = \sum_{\{\mathbf{s}\}} \Big[\prod_{\langle i,j \rangle} (u \pm x \pm y \pm z) \Big], \tag{A.5}$$

which can be further expanded and partially evaluated utilizing a graphical representation of the terms of the sum that involves the labeling of nearest neighbor bonds according to the constitution of the term in question. With the help of this representation, the partition function can be reduced to a sum over so-called effective patterns whose contributions do not vanish after carrying out the summation. On a square lattice of N sites, we get

$$\mathcal{Z} = 4^N \sum_{\{\text{eff. patt.}\}} u^{2N-(b+c+d)} x^b y^c z^d ., \tag{A.6}$$

where b, c, and d denote the number of pairs labeled with x, y, and z in each effective pattern.

Focusing on the domain structure of configurations leads to a different form of the partition function. Noticing that coordination provides the same payoff for all strategies, the potential of a configuration can be determined relative to perfect coordination by adding up losses along interfaces separating differently coordinated domains. With this in mind, a dual graphical representation of the partition function's terms can be constructed by drawing perpendicular lines across bonds connecting players who follow different strategies and labeling each line according to the payoff the two players receive instead of ε.

Let us use the following exponential weights derived from the payoffs as these labels:

$$\alpha = \exp\left(\frac{\varepsilon}{K}\right), \tag{A.7a}$$

$$\beta = \exp\left(\frac{\varepsilon'}{K}\right), \tag{A.7b}$$

$$\gamma = \exp\left(\frac{\varepsilon''}{K}\right), \tag{A.7c}$$

$$\delta = \exp\left(\frac{\varepsilon'''}{K}\right). \tag{A.7d}$$

It can be shown that the allowed $\beta\gamma\delta$ patterns of this representation are geometrically identical to the effective xyz-patterns of Eq. (A.6), provided that a large N number of players is considered and edge effects are neglected. Consequently, the partition function in this domain wall representation takes the form:

$$\mathcal{Z} = 4 \sum_{\{\text{eff. patt.}\}} \alpha^{2N-(b+c+d)} \beta^b \gamma^c \delta^d, \tag{A.8}$$

where b, c, and d are the total lengths of β, γ, and δ lines in a given effective pattern.

In the two-Ising-pair game defined by Eq. (A.1), $\varepsilon + \varepsilon' = 2\overline{\varepsilon} = 2\varepsilon'' = 2\varepsilon'''$ and $\Delta\varepsilon = \varepsilon - \overline{\varepsilon}$, where $\overline{\varepsilon}$ is the mean of the four defining parameters of the Ashkin–Teller model. Plugging these conditions into Eqs. (A.4a)-(A.4d) and Eqs. (A.7a)-(A.7d), comparing the results, and introducing $\vartheta = \exp\left(\overline{\varepsilon}/K\right)$ lead to the following set of equalities:

$$u = y + 1 = \frac{\vartheta}{2}\left(\cosh\left(\frac{\Delta\varepsilon}{K}\right) + 1\right), \tag{A.9a}$$

$$x = z = \frac{\vartheta}{2}\sinh\left(\frac{\Delta\varepsilon}{K}\right), \tag{A.9b}$$

$$\alpha = \frac{\vartheta^2}{\beta} = \exp\left(\frac{\varepsilon}{K}\right) = \vartheta \exp\left(\frac{\Delta\varepsilon}{K}\right), \tag{A.9c}$$

$$\gamma = \delta = \vartheta = \exp\left(\frac{\overline{\varepsilon}}{K}\right). \tag{A.9d}$$

With these in mind, we can further simplify both Eq. (A.6) and Eq. (A.8). The first expression becomes

$$\mathcal{Z} = 4^N \vartheta^{2N} \left(\cosh\left(\frac{\Delta\varepsilon}{2K}\right)\right)^{4N} \sum_{\{\text{eff. patt.}\}} \left(\tanh\left(\frac{\Delta\varepsilon}{2K}\right)\right)^{2m+n+l}, \tag{A.10}$$

while the second one at temperature K^* can be written as

$$\mathcal{Z}^* = 4(\vartheta^*)^{2N} \left(\exp\left(\frac{\Delta\varepsilon}{2K^*}\right)\right)^{4N} \sum_{\{\text{eff. patt.}\}} \left(\exp\left(-\frac{\Delta\varepsilon}{K^*}\right)\right)^{2m+n+l}. \tag{A.11}$$

According to Ref. [150], the partiton functions of Eq. (A.10) and Eq. (A.11) are reciprocity (or duality) related if i) there exists a $K^* = F(K)$ transformation that is an involution [i.e., $K = F(K^*)$] and ii) there also exists a function $G(K)$ with no singularities for real temperatures—with the possible exceptions of $K = 0$ and $K = \infty$—and

$$G(K)Z(K) = G(K^*)Z^*(K^*). \tag{A.12}$$

If these conditions are satisfied, then $\mathcal{Z}$ having a singularity at K implies $\mathcal{Z}^*$ having a corresponding singularity at $K^* = F(K)$.

In our case, the partition functions Eq. (A.10) and Eq. (A.11) are duality related through the transformation implicitly defined by

$$\tanh\left(\frac{\Delta\varepsilon}{2K}\right) = \exp\left(-\frac{\Delta\varepsilon}{K^*}\right). \tag{A.13}$$

Using the definition Eq. (A.7a), we can rewrite Eq. (A.13) as

$$\frac{\alpha - \vartheta}{\alpha + \vartheta} = \frac{\vartheta^*}{\alpha^*}, \tag{A.14}$$

and solving for ϑ/α we get

$$\frac{\vartheta}{\alpha} = \frac{\alpha^* - \vartheta^*}{\alpha^* + \vartheta^*}, \tag{A.15}$$

which means that the transformation satisfies condition i).

Comparing Eq. (A.10) and Eq. (A.11) and substituting Eq. (A.7a) and Eq. (A.13), we arrive at

$$4^N \left(\frac{(\alpha+\vartheta)^2}{\alpha}\right)^{-2N} \mathcal{Z} = \frac{1}{4}(\alpha^*)^{-2N}\mathcal{Z}^*. \tag{A.16}$$

Still following Ref. [150], we introduce $\lambda = \mathcal{Z}^{1/N}$, the per capita average of the partition function. In terms of this quantity the above equality becomes

$$\frac{4\alpha^2}{(\alpha+\vartheta)^4}\lambda = 4^{-1/N}\frac{1}{(\alpha^*)^2}\lambda^*. \tag{A.17}$$

Dividing both sides of the equation by $(\alpha^2+1)^2$ and rearranging some terms gives

$$\frac{1}{\vartheta^2}\left(\frac{\alpha}{\vartheta} + \frac{\vartheta}{\alpha}\right)^{-2}\lambda = 4^{-1/N}\frac{1}{(\vartheta^*)^2}\left(\frac{\alpha^*}{\vartheta^*} + \frac{\vartheta^*}{\alpha^*}\right)^{-2}\lambda^*. \tag{A.18}$$

If it were not for the $4^{-1/N}$ factor, this final equation would satisfy the second duality relation condition. However, if $N \to \infty$ then $4^{-1/N}$ tends to 1, and Eq. (A.18) becomes

$$\frac{1}{\vartheta^2}\left(\frac{\alpha}{\vartheta}+\frac{\vartheta}{\alpha}\right)^{-2}\lambda = \frac{1}{(\vartheta^*)^2}\left(\frac{\alpha^*}{\vartheta^*}+\frac{\vartheta^*}{\alpha^*}\right)^{-2}\lambda^*, \tag{A.19}$$

that clearly satisfies Eq. (A.12). Therefore the partition functions of Eq. (A.10) and Eq. (A.11) are reciprocity related. We have to emphasize, however, that this only holds in the $N \to \infty$ thermodynamic limit where edge effects and the $4^{-1/N}$ factor in Eq. (A.18) can be neglected.

We can now determine the critical transition temperature of the two-Ising-pair coordination game in the thermodynamic limit using Kramers and Wannier's argument presented in Refs. [156, 157]. Due to the duality relation, $\mathcal{Z}$ and $\mathcal{Z}^*$ have correspondig singularites, and under the assumption that only one such singularity exists, it must occur at $K = K^*$. Because $\Delta\varepsilon = 1 > 0$, K^* is a monotonically decreasing function of K, and K and K^* become equal at

$$K_\mathrm{c}(2) = \frac{\Delta\varepsilon}{\ln(\sqrt{2}+1)} \approx 1.1346\Delta\varepsilon. \tag{A.20}$$

If $\Delta\varepsilon < 0$, Eq. (A.13) has no real solutions, and the above established duality argument breaks down. On bipartite lattices, however, this anticoordinated version of the system can be mapped back onto its coordinated counterpart by simply exchanging the labels of the anticoordinated strategy pairs on one of the sublattices, and thus the duality argument can be recovered.

Bibliography

[1] P. Ball, *Why Society is a Complex Matter: Meeting Twenty-first Century Challenges with a New Kind of Science* (Springer, Heidelberg, Germany, 2012).

[2] L. Pásztor, Z. Botta-Dukát, G. Magyar, T. Czárán, and G. Meszéna, *Theory-based Ecology: A Darwinian Approach* (Oxford University Press, Oxford, UK, 2016).

[3] S. Azaele, S. Suweis, J. Grilli, I. Volkov, J. R. Banavar, and A. Maritan, "Statistical mechanics of ecological systems: Neutral theory and beyond," Rev. Mod. Phys. **88**, 035003 (2016).

[4] R. N. Mantegna and H. E. Stanley, *Introduction to Econophysics: Correlations and Complexity in Finance* (Cambridge University Press, Cambridge, UK, 1999).

[5] J.-P. Bouchaud, "Crises and collective socio-economic phenomena: Simple models and challenges," J. Stat. Phys. **151**, 567 (2013).

[6] D. Sornette, "Physics and financial economics (1776–2014): Puzzles, Ising and agent-based models," Rep. Prog. Phys. **77**, 062001 (2014).

[7] W. Weidlich, "Physics and social science: The approach of synergetics," Physics Reports **204**, 1 (1991).

[8] C. Castellano, S. Fortunato, and V. Loreto, "Statistical physics of social dynamics," Rev. Mod. Phys. **81**, 591 (2009).

[9] S. Galam, *Sociophysics: A Physicist's Modeling of Psycho-political Phenomena*, Understanding Complex Systems (Springer, New York, NY, 2012).

[10] F. Abergel, H. Aoyama, B. K. Chakrabarti, A. Chakraborti, N. Deo, D. Raina, and I. Vodenska, eds., *Econophysics and Sociophysics: Recent Progress and Future Directions*, New Economic Windows (Springer, Cham, Switzerland, 2017).

[11] R. Albert and A.-L. Barabási, "Statistical mechanics of complex networks," Rev. Mod. Phys. **74**, 47 (2002).

[12] A.-L. Barabási and M. Pósfai, *Network Science* (Cambridge University Press, Cambridge, UK, 2016).

[13] C. Schinckus, "Ising model, econophysics and analogies," Physica A **508**, 95 (2018).

[14] S. de Marchi and S. E. Page, "Agent-based models," Annual Review of Political Science **17**, 1 (2014).

[15] H. Gintis, *The Bounds of Reason: Game Theory and the Unification of the Behavioral Sciences* (Princeton University Press, Princeton, NJ, 2009).

[16] J. Maynard Smith, *Evolution and the Theory of Games* (Cambridge University Press, Cambridge, UK, 1982).

[17] R. Axelrod, *The Evolution of Cooperation* (Basic Books, New York, NY, 1984).

[18] R. Axelrod, *The Complexity of Cooperation: Agent-based Models of Competition and Collaboration* (Princeton University Press, Princeton, NJ, 1997).

[19] S. Bowles and H. Gintis, *A Cooperative Species: Human Reciprocity and Its Evolution* (Princeton University Press, Princeton, NJ, 2011).

[20] M. Perc, J. J. Jordan, D. G. Rand, Z. Wang, S. Boccaletti, and A. Szolnoki, "Statistical physics of human cooperation," Phys. Rep. **687**, 1 (2017).

[21] J. von Neumann and O. Morgenstern, *Theory of Games and Economic Behaviour* (Princeton University Press, Princeton, NJ, 1953), 3rd ed.

[22] S. Karlin, *Matrix Games, Programming, and Mathematical Economics*, vol. 1 of *Mathematical Methods and Theory in Games, Programming, and Economics* (Pergamon, London, UK, 1959).

[23] N. N. Vorob'ev, *Game Theory: Lectures for Economists and Systems Scientists*, vol. 7 of *Applications of Mathematics* (Springer, New York, NY, 1977).

[24] J. Szép and F. Forgó, *Introduction to the Theory of Games*, vol. 3 of *Mathematics and Its Applications, East European Series* (D. Reidel, Dordrecht, The Netherlands, 1985).

[25] D. Fudenberg and J. Tirole, *Game Theory* (MIT Press, Cambridge, MA, 1991).

[26] R. Gibbons, *Game Theory for Applied Economists* (Princeton University Press, Princeton, NJ, 1992).

[27] M. J. Osborne and A. Rubinstein, *A Course in Game Theory* (MIT Press, Cambridge, MA, 1994).

[28] J. W. Weibull, *Evolutionary Game Theory* (MIT Press, Cambridge, MA, 1995).

[29] J. Hofbauer and K. Sigmund, *Evolutionary Games and Population Dynamics* (Cambridge University Press, Cambridge, UK, 1998).

[30] L. Samuelson, *Evolutionary Games and Equilibrium Selection*, vol. 1 of *Economic Learning and Social Evolution* (MIT Press, Cambridge, MA, 1998).

[31] R. Cressman, *Evolutionary Dynamics and Extensive Form Games*, vol. 5 of *Economic Learning and Social Evolution* (MIT Press, Cambridge, MA, 2003).

[32] G. Szabó and G. Fáth, "Evolutionary games on graphs," Phys. Rep. **446**, 97 (2007).

[33] H. Gintis, *Game Theory Evolving: A Problem-Centered Introduction to Modeling Strategic Interaction* (Princeton University Press, Princeton, NJ, 2009), 2nd ed.

[34] W. H. Sandholm, *Population Games and Evolutionary Dynamics*, vol. 8 of *Economic Learning and Social Evolution* (MIT Press, Cambridge, MA, 2010).

[35] K. Sigmund, *The Calculus of Selfishness*, vol. 6 of *Princeton Series in Theoretical and Computational Biology* (Princeton University Press, Princeton, NJ, 2010).

[36] G. Szabó and I. Borsos, "Evolutionary potential games on lattices," Phys. Rep. **624**, 1 (2016).

[37] J. F. Nash, Jr., "Equilibrium points in n-person games," Proc. Natl. Acad. Sci. USA **36**, 48 (1950).

[38] J. Nash, "Non-cooperative games," Ann. Math. **54**, 286 (1951).

[39] W. Poundstone, *Prisoner's Dilemma* (Anchor Books, New York, NY, 1993).

[40] A. Rapoport, A. M. Chammah, and C. J. Orwant, *Prisoner's Dilemma: A Study in Conflict and Cooperation* (University of Michigan Press, Ann Arbor, MI, 1965).

[41] D. Monderer and L. S. Shapley, "Potential games," Games Econ. Behav. **14**, 124 (1996).

[42] G. Szabó, K. S. Bodó, B. Allen, and M. A. Nowak, "Fourier decomposition of payoff matrix for symmetric three-strategy games," Phys. Rev. E **90**, 042811 (2014).

[43] G. Szabó, K. S. Bodó, B. Allen, and M. A. Nowak, "Four classes of interactions for evolutionary games," Phys. Rev. E **92**, 022820 (2015).

[44] G. Szabó, K. S. Bodó, and K. A. Samani, "Separation of cyclic and starlike hierarchical dominance in evolutionary matrix games," Phys. Rev. E **95**, 012320 (2017).

[45] G. Szabó and G. Bunth, "Social dilemmas in multistrategy evolutionary potential games," Phys. Rev. E **97**, 012305 (2018).

[46] O. Candogan, I. Menache, A. Ozdaglar, and P. A. Parrilo, "Flows and decomposition of games: Harmonic and potential games," Math. Oper. Res. **36**, 474 (2011).

[47] S.-H. Hwang and L. Rey-Bellet, "Decompositions of two player games: Potential, zero-sum, and stable games," CoRR **abs/1106.3552** (2011), arXiv:1106.3552.

[48] S.-H. Hwang and L. Rey-Bellet, "Strategic decompositions of normal form games: Zero-sum games and potential games," CoRR **abs/1602.06648** (2016), arXiv:1602.06648.

[49] M. W. Macy and A. Flache, "Learning dynamics in social dilemmas," Proc. Natl. Acad. Sci. USA **99**, 7229 (2002).

[50] F. C. Santos, J. M. Pacheco, and T. Lenaerts, "Evolutionary dynamics of social dilemmas in structured heterogeneous populations," Proc. Natl. Acad. Sci. USA **103**, 3490 (2006).

[51] J.-J. Rousseau, *The Social Contract and The First and Second Discourses*, Rethinking the Western Tradition (Yale University Press, New Haven, CT, 2002).

[52] J. Maynard Smith and G. R. Price, "The logic of animal conflict," Nature **246**, 15 (1973).

[53] C. Hauert and M. Doebeli, "Spatial structure often inhibits the evolution of cooperation in the snowdrift game," Nature **428**, 643 (2004).

[54] R. M. Alston and C. Nowell, "Implementing the voluntary contribution game," J. Econ. Behav. Organ. **31**, 357 (1996).

[55] C. Hauert, S. De Monte, J. Hofbauer, and K. Sigmund, "Volunteering as Red Queen mechanism for cooperation in public goods game," Science **296**, 1129 (2002).

[56] G. Szabó and C. Hauert, "Evolutionary prisoner's dilemma games with voluntary participation," Phys. Rev. E **66**, 062903 (2002).

[57] R. M. May, "Hypercycles spring to life," Nature **353**, 607 (1991).

[58] A. Szolnoki, M. Mobilia, L.-L. Jyian, B. Szczesny, A. M. Rucklidge, and M. Perc, "Cyclic dominance in evolutionary games: A review," J. R. Soc. Interface **11**, 20140735 (2014).

[59] J. Carroll, "The backward induction argument," Theory and Decision **48**, 61 (2000).

[60] R. D. McKelvey and T. Palfrey, "An experimental study of the centipede game," Econometrica **60**, 803 (1992).

[61] J. Andreoni and J. H. Miller, "Rational cooperation in the finitely repeated prisoner's dilemma: Experimental evidence," Econ. J. **103**, 570 (1993).

[62] J. Hofbauer and K. Sigmund, "Evolutionary game dynamics," Bull. Am. Math. Soc. **40**, 479 (2003).

[63] W. Choi, S.-H. Yook, and Y. Kim, "Percolation in spatial evolutionary prisoner's dilemma game on two-dimensional lattices," Phys. Rev. E **92**, 052140 (2015).

[64] H. Nishiuchi, N. Hatano, and K. Kubo, "Vortex generation in the RSP game on the triangular latice," Physica A **387**, 1319 (2008).

[65] G. Szabó, J. Vukov, and A. Szolnoki, "Phase diagrams for an evolutionary prisoner's dilemma game on two-dimensional lattices," Phys. Rev. E **72**, 047107 (2005).

[66] J. Vukov and G. Szabó, "Evolutionary prisoner's dilemma game on hierarchical lattices," Phys. Rev. E **71**, 036133 (2005).

[67] A.-L. Barabási and R. Albert, "Emergence of scaling in random networks," Science **286**, 509 (1999).

[68] L. N. A. Amaral, A. Scala, M. Barthélémy, and H. E. Stanley, "Classes of small-world networks," Proc. Natl. Acad. Sci. USA **97**, 11149 (2000).

[69] S. N. Dorogovtsev and J. F. F. Mendes, *Evolution of Networks: From Biological Nets to the Internet and WWW* (Oxford University Press, Oxford, UK, 2003).

[70] M. E. J. Newman, "The structure and function of complex networks," SIAM Review **45**, 167 (2003).

[71] S. Boccaletti, V. Latora, Y. Moreno, M. Chavez, and D. Hwang, "Complex networks: Structure and dynamics," Phys. Rep. **424**, 175 (2006).

[72] J. M. Pacheco, A. Traulsen, and M. A. Nowak, "Coevolution of strategy and structure in complex networks with dynamical linking," Phys. Rev. Lett. **97**, 258103 (2006).

[73] T. Gross and B. Blasius, "Adaptive coevolutionary networks: A review," J. R. Soc. Interface **5**, 259 (2008).

[74] J. Hofbauer, "Evolutionary dynamics for bimatrix games: A Hamiltonian system?," J. Math. Biol. **34**, 675 (1996).

[75] H. Ohtsuki, "Stochastic evolutionary dynamics of bimatrix games," J. Theor. Biol. **264**, 136 (2010).

[76] A. McAvoy and C. Hauert, "Asymmetric evolutionary games," PLoS Comp. Biol. **11**, e1004349 (2015).

[77] H. Fort, "On evolutionary spatial heterogeneous games," Physica A **387**, 1613 (2008).

[78] H. Fort, "A minimal model for the evolution of cooperation through evolving heterogenous games," EPL **81**, 48008 (2008).

[79] T. Killingback, M. Doebeli, and N. Knowlton, "Variable investment, the continuous prisoner's dilemma, and the origin of cooperation," Proc. R. Soc. Lond. B **266**, 1723 (1999).

[80] M. Perc, J. Gómez-Gardeñes, A. Szolnoki, L. M. Floría, and Y. Moreno, "Evolutionary dynamics of group interactions on structured populations: A review," J. R. Soc. Interface **10**, 20120997 (2013).

[81] P. Taylor and L. Jonker, "Evolutionary stable strategies and game dynamics," Math. Biosci. **40**, 145 (1978).

[82] J. A. J. Metz, S. A. H. Geritz, G. Meszéna, F. J. A. Jacobs, and J. S. van Heerwaarden, "Adaptive dynamics, a geometrical study of the consequences of nearly faithful reproduction,", in *Stochastic and Spatial Structures of Dynamical Systems*, edited by S. J. van Strien and S. M. Verduyn Lunel (North-Holland, Amsterdam, The Netherlands, 1996), pp. 183–231.

[83] L. E. Blume, "The statistical mechanics of strategic interactions," Games Econ. Behav. **5**, 387 (1993).

[84] J. Cramer, *Logit Models from Economics and Other Fields* (Cambridge University Press, 2003).

[85] G. Szabó and C. Tőke, "Evolutionary prisoner's dilemma game on a square lattice," Phys. Rev. E **58**, 69 (1998).

[86] R. J. Baxter, *Exactly Solved Models in Statistical Mechanics* (Academic, London, UK, 1982).

[87] D. H. Rothman and S. Zaleski, "Lattice-gas models of phase separation: Interfaces, phase transitions, and multiphase flow," Rev. Mod. Phys. **66**, 1417 (1994).

[88] H. Föllmer, "Random economies with many interacting agents," J. Math. Econ. **1**, 51 (1974).

[89] W. A. Brock and S. N. Durlauf, "Discrete choice with social interactions," Rev. Econ. Stud. **68**, 235 (2001).

[90] K. Sznajd-Weron and R. Weron, "A simple model of price formation," Int. J. Mod. Phys. C **13**, 115 (2002).

[91] S. M. Krause and S. Bornholdt, "Spin models as microfundation of macroscopic market models," Physica A **392**, 4048 (2013).

[92] K. Sznajd-Weron and J. Sznajd, "Opinion evolution in closed community," Int. J. Mod. Phys. C **11**, 1157 (2000).

[93] D. Stauffer, "Sociophysics: The Sznajd model and its applications," Comput. Phys. Commun. **146**, 93 (2002).

[94] S. Galam, "Sociophysics: A review of Galam models," Int. J. Mod. Phys. C **19**, 409 (2008).

[95] T. C. Schelling, "Models of segregation," Am. Econ. Rev. **59**, 488 (1969).

[96] T. C. Schelling, "Dynamic models of segregation," J. Math. Sociol. **1**, 143 (1971).

[97] S. Grauwin, D. Hunt, E. Bertin, and P. Jensen, "Effective free energy for individual," Adv. Complex Syst. **14**, 529 (2011).

[98] B. Oborny, G. Szabó, and G. Meszéna, "Survival of species in patchy landscapes: Percolation in space and time,", in *Scaling Biodiversity*, edited by D. Storch, P. A. Marquet, and J. H. Brown (Cambridge University Press, Cambridge, UK, 2007), Ecological Reviews, pp. 409–440.

[99] R. Pastor-Satorras, C. Castellano, P. Van Mieghem, and A. Vespignani, "Epidemic processes in complex networks," Rev. Mod. Phys. **87**, 925 (2015).

[100] K. Binder, "Application of Monte Carlo methods to statistical physics," Rep. Prog. Phys. **60**, 487 (1997).

[101] W. Janke, "Monte Carlo methods in classical statistical physics,", in *Computational Many-Particle Physics* (Springer, Berlin, Germany, 2008), vol. 739 of *Lecture Notes in Physics*, pp. 79–140.

[102] N. Metropolis, A. W. Rosenbluth, M. N. Rosenbluth, A. H. Teller, and E. Teller, "Equation of state calculations by fast computing machines," J. Chem. Phys. **21**, 1087 (1953).

[103] R. Kikuchi, "A theory of cooperative phenomena," Phys. Rev. **81**, 988 (1951).

[104] R. Kikuchi, "A theory of cooperative phenomena II. Equation of states for classical statistics," J. Chem. Phys. **19**, 1230 (1951).

[105] R. Kikuchi and S. Brush, "Improvement of the cluster-variation method," J. Chem. Phys. **47**, 195 (1967).

[106] D. de Fontaine, "Cluster variation and cluster statics,", in *Theory and Applications of the Cluster Variation and Path Probability Methods*, edited by J. L. Morán-López and J. M. Sanchez (Plenum, New York, NY, 1996), pp. 125–144.

[107] T. Morita, "Formal structure of the cluster variation method," Prog. Theor. Phys. Suppl. **115**, 27 (1994).

[108] R. Dickman, "Kinetic phase transitions in a surface-reaction model: Mean-field theory," Phys. Rev. A **34**, 4246 (1986).

[109] R. Dickman, "Mean-field theory of the driven diffusive lattice gas," Phys. Rev. A **38**, 2588 (1988).

[110] R. Dickman, "Driven lattice gas with repulsive interaction: Mean-field theory," Phys. Rev. A **41**, 2192 (1990).

[111] J. Vukov, G. Szabó, and A. Szolnoki, "Cooperation in the noisy case: Prisoner's dilemma game on two types of regular random graphs," Phys. Rev. E **73**, 067103 (2006).

[112] G. Szabó and B. Király, "Extension of a spatial evolutionary coordination game with neutral options," Phys. Rev. E **93**, 052108 (2016).

[113] R. W. Cooper, *Coordination Games: Complementarities and Macroeconomics* (Cambridge University Press, Cambridge, UK, 1999).

[114] E. Ising, "Beitrag zur Theorie des Ferromagnetismus," Z. Physik **31**, 253 (1925).

[115] H. E. Stanley, *Introduction to Phase Transitions and Critical Phenomena* (Clarendon, Oxford, UK, 1971).

[116] C. Domb, "Ising model,", in *Series Expansions for Lattice Models*, edited by C. Domb and M. S. Green (Academic, London, UK, 1974), vol. 3 of *Phase Transitions and Critical Phenomena*, pp. 357–484.

[117] R. Tamura, S. Tanaka, and N. Kawashima, "Phase transition in Potts model with invisible states," Prog. Theor. Phys. **124**, 381 (2010).

[118] S. Tanaka, R. Tamura, and N. Kawashima, "Phase transition of generalized ferromagnetic Potts model: Effect of invisible states," J. Phys.: Conf. Ser. **297**, 012022 (2011).

[119] S. Tanaka and R. Tamura, "Dynamical properties of Potts model with invisible states," J. Phys.: Conf. Ser. **320**, 012025 (2011).

[120] A. C. D. van Enter, G. Iacobelli, and S. Taati, "First-order transition in Potts models with "invisible" states," Prog. Theor. Phys. **126**, 983 (2011).

[121] A. C. D. van Enter, G. Iacobelli, and S. Taati, "Potts model with invisible colors: Random-cluster representation and Pirogov–Sinai analysis," Rev. Math. Phys. **24**, 1250004 (2012).

[122] D. A. Johnston and R. P. K. C. M. Ranasinghe, "Potts model with (17) invisible states on thin graphs," J. Phys. A: Math. Theor. **46**, 225001 (2013).

[123] N. Ananikian, N. S. Izmailyan, D. A. Johnston, R. Kenna, and R. P. K. C. M. Ranasinghe, "Potts model with invisible states on general Bethe lattices," J. Phys. A: Math. Theor. **46**, 385002 (2013).

[124] M. Krasnytska, P. Sarkanych, B. Berche, Y. Holovatch, and R. Kenna, "Marginal dimensions of the Potts model with invisible states," J. Phys. A: Math. Theor. **49**, 255001 (2016).

[125] P. Sarkanych, Y. Holovatch, and R. Kenna, "Exact solution of a classical short-range spin model with a phase transition in one dimension: The Potts model with invisible states," Phys. Lett. A **381**, 3589 (2017).

[126] O. N. Senkov, G. B. Wilks, D. B. Miracle, C. P. Chuang, and P. K. Liaw, "Refractory high-entropy alloys," Intermetallics **18**, 1758 (2010).

[127] J.-W. Yeh, "Alloy design strategies and future trends in high-entropy alloys," J. Metals **65**, 1759 (2013).

[128] R. Carroll, C. Li, C.-W. Tsai, J.-W. Yeh, J. Antonaglis, B. A. W. Brinkman, M. LeBlanc, X. Xie, S. Chen, P. K. Liaw, et al., "Experiments and model for serration statistics in low-entropy, medium-entropy, and high-entropy alloys," Sci. Rep. **5**, 16997 (2015).

[129] L. Onsager, "Crystal statistics. I. A two-dimensional model with an order-disorder transition," Phys. Rev. **65**, 117 (1944).

[130] F. Y. Wu, "The Potts model," Rev. Mod. Phys. **54**, 235 (1982).

[131] V. Spirin, P. L. Krapivsky, and S. Redner, "Fate of zero-temperature Ising ferromagnets," Phys. Rev. E **63**, 036118 (2001).

[132] V. Spirin, P. L. Krapivsky, and S. Redner, "Freezing in Ising ferromagnets," Phys. Rev. E **65**, 016119 (2001).

[133] J. Olejarz, P. L. Krapivsky, and S. Redner, "Fate of 2D kinetic ferromagnets and critical percolation crossing probabilities," Phys. Rev. Lett. **109**, 195702 (2012).

[134] R. B. Potts, "Some generalized order-disorder transformations," Math. Proc. Camb. Phil. Soc. **48**, 106 (1952).

[135] B. Király and G. Szabó, "Evolutionary games with coordination and self-dependent interactions," Phys. Rev. E **95**, 012303 (2017).

[136] M. Blume, "Theory of the first-order magnetic phase change in UO_2," Phys. Rev. **141**, 517 (1966).

[137] H. W. Capel, "On the possibility of first-order transitions in Ising systems of triplet ions with zero-field splitting," Physica **32**, 966 (1966).

[138] H. W. Capel, "On the possibility of first-order transitions in Ising systems of triplet ions with zero-field splitting II," Physica **33**, 295 (1967).

[139] H. W. Capel, "On the possibility of first-order transitions in Ising systems of triplet ions with zero-field splitting III," Physica **37**, 423 (1967).

[140] J. Zierenberg, N. G. Fytas, M. Weigel, W. Janke, and A. Malakis, "Scaling and universality in the phase diagram of the 2D Blume–Capel model," Eur. Phys. J. Special Topics **226**, 789 (2017).

[141] P. D. Beale, "Finite-size scaling study of the two-dimensional Blume–Capel model," Phys. Rev. B **33**, 1717 (1986).

[142] C. J. Silva, A. A. Caparica, and J. A. Plascak, "Wang–Landau Monte Carlo simulation of the Blume–Capel model," Phys. Rev. E **73**, 036702 (2006).

[143] A. Malakis, A. N. Berker, I. A. Hadjiagapiou, N. G. Fytas, and T. Papakonstantinou, "Multicritical points and crossover mediating the strong violation of universality: Wang–Landau determinations in the random-bond $d = 2$ Blume–Capel model," Phys. Rev. E **81**, 041113 (2010).

[144] W. Kwak, J. Jeong, J. Lee, and D.-H. Kim, "First-order phase transition and tricritical scaling behavior of the Blume–Capel model: A Wang–Landau sampling approach," Phys. Rev. E **92**, 022134 (2015).

[145] M. Blume, V. J. Emery, and R. B. Griffiths, "Ising model for the λ transition and phase separation in He^3-He^4 mixtures," Phys. Rev. A **4**, 1071 (1971).

[146] A. N. Berker and M. Wortis, "Blume–Emery–Griffiths–Potts model in two dimensions: Phase diagram and critical properties from a position-space renormalization group," Phys. Rev. B **14**, 4946 (1976).

[147] B. Király and G. Szabó, "Evolutionary games combining two or three pair coordinations on a square lattice," Phys. Rev. E **96**, 042101 (2017).

[148] M. Suzuki, "Solution of Potts model for phase transition," Prog. Theor. Phys. **37**, 770 (1967).

[149] J. Tobochnik, "Properties of the q-state clock model for $q = 4$, 5, and 6," Phys. Rev. B **26**, 6201 (1982).

[150] J. Ashkin and E. Teller, "Statistics of two-dimensional lattices with four components," Phys. Rev. **64**, 178 (1943).

[151] C. Fan, "On critical properties of the Ashkin–Teller model," Phys. Lett. A **39**, 136 (1972).

[152] D. D. Betts, "The exact solution of some lattice statistics models with four states per site," Can. J. Phys. **42**, 1564 (1964).

[153] F. Y. Wu and K. Y. Lin, "Two phase transitions in the Ashkin–Teller model," J. Phys. C: Solid State Phys. **7**, L181 (1974).

[154] F. J. Wegner, "Duality relation between the Ashkin–Teller and the eight-vertex model," J. Phys. C: Solid State Phys. **5**, L131 (1972).

[155] R. V. Ditzian, J. R. Banavar, G. S. Grest, and L. P. Kadanoff, "Phase diagram for the Ashkin–Teller model in three dimensions," Phys. Rev. B **22**, 2542 (1980).

[156] H. A. Kramers and G. H. Wannier, "Statistics of two-dimensional ferromagnet. Part I," Phys. Rev. **60**, 252 (1941).

[157] H. A. Kramers and G. H. Wannier, "Statistics of two-dimensional ferromagnet. Part II," Phys. Rev. **60**, 263 (1941).

[158] J. Chen, H.-J. Liao, H.-D. Xie, X.-J. Han, R.-Z. Huang, S. Cheng, Z.-C. Wei, Z.-Y. Xie, and T. Xiang, "Phase transition of the q-state clock model: Duality and tensor renormalization," Chin. Phys. Lett. **34**, 050503 (2017).

[159] B. Király and G. Szabó, "Entropy affects the competition of ordered phases," Entropy **20(2)**, 115 (2018).

[160] K. Binder, "Static and dynamic critical phenomena of the two-dimensional q-state Potts model," J. Stat. Phys. **24**, 69 (1981).

[161] E. Luijten, "Introduction to cluster Monte Carlo algorithms,", in *Computer Simulations in Condensed Matter Systems: From Materials to Chemical Biology Volume 1*, edited by M. Ferrario, G. Ciccotti, and K. Binder (Springer, Berlin, Germany, 2006), vol. 703 of *Lecture Notes in Physics*, pp. 13–38.

[162] J. Cardy, *Scaling and Renormalization in Statistical Physics* (Cambridge University Press, Cambridge, UK, 1996).

[163] M. E. Fisher, "Renormalization group theory: Its basis and formulation in statistical physics," Rev. Mod. Phys. **70**, 653 (1998).

[164] M. Levin and C. P. Nave, "Tensor renormalization group approach to two-dimensional classical lattice models," Phys. Rev. Lett. **99**, 120601 (2007).

[165] A. Wipf, "High-temperature and low-temperature expansions,", in *Statistical Approach to Quantum Field Theory: An Introduction* (Springer, Heidelberg, Germany, 2013), vol. 864 of *Lecture Notes in Physics*, pp. 173–204.

[166] K. G. Wilson and M. E. Fisher, "Critical exponents in 3.99 dimensions," Phys. Rev. Lett. **28**, 240 (1972).

[167] G. Szabó, L. Varga, and M. Szabó, "Anisotropic invasion and its consequences in two-strategy evolutionary games on a square lattice," Phys. Rev. E **94**, 052314 (2016).

[168] E. C. Zeeman, "Population dynamics from game theory,", in *Global Theory of Dynamical Systems*, edited by Z. Nitecki and C. Robinson (Springer, Berlin, Germany, 1980), vol. 819 of *Lecture Notes in Mathematics*, pp. 471–497.